Mass Spectrometry Analysis of Nrf2-Keap1 Chemoprevention Signaling Pathway

BY

CHENQI HU
B.E, B.S, Shanghai Jiao Tong University, Shanghai, China, 2003
M.S., University of Nanyang Technological University, Singapore and Stanford University, 2004

DISSERTATION

Submitted as partial fulfillment of the requirements
For the degree of Doctor of Philosophy in Medicinal Chemistry
In the Graduate College of the
University of Illinois at Chicago, 2012

Chicago, Illinois

Defense Committee:

Richard B. van Breemen, Chair and Advisor
John F. Fitzloff
Steven M. Swanson
Joanna E. Burdette
Bao-Shiang (Bob) Lee, UIC Research Resources Center

This dissertation is dedicated to my husband Zichong Wang, my son Andrew Wang, my parents Xiaoyuan Hu and Haihui Chen, as well as my friends for their support, encouragement and providing the strength to complete this Ph.D.

ACKNOWLEDGMENTS

I would like to express my utmost gratitude to my supervisor, Professor Richard B. van Breemen for entrusting me with such an exciting and promising dissertation project, guiding me toward cancer chemoprevention and proteomics. I appreciate his vast knowledge and skill, which provided me invaluable guidance in the mass spectrometry field. During four years of study, his patience and encouragement provided me with an environment to think and learn independently, which is one of the most important qualities essential to my future career.

I thank Professor John F. Fitzloff for his guidance in my graduate studies. As the director of graduate studies in Medicinal Chemistry, he has provided me with help and support during my graduate study. I especially thank him for his participation in both my preliminary examination and dissertation defense committees.

I acknowledge the other committee members of my preliminary examination and dissertation defense - Professor Steven M. Swanson, Dr. Bob Lee and Professor Joanne E. Burdette- for all their time and assistance to help me improve my work.

I express my gratitude and respect to Professor Andrew D. Mesecar in the collaboration of the Keap1 project. I thank Dr. Evan Small for supplying us with the recombinant proteins and cross-linking sample preparation. A very special thanks to Dr. Aimee L. Eggler for the wonderful and pleasant collaboration during this project as well as tremendous suggestions and inspirations that will benefit me throughout my life.

ACKNOWLEDGMENTS (continued)

I shall always feel grateful to Dr. Alexander Schilling, Dr, Carrie Crot, Dr. Larry Helseth, Dr. Hua Xu, and Mr. Rod Davis from the Proteomics and Informatics Services Facility for providing me with experience in operating and maintaining a variety of analytical instruments.

I appreciate Dr. Dejan Nikolic, Dr. Yan Wang, Dr. Yan Luo, Dr. Hongmei Cao, Dr. Jinghu Li, Dr. Jeffery Dahl, Dr. Soyoun Ahn and all other senior researchers in this lab, who assisted me in the operation of the mass spectrometers. I also thank Dr. Shunyan Mo, Dr. Yongsoo Choi, Linlin Dong, Yang Yuan, and Yang Song for their helpful discussions for my research project. Finally, I thank Xi Qiu, Jerry White, Zhiyuan Sun, and all the other members in Dr. van Breemen's lab for their friendship and assistance.

Finally, I would like to acknowledge Dr. Chaoran (Ron) Huang, Dr. Liyu Yang and Dr. Wei (Don) Dong for the internship opportunity at Biogen Idec where I learned a lot of practical skills in mass spectrometry, which became helpful to my dissertation work.

I acknowledge the Department of Medicinal Chemistry and Pharmacognosy for financial support. This work was supported by grant P01 CA48112 from the National Cancer Institute.

CQHU

TABLE OF CONTENTS

TABLE OF CONTENTS (continued)

TABLE OF CONTENTS (continued)

LIST OF TABLES

LIST OF FIGURES

FIGURE PAGE

LIST OF FIGURES (continued)

FIGURE PAGE

LIST OF FIGURES (continued)

FIGURE PAGE

LIST OF ABBREVIATIONS

4-HNE	4-hydroxynonenal
15d-PGJ_2	15-deoxy-$^{\Delta 12,14}$-prostaglandin J_2
ARE	Antioxidant response element
BME	β-mercaptoethanol
BS^3	Bis(sulfosuccinimidyl) suberate
CDDO-Im	1-[2-cyano-3-,12-dioxooleana-1,9(11)-dien-28-oyl]imidazole
CID	Collision-induced dissociation
Cul3	Cullin3-based E3-ligase ubiquitination complex
DTT	D,L-dithiothreitol
FPLC	Fast protein liquid chromatography
FT ICR	Fourier transform ion cyclotron resonance
GSH	Glutathione
HCD	Higher-energy collisional dissociation
HPLC	High performance liquid chromatography
IAB	*N*-iodoacetyl-*N*-biotinylhexylenediamine
IT	Ion trap
ITC	Isothermal titration calorimetry
Keap1	Kelch-like ECH-associated protein 1
LC-MS/MS	Liquid chromatography tandem mass spectrometry
LTQ	Linear quadrupole ion trap
MALDI	Matrix-assisted laser desorption ionization

LIST OF ABBREVIATIONS (continued)

MS	Mass spectrometry
NMR	Nuclear magnetic resonance
Nrf2	NF-E2-related factor-2
PGA_2	Prostaglandin A_2
PKC	Protein kinase C
PTMs	Post translational modifications
S-lens	Stacked ring ion guide
tBHQ	*tert*-butylhydroquinone
TCEP	Tris[2-carboxyethyl]phosphine hydrochloride
TOF	Time-of-flight

SUMMARY

Chemoprevention is an active cancer preventive strategy to inhibit, delay or reverse human carcinogenesis using naturally occurring or synthetic chemical agents. In recent years, it has emerged as one of the major approaches for reducing cancer. Dietary natural products and diet-derived agents are potential chemopreventive agents since they are relatively safe and exhibit no or low toxicity.

Activation of the transcription factor NF-E2-related factor-2 (Nrf2), leading to up-regulation of the antioxidant response element (ARE) for cellular defense against reactive oxygen species and xenobiotic electrophiles, is an important strategy for cancer chemoprevention. Under basal conditions, Nrf2 is anchored in the cytosol by a Kelch-like ECH-associated protein 1 (Keap1) dimer. Keap1 serves as an adaptor between the Cullin3 (Cul3)-based E3-ligase ubiquitination complex and Nrf2, directing constitutive ubiquitination of Nrf2 and thus its proteasomal degradation. The low concentration of Nrf2 in the nucleus results in low expression of ARE-driven genes. Upon exposure of cells to the ARE activators, Nrf2 ubiquitination is inhibited, leading to the stabilization and accumulation of Nrf2 in the nucleus, where it dimerizes with a small Maf protein, binds to AREs and stimulates cytoprotective gene transcription.

Numerous potential ARE activators have been identified, many of which are abundant in natural plants. However, how these chemopreventive agents activate ARE through Nrf2-Keap1 signaling pathway is still unclear. In this dissertation, mass spectrometry was employed to improve the high-throughput screening assay we developed previously to find compounds that modify Keap1, and to facilitate elucidation of the mechanism of the Nrf2-Keap1 signaling pathway in response to ARE activators.

Firstly, since our previous matrix-assisted laser desorption time-of-flight mass spectrometry (MALDI-TOF MS) based screening method to discover natural products that modify Keap1 is not able to detect some of agents such as sulforaphane, a potent ARE activator, a more sensitive screening assay was developed. In this new method, electrophiles that reversibly modify Keap1 protein can be trapped by BME and identified by mass spectrometry as adducts. Isoliquiritigenin, a known ARE activator that targets Keap1, was used to validate the method by using liquid chromatography-tandem mass spectrometry (LC-MS-MS). To evaluate the screening assay, sulforaphane was spiked into a crude extract of cocoa nibs. Use of high resolution accurate mass measurement on a HPLC-ion trap-TOF mass spectrometer (IT-TOF MS) and automated peak detection software, permitted approximately 20-fold more sensitive detection than our previously developed MALDI-TOF MS-based assay and improved other aspects of that assay. This new screening method is applicable to detection of low abundance reversible chemopreventive agents in natural product mixtures.

Modification of Keap1 cysteines has been demonstrated to be a critical step for chemopreventive agents to active the ARE. Significant effort has been undertaken to identify the key cysteines in Keap1 and their function. However, there are conflicting in vitro and in vivo data regarding which Keap1 cysteine residues become modified for some ARE activators such as sulforaphane. Although most biological data indicate that modification at C151 is essential for sulforaphane action, some recent studies using mass spectrometry have failed to identify C151 as a site of Keap1 modification by sulforaphane. To address this issue, a revised sample preparation protocol was developed.

Our studies indicate that iodoacetamide treatment usually used during sample preparation promotes dissociation of sulforaphane-cysteine adducts, especially adducts with C151 of Keap1. By eliminating the iodoacetamide treatment step and reducing sample preparation time, we showed that C151 is detected as one of the four most reactive cysteine residues in Keap1 towards sulforaphane. These results are consistent with cell studies and in vivo findings.

Next, in order to investigate whether iodoacetamide treatment will affect other ARE activators' modification pattern during in vitro experiments, the reversibility of another five activators including isoliquiritigenin, xanthohumol, 1-[2-cyano-3-,12-dioxooleana-1,9(11)-dien-28-oyl]imidazole (CDDO-Im), prostaglandin A_2 (PGA_2), and 15-deoxy-$\Delta^{12,14}$-prostaglandin J_2 (15d-PGJ_2) were evaluated. Subsequently, the Keap1 cysteine alkylation pattern of PGA_2 and 15d-PGJ_2 was investigated using a linear ion trap Fourier transform ion cyclotron resonance mass spectrometer (LTQ-FT ICR) with an appropriate sample preparation protocol. Contrary to most of the ARE activators reported previously, we found that C151 is not detected as one of the most reactive cysteine residues in Keap1 towards either PGA_2 or 15d-PGJ_2. These in vitro results are consistent with some in vivo evidence reported recently that PGA_2 and 15d-PGJ_2 are Keap1 C151-independent.

Alteration of the Keap1-Cul3 interaction is a promising mechanism of regulating ARE activation by decreasing Nrf2 ubiquitination. To support this mechanistic study, mass spectrometry was used to help elucidate how Keap1 conformation changes upon

C151 modification by an ARE activator and subsequently alters the binding to Cul3. First, we used an indirect method to investigate the protein structure change that occurs when isoliquiritigenin, a well studied ARE activator reported previously, binds covalently to Keap1. The conformation of Keap1 may affect its reactivity, and the 27 cysteines of Keap1 may be used as conformational probes. To investigate whether modification of Keap1 C151 leads to a conformational change, both wt Keap1 and a Keap1 C151W mutant, which simulates the modification of C151 by electrophiles, were modified by isoliquiritigenin, either with or without the presence of Cul3, and modified cysteines were monitored. We found that there is no significant difference between wt Keap1 and the Keap1 C151W mutant in terms of their reaction with isoliquiritigenin. However, Cul3 C636 is differentially modified by isoliquiritigenin when binding to wt Keap1 or Keap1 C151W mutant. This observation implies a change in the Keap1-Cul3 interaction induced by the modification of Keap1 C151, apart from a simple disruption of the Keap1-Cul3 complex, changing the current model in the field. The most reactive cysteine of Cul3, C636, may play a functional role in the signaling pathway, and this needs further investigation.

Next, considering the unavailability of the three dimensional structure of either Keap1 or Cul3 protein, we covalently linked Keap1 and Cul3 using a cross-linker and used mass spectrometry to probe directly the Keap1 and Cul3 structure, as well as their interaction interface. After the optimization of sample preparation conditions, thirty intra- or intermolecular cross-linked peptides were identified. These results can be further used

for protein docking models. In addition, we found that the cross-linker bis(sulfosuccinimidyl) suberate (BS^3) is more suitable for intermolecular cross-linking studies than is glutaraldehyde due to its longer spacer and reaction specificity. Finally, we found that with a much faster scanning speed, more efficient fragmentation and high mass accuracy of both precursor and product ions, the LTQ Orbitrap Velos is a more suitable instrument for cross-linked peptides identification than the LTQ FT-ICR mass spectrometer.

In conclusion, these mass spectrometry-based methods were developed to 1) screen natural product extracts for possible chemopreventive agents that can activate ARE-mediated gene expression; and 2) facilitate clarification of the Nrf2-Keap1 signaling pathway mechanism in terms of cysteine alkylation, reversibility of the cysteine-electrophile adducts and protein 3D structure. The methods developed here can also be used in studies of other signaling pathways that have a similar mechanism.

1 INTRODUCTION

1.1 Cancer chemoprevention by natural products

1.1.1 Cancer chemoprevention

Cancer is a major public health problem in the United States and many other parts of the world. Currently, one out of every four deaths in United States is due to cancer. Prostate, lung, breast and colorectal cancers are the most common cancers in both men and women according to the American Cancer Society [1]. However, the overall new diagnoses and death rates from all cancers are declined in the recent ten years, which may be at least partially attributed to the progress in cancer prevention, early detection, and treatment.

Various human diseases, including cancer can be effectively prevented by avoidable causes such as cigarette smoking and reduction of environmental toxins, in combination with a healthy diet and regular physical activities [2-4]. The concept of chemoprevention, as first proposed by Dr. Michael B. Sporn in the early 1970s, was defined as the use of natural or synthetic compounds to inhibit, suppress or reverse the development and progression of cancer [5]. Since Dr. Lee W. Wattenberg articulated the concept of selective inhibition of carcinogenesis during either initiation, promotion or progression phases [6], the field of cancer chemoprevention has grown rapidly.

Recently, it has become increasingly clear that chemoprevention is a rational and appealing strategy. It is applicable to healthy individuals or to individuals who may be at a higher risk of developing cancer due to family history. For cancer patients being treated

with the goal of killing cancer cells, chemopreventive agents may be used along with chemotherapeutic agents to provide additive or synergistic effects with fewer side effects. Moreover, chemopreventive agents are becoming an important component in the post-therapy of cancer patients to prevent the recurrence of the disease (as shown in Figure 1) [7].

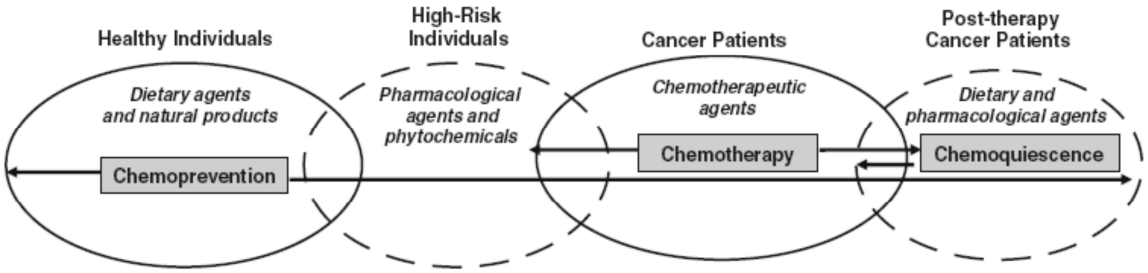

Figure 1. Selective responsiveness of a healthy population as well as cancer patients to chemopreventive agents [7].

Numerous cancer cell lines and animal models have been used to evaluate the chemopreventive effects of dietary compounds. These efforts have yielded great success in the discovery of novel chemopreventive agents such as polyphenols from green and black tea, and flavonoids from soybeans. For example, isothiocyanates from cruciferous vegetables have progressed from the bench to clinical trials [8]. Considering that the overall cancer preventive effects of these chemopreventive agents are contributed by a complex cellular process involving altered protein expression and signaling transduction modulation, elucidation of their underlying mechanisms of cancer prevention action at the molecular level plays a pivotal role in understanding their uses. Recently, some of the most promising molecular targets for chemoprevention studies are the cellular signaling cascades mediated by nuclear factor E2-related factor 2 (Nrf2), nuclear factor-kappaB

(NF-κB), cyclooxy-genase-2 (COX-2), activator protein-1 (AP-1), and mitogen-activated protein kinases (MAPKs) [9].

1.1.2 Natural products in chemoprevention

Natural products, herbs and spices have been used for preventing several diseases since ancient times. Despite the great interest in diet as a strategy to prevent and cure cancer with little or no toxicity, it was not until the late twentieth century that diet-derived chemoprevention mechanisms began to be understood. Since the National Cancer Institute initiated a Diet and Cancer Program approximately 35 years ago, studies have shown that the high content of bioactive compounds present in fruits and vegetables has important roles in the prevention of chronic diseases, including cancer, diabetes and hypercholesteremia [7, 10]. Some of the diet-derived substances widely consumed in the United States that have been reported to reduce experimental carcinogenesis are indole-3-carbinol (I3C) from cruciferous vegetable [11], curcumin from the root of curcuma, present in the Indian spice turmeric [12], resveratrol from grapes [13], and epigallocatechin gallate (EGCG) from tea [14]. Other commonly consumed foods and their targets are shown in Figure 2.

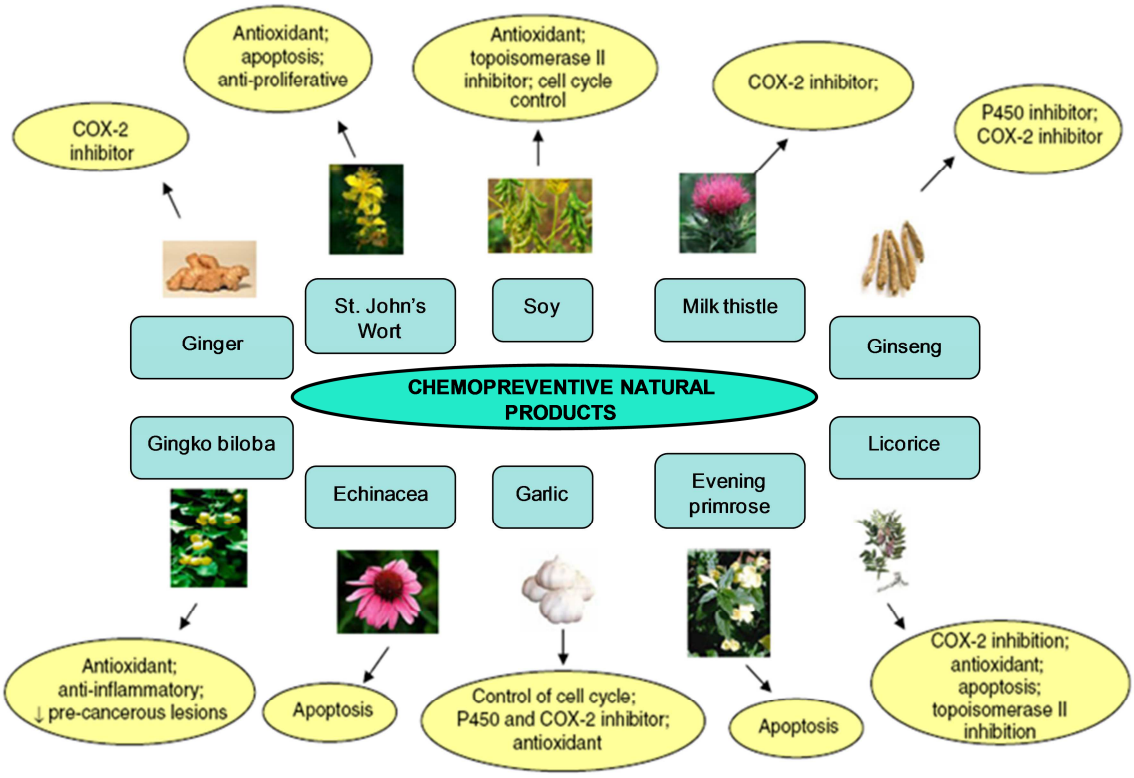

Figure 2. Some of the chemopreventive natural products widely consumed in the United States and reported to have chemopreventive efficacy. The circles indicate reported mechanism(s) of action for these agents [7].

Recently, the use of natural agents as nutritional supplements or alternative medicines has grown and continues to show an upward trend. The general public as well as cancer patients use natural agents for prevention or even for treatment of cancer. Data from 2004 show that natural products and their derivatives account for 44% of all new drugs [15]. Since natural products may not be ideal chemopreventive or chemotherapeutic agents as found in nature, natural agents could still guide medicinal chemists toward the synthesis of more effective and safer analogs, which could become novel therapeutic agents for the treatment or prevention of various cancers in the future.

In addition, studies of underlying mechanisms of natural agents' action at a molecular level will facilitate evaluation of the potential of natural agents in chemoprevention, as well as the basis of mechanism-based biomarker development, both of which are important for winning the battle against cancer.

1.2 Molecular mechanisms of the Nrf2-Keap1 chemoprevention pathway

Induction of phase II detoxification enzymes such as NAD(P)H-quinone oxidoreductase 1 (NQO1) and glutathione S-transferases (GSTs), and endogenous antioxidant enzymes such as heme oxygenase-1 (HO-1) by natural chemopreventive agents is a promising strategy for reducing the risk of cancer and other chronic diseases [16]. In the early 1990's, Pickett and colleagues first discovered a regulatory element in the promoter region of rat *Gst-Ya* and termed it the antioxidant responsive element (ARE) [17]. Mutational analysis further revealed 5'-GTGACnnnGC-3' to be the core sequence of the ARE in the same laboratory, where n represents any base [18]. Numerous subsequent analyses have demonstrated that ARE encodes a battery of cytoprotective enzymes [19-21] and is upregulated in response to a wide range of chemicals including oxidative stress, xenobiotic electrophiles, endogenous oxidized metabolites, toxic heavy metals, UV irradiation, and natural products [16, 22-26]. Up-regulation of the ARE causes cells to produce more cytoprotective enzymes.

The NF-E2-related factor 2 (Nrf2), a member of the Cap-N-Collar (CNC) of basic-leucine zipper NF-E2 family, is ubiquitously expressed at low levels in all human organs [27]. It was first cloned and characterized by Kan (human Nrf2) in 1994 [28] and Yamamoto (chicken Nrf2) [29] independently as a factor that binds to the NF-E2/AP-1

repeat of the β-globin gene promoter. Soon after, Kensler and coworkers provided convincing evidence demonstrating that Nrf2 is a critical regulator of ARE-dependent transcription. They showed that Nrf2-knockout mice had reduced levels and impaired induction of a variety of phase II detoxifying enzymes and endogenous antioxidants, rendering the knockout mice more susceptible to carcinogen-induced cancers [30]. Several other groups showed that Nrf2 initiates transcription of ARE-driven phase II genes, upon translocation to the nucleus, formation of a heterodimer with a small Maf protein and binding to the ARE [31-34]. Since then, Nrf2 has emerged as the master regulator of a cellular defense mechanism to protect cells against various electrophilic and oxidative damages.

The activity of Nrf2 is negatively regulated by a cysteine-rich protein termed Kelch-like ECH-associated protein 1 (Keap1). Gene knockout of Keap1 resulted in constitutively hyperactive Nrf2 signaling both in cells and animal models [35-38]. Keap1 was first identified and cloned using the Neh2 domain (approximately the first 100 residues) of Nrf2 as bait in a yeast two-hybrid screen by Itoh and colleagues from Yamamoto's group in 1999 [37]. Keap1 mainly distributes in the cytoplasm, immobilized by binding to actin cytoskeleton [39-41]. The human Keap1 consists of five domains shows in Figure 3: an amino-terminal region (NTR), a bric-a-brac, tramtrack, broad complex (BTB), an intervening region (IVR), a Kelch/double glycine repeat (DGR), and a carboxyl terminal region (CTR) [37]. The BTB domain is required for Keap1 homodimerization [42]. The DGR and CTR domain binds to two Neh2 motifs, termed the DLG (low-affinity) and ETGE (high-affinity) motifs, so that the Keap1 dimer recognizes one molecule of Nrf2 and prevents constitutive Nrf2 nuclear accumulation

[43, 44]. The IVR domain is the most cysteine-rich domain and is indispensable for cytoplasmic sequestration of Nrf2 [45].

In 2004, Keap1 was proved to be a substrate adaptor protein for a Cullin3 (Cul3)-based E3-ligase ubiquitination complex, responsible for Nrf2 degradation, by four independent groups [46-49]. Keap1 serves as a bridge between Nrf2 and Cul3. Keap1 brings Nrf2 into the E3 ligase complex through interacting Cul3 with BTB domain, and binding Nrf2 with DGR domain. Under basal conditions, the concentration of Nrf2 is low due to constitutive ubiquitination by the Cul3-based E3-ligase ubiquitination complex and then degradation by the 26S proteasome; this results in low expression of ARE-driven genes [47]. Upon exposure of cells to ARE activators, Nrf2 ubiquitination is inhibited, and Nrf2 accumulates in the nucleus where it forms a heterodimer with a small Maf protein and binds to the ARE to stimulate cytoprotective gene transcription [37] (Figure 4A). Activation of this pathway is a promising strategy for the prevention of numerous human diseases including cancer.

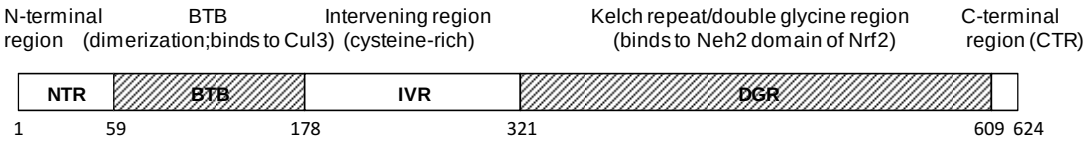

Figure 3. Schematic representation of five regions of human Keap1 protein.

Although numerous ARE activators have been identified, they share few structural similarities [50]. Talalay and coworkers [35, 51, 52] have noted that the majority of ARE activators are electrophilic and can covalently modify cysteine

sulfhydryl groups. Since human Keap1 binds Nrf2 and contains 27 cysteine residues, Dinkova-Kostova in Talalay's group proposed in 2002 that Keap1 might be a regulatory sensor for the ARE pathway and provided the first in vitro evidence that four cysteines C257, C273, C288, and C297 in mouse Keap1 were the most reactive toward dexamethasone, a thiol reagent using mass spectrometry (MS) [52]. However, how signals from these compounds are transmitted to the Nrf2-Keap1-Cul3 system and activate the ARE response is still unclear. Based on a number of studies, several mechanisms have been proposed for Nrf2 nucleus accumulation in response to the activators and are shown in Figure 4.

Itoh and co-workers [53] first postulated that Nrf2 is released from the Nrf2-Keap1 complex in the cytoplasm in response to interaction with electrophiles or oxidative stressors and translocates to the nucleus resulting in nuclear accumulation and ARE-regulated gene expression in 1999 (Figure 4B). Based on a primarily study by Dinkova-Kostova et al., in which native EMSAs conducted with mouse Keap1 and Neh2 proteins show that the Keap1-Neh2 complex band is disrupted by the addition of sulforaphane, a direct Nrf2-Keap1 dissociation model was established in 2002 [52]. Since then, significant effort has been undertaken to identify the critical cysteines in Keap1 and their function. Keap1 C273 and C288 located in the IVR domain, are required for efficient ubiquitination and basal inhibition of Nrf2 [35, 45, 54, 55]. Zhang *et al.*, first demonstrated in cell that C151 was the only cysteine determined to be required for stabilization and activation of Nrf2 in response to ARE activators such as sulforaphane and tert-butylhydroquinone (tBHQ) using mutagenesis approach [45]. Located in the BTB domain (Figure 3), Keap1 C151 is a 100% conserved cysteine among species.

Modification of C151 might play a critical role in regulating electrophile signaling. However, mass spectrometry studies showed conflicting Keap1 cysteine adduction patterns in vitro by different groups. Our group showed that C151 is the three most reactive cysteines in human Keap1 towards biotinylated iodoacetamide (BIA) [56], 1-biotinamido-4-(4′-[maleimidoethyl-cyclohexane]-carboxamido) butane (BMCC) [57], as well as the natural product ARE activators xanthohumol from hops, isoliquiritigenin from licorice and 10-shogaol from ginger [57]. Independently, Hong *et al.* showed 15 cysteines of human Keap1 modified by BIA without C151 [58]. To reconcile the contradict results, our group evaluated the methods used by both groups and found C151 is one of the most highly reactive cysteines in human Keap1 agreed well with other biological evidence. The no detection of C151 by Liebler's group is due to the relatively harsh treatment of Keap1 in the membrane method, which probably results in an unfolded or misfolded Keap1 at the time of BIA modification [56]. Subsequent analysis further confirmed that C151 is the most reactive cysteine towards most of the ARE activators including sulforaphane [59], 1-[2-cyano-3-,12-dioxooleana-1,9(11)-dien-28-oyl]imidazole (CDDO-Im) [59], ebselen (a seleno-organic antioxidant) [60], and neurite outgrowth-promoting prostaglandin (NEPP), which protects neurons from oxidative insults [61]. Recently, we showed that a C151W mutation to mimic electrophilic modification was sufficient for Keap1 to lose the ability to repress Nrf2 [59]. Kobayashi *et al.* [62] have categorized ARE activators into six classes using a "cysteine code", which defines the preferential target cysteine(s) and distinct biological effects. Most ARE activators belong to class 1 of the "cysteine code", where C151 is essential for activity.

Although the model of direct disruption of Nrf2-Keap1 complex by alkylation on the Keap1 had become widely accepted, evidences from two independent groups showed that the direct disruption model is invalid [47, 63]. Zhang *et al.* showed that neither sulforaphane nor quinone-induced oxidative stress results in quantitative release of Nrf2 from Keap1 as determined by immunoblot analysis following immunoprecipitation [47]. In 2005, through a combination of chemical, mass spectrometry, and isothermal titration calorimetry methods, our group found that the human Keap1 and Neh2 proteins bind with a high affinity Kd of 9 nM. Modification of human Keap1 by a variety of ARE activators including sulforaphane, isoliquiritigenin, 15-deoxy-Δ12, 14-prostaglandin-J2, and menadione, does not alter the affinity of Keap1 for the Neh2 domain protein of Nrf2, nor does it alter the binding stoichiometry [63]. These findings unambiguously indicated that C151 is extremely reactive and plays a critical role in the Nrf2-Keap1 signaling pathway, but modification of C151 by an electrophile is not sufficient to disrupt the Nrf2-Keap1 interaction.

While modification of Keap1 cysteines does not alter the affinity of Keap1 for Nrf2, several studies indicated that the Keap1-Cul3 interaction is disrupted by modification of Keap1 C151 by electrophiles, which downregulates Nrf2 ubiquitination and degradation (Figure 4C). Zhang *et al.* first demonstrated that less Cul3 precipitated with Keap1 when treated with sulforaphane or tBHQ using coimmunoprecipitation, whereas a C151S mutation largely abrogated this effect [47]. Afterwards, consensus results were obtained by two independent groups. Using coimmunoprecipitation, Gao *et al.* showed a reduced association of Cul3 with Keap1 upon modification of Keap1 cysteines by oxidized eicosapentaenoic acid (EPAox), a major component of fish oil [64].

Rachakonda *et al.* from Liebler's group observed a progressive loss of protein secondary structure of wild type Keap1 assessed by CD spectroscopy, accompanied by dissociation of the Keap1 and Cul3 complex after exposure to *N*-iodoacetyl-*N*-iotinylhexylenediamine (IAB). In contrast, a C151S mutant of Keap1 was significantly resistant to IAB-induced structural change and did not dissociate from Cul3 [65]. However, it is unknown whether modification of other Keap1 cysteines in addition to C151 is required to alter the Keap1 and Cul3 interaction.

Recently, to address this question, our collaborator Eggler *et al*., mutated Keap1 C151 to the amino acid with the largest partial molar volume, tryptophan, to mimic sterically the modification of C151 by electrophilic molecules. Remarkably, transfection with Keap1 C151W was largely unable to catalyze Nrf2 ubiquitination, resulting in a level of Nrf2 that was similar to that observed in the absence of overexpressed Keap1. Moreover, immunoblot analysis and isothermal titration calorimetry indicated that modification of Keap1 C151 to a tryptophan destabilized Keap1-Cul3 interaction but did not alter the affinity of C151W Keap1 for Nrf2. Examining a homology model of the interaction of the BTB domain of Keap1 with Cul3 (Figure 5), it appears that a bulky modification at C151 does not impose a loss of secondary structure that could disrupt Keap1-Cul3 binding. It is probable that a bulky modification at C151 alters the interaction between two helices via a steric clash of the tryptophan side chain with K131, thereby forcing the α-helix containing K131 away from position C151. The R135 residue, depending on its orientation, is also close enough to clash with the tryptophan. Movement of this helix on which two residues reside, would then affect the positioning of residues 125-127 relative to Cul3, altering Keap1-Cul3 binding. Considering that residues K131

and R135 are conserved in sequences of Keap1 proteins from divergent species, we hypothesize that modification of Keap1 C151 by an electrophile of sufficient partial molar volume alters the secondary structure of Keap1 through steric clashes, which results in an alteration of Keap1-Cul3 binding and decreasing of Nrf2 ubiquitination [59] (Figure 4D). However, 15d-PGJ_2, a reactive endogenous lipid electrophile with large partial molar volume, has recently been reported to be independent of C151 in a zebrafish model [62]. This result indicates that Keap1 differentially responds to activators of Nrf2-dependent transcription. Further investigation is required to determine how Keap1 modifications alter the Keap1-Cul3 interface and change Nrf2 ubiquitination, and what is the sensor for other C151 independent ARE activators such as 15d-PGJ_2.

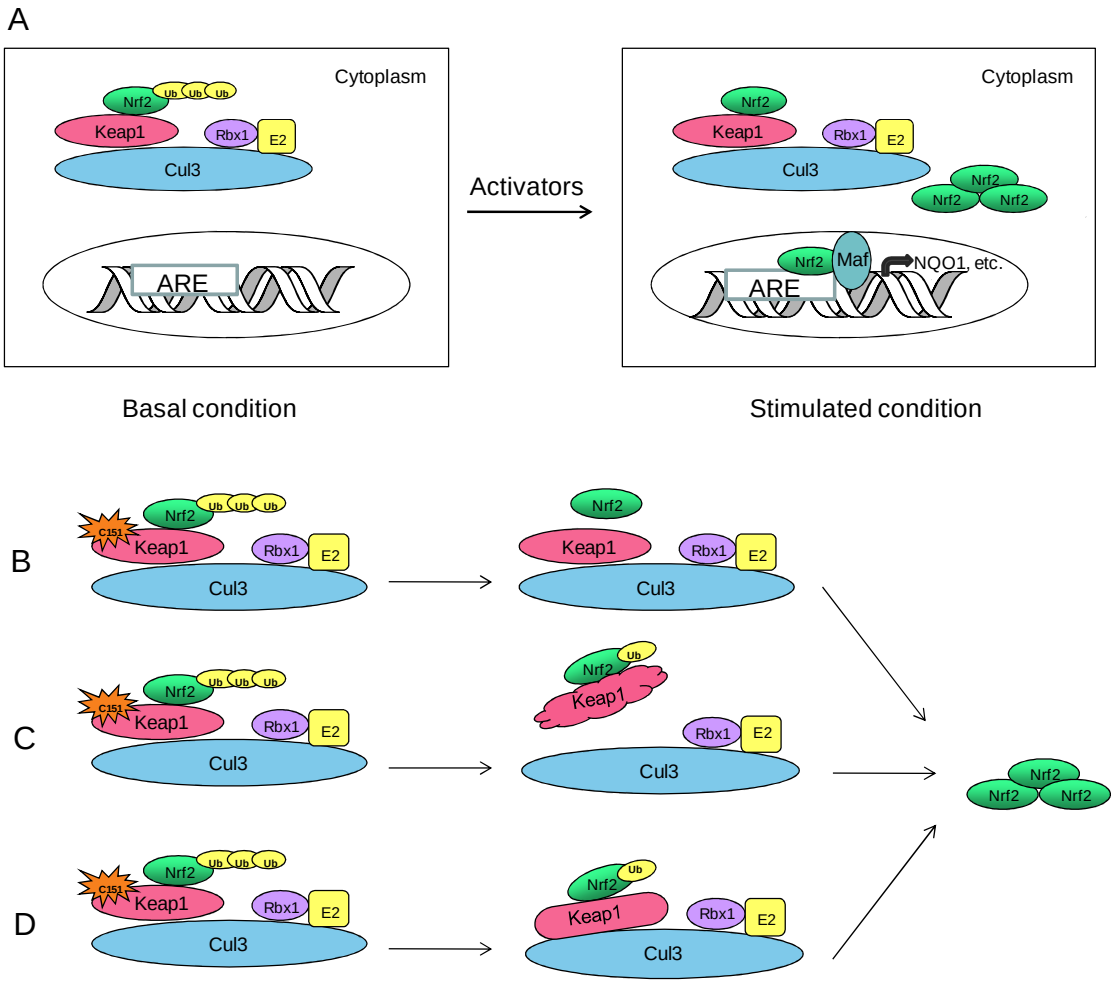

Figure 4. Schematic potential mechanisms of Nrf2-Keap1 signaling pathways leading to Nrf2 nuclear accumulation and ARE activation by chemopreventive agents. A) Nrf2 is constitutively ubiquitinated and degraded under basal condition. Nrf2 ubiquitination is inhibited upon cells exposure to ARE activators, leading to Nrf2 accumulation and cytoprotective enzyme transcription activation. B) Direct Nrf2-Keap1 disruption model. Nrf2 is released from Keap1 upon modification of Keap1 cysteines by ARE activatiors. C) Keap1 dissociates from Cul3 accompanied by loss of Keap1 secondary structure when Keap1 C151 is modified. D) Modification of Keap1 C151 alters the interaction between Keap1 and Cul3, which downregulates Nrf2 ubiquitination.

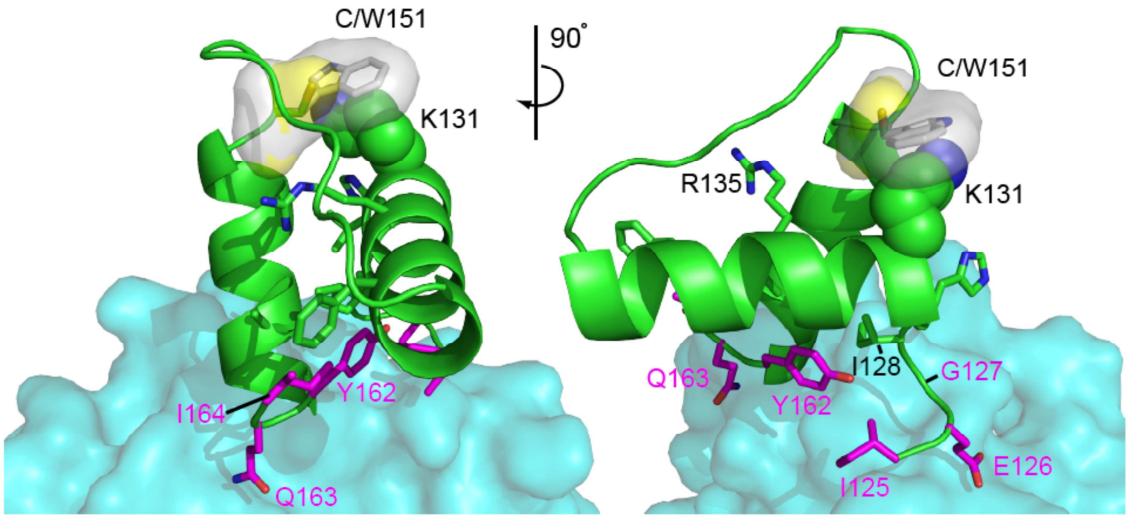

Figure 5. Hypothetical model of the putative Keap1 BTB-Cul3 interaction interface and the location of residue 151 of Keap1. A portion of the modeled TB domain of Keap1 is shown as a ribbon diagram in green, and a portion of the modeled Cul3 surface is shown in teal. Keap1 residue 151 is modeled both as a cysteine (yellow) and as a tryptophan (white). The locations of the Keap1 residues 125-127 and 162-164 in the putative Cul3 binding region are shown colored in magenta [59].

Although, significant progress has been made by a large number of studies over the past decade, there are still a lot of puzzle needed to be solved to clarify the molecular pathway. For instance, whether the screening assay that our group developed previously [66] is sensitive enough to identify the ARE activators from complex natural product extracts? Why contradictory in vitro and in vivo results were observed regarding which Keap1 cysteine residues become modified towards sulforaphane, a potent natural ARE activator? Considering the huge amount of IAB, a synthetic ARE activator Rachakonda *et al.* used in the experiment [65], whether other activators, especially a natural product will result in a similar Keap1-Cul3 dissociation or an alteration of Keap1-Cul3 interaction at a much lower concentration?

To address these questions, in this dissertation, we improved our high throughput Keap1 screening assay. We investigated whether the apparent unreactivity of C151 towards sulforaphane reported by Hong *et al.* [67] was a methodological artifact due to the reversible binding of sulforaphane to Keap1 cysteine residues. In addition, to support our recent model, we investigated the Keap1-Cul3 interaction change using two approaches using mass spectrometry: 1) the reactivity of the cysteines was used to indirectly probe Keap1-Cul3 conformational change; 2) cross-linking coupled with mass spectrometry was used to directly probe the Keap1 and Cul3 three dimensional structures, as well as their interaction interface. Finally, a titration approach was used to determine the relative reactivity of Keap1 cysteines towards 15d-PGJ_2 and PGA_2, which might imply a common sensor for C151-independent ARE activators.

1.3 Mass spectrometry-based proteomics

Mass spectrometry has emerged as an indispensable technique to understand complex systems and diseases from a molecular level to the organism level. Its excellent sensitivity and selectivity have facilitated successful applications to protein analysis including primary sequence, post-translational modifications (PTMs) and protein-protein interactions [68]. Mass spectrometric measurements are carried out in three general steps: 1) ionization of the analyte; 2) separation of the analyte in an electromagnetic field based on the mass to charge ratio (*m/z*); and 3) detection of the separated ions using a detector. In order to interpret the tremendous quantities of data that can be acquired by the mass spectrometer in an automated fashion when mass spectrometers are interfaced to chromatography systems such as HPLCs, database searching is required. Figure 6 shows the general process of a mass spectrometry-based proteomics experiment. In the context

of proteomics, the key parameters are sensitivity, resolution, mass accuracy, and the ability to generate information-rich peptide fragments. These parameters are closely associated with the ion source and the mass analyzer, as well as the database searching algorithm for post-analysis.

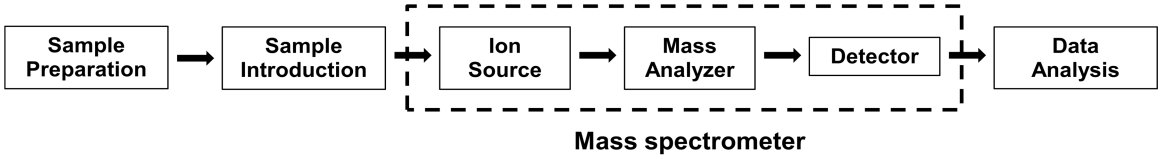

Figure 6. Schematic of a typical mass spectrometry-based proteomics experiment.

1.3.1 Ion source

Electrospray ionization and matrix-assisted laser desorption/ionization (MALDI) are the two ionization techniques most commonly used to volatize and ionize proteins and peptides during the mass spectrometry studies [69, 70]. Electrospray ionizes molecules directly from solution, either by evaporation of the solvent from charged analyte molecules or through analyte ion evaporation from droplets. Multiply charged ions are usually observed using electrospray, which facilitates the analysis of ions of several thousand Da. When sample size is small, the most sensitive form of electrospray is nanospray, which allows protein amounts in the low fmol range to be ionized and measured.

MALDI relies on the utilization of a matrix capable of absorbing strongly at the wavelength of the incident laser light. Ultraviolet and infrared lasers are used for MALDI mass spectrometry, and UV lasers predominate since they are less expensive to purchase

and maintain. Proteins or peptides in the appropriate solvent are mixed and co-crystallized with matrix. When the probe is hit by a pulsed UV laser beam, the energy is absorbed by the matrix and protons are exchanged between analytes and matrix molecules in the gas phase [70-72]. The advantage of MALDI over electrospray is that it is more tolerant of sample contaminants like buffers and salts.

1.3.2 Hybrid mass spectrometers

There are five basic types of mass analyzer commonly used in proteomics. These are ion trap, time-of-flight (TOF), quadrupole, Fourier transform ion cyclotron resonance (FT-ICR), and orbitrap. They have distinct designs and performance specifications with their own advantages and disadvantages. These mass analyzers can be used alone or put together in tandem to take advantage of complementary mass spectrometry technology. As described in the next sections, three hybrid mass spectrometers that are widely used in proteomics due to their high sensitivity, resolution, and mass accuracy were applied to Nrf2-Keap1 chemoprevention pathway studies during this dissertation.

1.3.2.1 Ion trap-time of flight mass spectrometer (IT-TOF MS)

IT-TOF mass spectrometers consist of an ion trap that is used for ion storage, selection and fragmentation, followed by a reflectron TOF analyzer for accurate mass measurement with a high mass range (Figure 7). With the combination of these two mass analyzers, high resolution (resolving power >10,000) and high mass accuracy (5 ppm) are achievable in all modes including MS, MS/MS, and MS^n. High scanning speed coupled with rapid polarity switching allows analysis of different types of ions during a single LC-MS^n analysis.

With the use of accurate mass measurement and software designed for LC-MS/MS studies of proteomics and metabolism, the IT-TOF mass spectrometer may be used to determine elemental compositions and structural analysis of peptides and proteins. For example, the Shimadzu MetID software will compare data from an unmetabolized control sample and a metabolized target sample to detect metabolites and then determine elemental compositions with great reliability due to high resolution accurate mass measurement. It should be noted that the quadrupole TOF hybrid mass spectrometer has performance specifications that are similar to the IT-TOF MS (except that only MS and MS^2 measurements are possible) and is also widely used for proteomics analyses

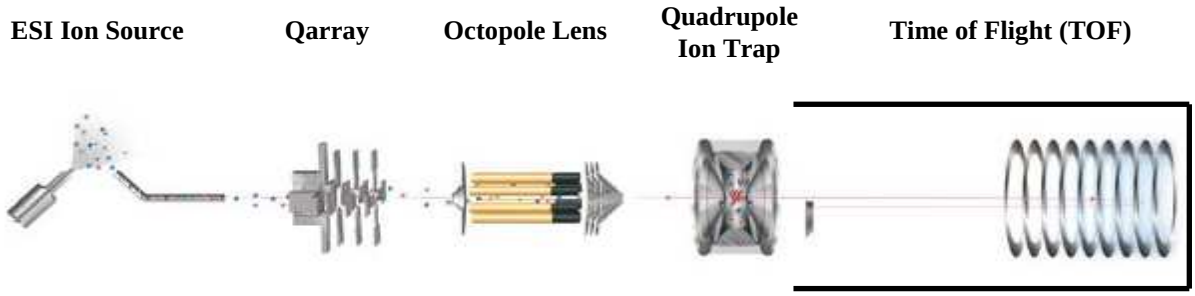

Figure 7. Schematic of an ion trap-TOF mass spectrometer (IT-TOF MS) [73].

1.3.2.2 Linear ion trap Fourier transform ion cyclotron resonance mass spectrometer (LTQ FT-ICR MS)

The Thermo hybrid LTQ FT-ICR mass spectrometer (Figure 8) is one of the highest resolving power mass spectrometers available for proteomics research. ICR mass spectrometry was first described in the late 1940s, but it was not until Marshall and Comisarow invented the FT-ICR mass spectrometer in 1974 that the technique could be

used to detect multiple ions simultaneously [74]. The LTQ FT-ICR mass spectrometer is designed with a standard linear ion trap as the first stage for ion regulation and rapid MS^n capability, combined with a Fourier transform ion cyclotron resonance mass spectrometer for ultrahigh resolving power that can exceed 600,000. Ions are accumulated in the linear ion trap before being transferred to the ICR cell for high mass accuracy (<1 ppm) measurements. Precursor ions can be selected using the ion trap, fragmented using collision-induced dissociation, and then transferred to the ICR for mass measurement at high resolving power using a fast Fourier transformation, peak detection, and mass calculation. During the time in which the FT-ICR is acquiring a high resolution spectrum, the LTQ is able to perform fragmentation and acquire MS/MS data for the next measurement.

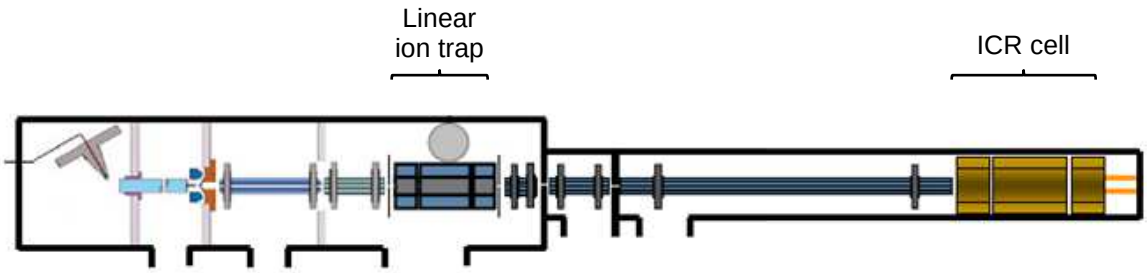

Figure 8. Schematic of a linear ion trap Fourier transform ion cyclotron resonance mass spectrometer (LTQ FT-ICR MS) [75].

The LTQ FT-ICR mass spectrometer routinely operates in parallel detection mode, which provides both MS and MS/MS data during sample analysis. This information allows a higher confidence level for peptide and protein sequence assignments for complex proteomics work.

With the high sensitivity, high mass resolution and high mass accuracy, LTQ FT-ICR mass spectrometry is ideal for analysis of proteolytic peptides (bottom-up approach to proteomics) and for analysis of intact proteins (top-down proteomics) [76, 77].

1.3.2.3 Linear ion trap orbitrap mass spectrometer

The LTQ orbitrap mass spectrometer such as the Thermo LTQ Orbitrap Velos (Figure 9) is becoming a popular technological platform for proteomics research because it combines the sensitivity, speed, and robustness of linear ion trap with the high resolution capabilities of the orbitrap analyzer developed by Makarov [78]. During operation, ions are accumulated in the linear ion trap and transferred into a radio frequency-only quadrupole called a C-trap due to its letter 'C' shape. This additional storage improves the analytical capabilities of the instrument because structurally informative fragmentation may be carried out at higher energy than is possible in the ion trap. Subsequently, the ions accumulated in the C-trap are transferred to the orbitrap by a pulse [78]. The orbitrap functions like a high (60,000) resolving power ion trap. Similar to LTQ FT-ICR mass spectrometry, a typical operational setup in LTQ Orbitrap mass spectrometer is that both mass analyzers work in parallel. While a high resolution accurate mass spectrum is acquired in the orbitrap, the fast linear ion trap carries out fragmentation and may be used to acquire MS/MS spectra of selected peptides. Depending on the requirement of the experiments, the linear ion trap can send precursors or MS^n product ions to the orbitrap for accurate mass measurements. Precursor ions can also be sent to the C-trap for fragmentation at higher energy before being measured in the orbitrap.

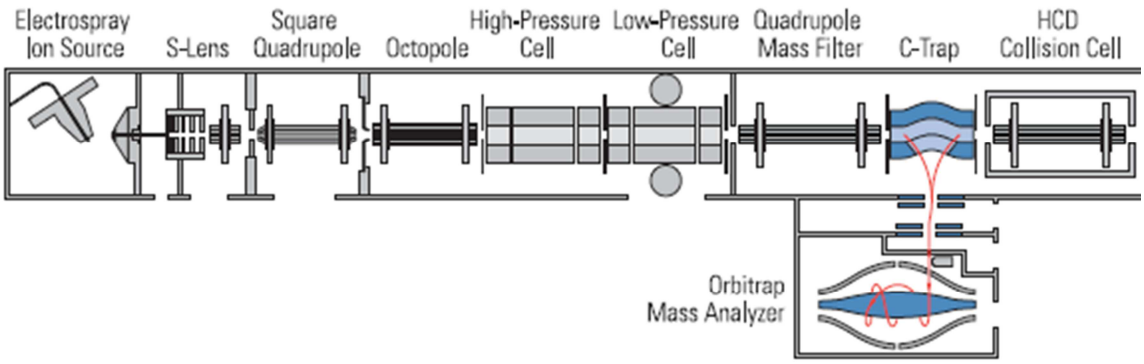

Figure 9. Schematic of linear ion trap orbitrap mass spectrometer (LTQ Orbitrap Velos) [79].

The 2nd generation Thermo LTQ Orbitrap system termed Velos that was used in this investigation provided significantly improved sensitivity and higher scan speeds compared with the 1st generation LTQ Orbitrap and LTQ FT-ICR mass spectrometers. These improvements enabled more proteome coverage during peptide mapping. In addition, the combo C-trap and higher-energy collisional dissociation (HCD) cell with an applied axial field improved fragment ion extraction, trapping capabilities and enhanced sequence ion formation [79].

1.3.3 Data analysis

Database searching is an essential element of proteomics that facilitates peptide and protein identification based on tandem mass spectra at minimal computational expense [80]. The principle of this approach is to correlate the tandem mass spectra in the data set with the theoretical spectra created from the sequence database via protease digestion in an automated fashion. The scores returned from the search reflect the probability that a match is a random occurrence. Various probability-based post-search

algorithms have been developed to analyze proteomic data sets automatically. The key difference among these algorithms lies in how each approach scores a potential match between experimental and theoretical spectra. They rely on four basic approaches of score models: descriptive, interpretative, stochastic, and statistical/probabilistic models [80, 81].

1.3.3.1 SEQUEST

SEQUEST is the first software designed to automate protein identification, and was developed by Eng *et al.* [82]. It is still one of the most commonly used database searching programs that use a descriptive score model. The algorithm of SEQUEST is illustrated in Figure 10A. The strategy begins with reducing background noise by performing an initial reduction of the MS/ms data. All but the 200 most abundant fragment ions are removed. Amino acid sequences are then identified in a protein database by matching the molecular mass of the peptide to a sequence within the defined mass tolerance. The preliminary scores Sp are assigned to these candidates by evaluating the number and quality of the fragment ions matching the predicted ones derived from the database. With a generated ranking list, the top 500 best fit sequences are then subjected to a correlation-based analysis to generate a final score and ranking of the sequences [82].

Two parameters X_{corr} and ΔC_n from the cross-correlation analysis have shown a trend that is useful for distinguishing correct identifications from false positives. X_{corr} value is an absolute measure of spectral quality and closeness of fit to the predicted spectrum in the search. ΔC_n is the difference between the normalized correlation score of the first- and second-ranked sequences in the search results. It is useful to determine the uniqueness of the match. X_{corr} is independent of the database size and reflects the quality

of the match between spectrum and sequence; whereas ΔC_n is database size dependent and reflects the quality of the match relative to near misses [80, 83]. A general rule is that an X_{corr} value greater than 2.0, 2.2 and 3.75 for 1+, 2+ and 3+ charge-state peptides, respectively, and a ΔC_n value over 0.1 indicate a good correlation [84].

1.3.3.2 MassMatrix

MassMatrix is a newly developed database search software package [85] for characterization of peptides, proteins and their posttranslational modifications from MS/MS data (Figure 10B). This probability-based algorithm incorporates mass accuracy into scoring the potential peptide and protein matches. It uses two independent scoring models, a descriptive model and a mass accuracy sensitive statistical model, to calculate three distinct scores for a peptide match. The two statistical scores, pp and pp2 are calculated as the negative logarithm of the probability that a peptide match is a random occurrence. The pp score is based on the number of matched product ions, and the pp2 score is based on the total abundance of matched product ions in the experimental spectrum. The pp_{tag} score is a statistical score based on a Monte Carlo simulation, and it is a standard to discriminate true matches from false ones. Each of the scores can be used to ascertain the quality of the match independently. The combination of the scores reflects the significance of protein matches and can be used to differentiate true protein matches from random ones [86, 87].

Traditionally used database search programs such as SEQUEST, Mascot, OMSSA, and X!Tandem are not applicable to cross-linking analysis. Due to the exponentially increased search space by cross-links, false positives need to be controlled by validated scoring algorithms and by decoy search strategy [88, 89]. MassMatrix has an

option to perform analysis of tandem MS data from cross-linked peptides. It is an extension of a validated database search engine with three probability-based scoring algorithms, and cross-links can be identified along with other fixed and/or variable modifications in tandem MS data [87, 90].

The three independent statistical scores, pp, pp_2, and pp_{tag} from the scoring models are mainly used to evaluate the quality of peptide-spectrum matches for both cross-linked and non-cross-linked peptides. A posthoc analysis program XMapper is used to calculate the overall score for cross-link assignments using the following equation and to generate a heat map figure for each match [90].

$$\text{Cross-link score} = \sum_{p=1}^{N}\left[\left(\frac{1}{2}max_{m=1}^{p_n} pp_m + \frac{1}{2}max_{m=1}^{p_n} pp_{2_m} + max_{m=1}^{n_p} pp_{tag_m}\right) \times log_3(n_p + 2)\right]$$

N: the number of peptides assigned to the cross-link

n_p: the number of spectral matches for peptide p with the cross-link

pp, pp_2, and pp_{tag}: the statistical scores for a spectral match

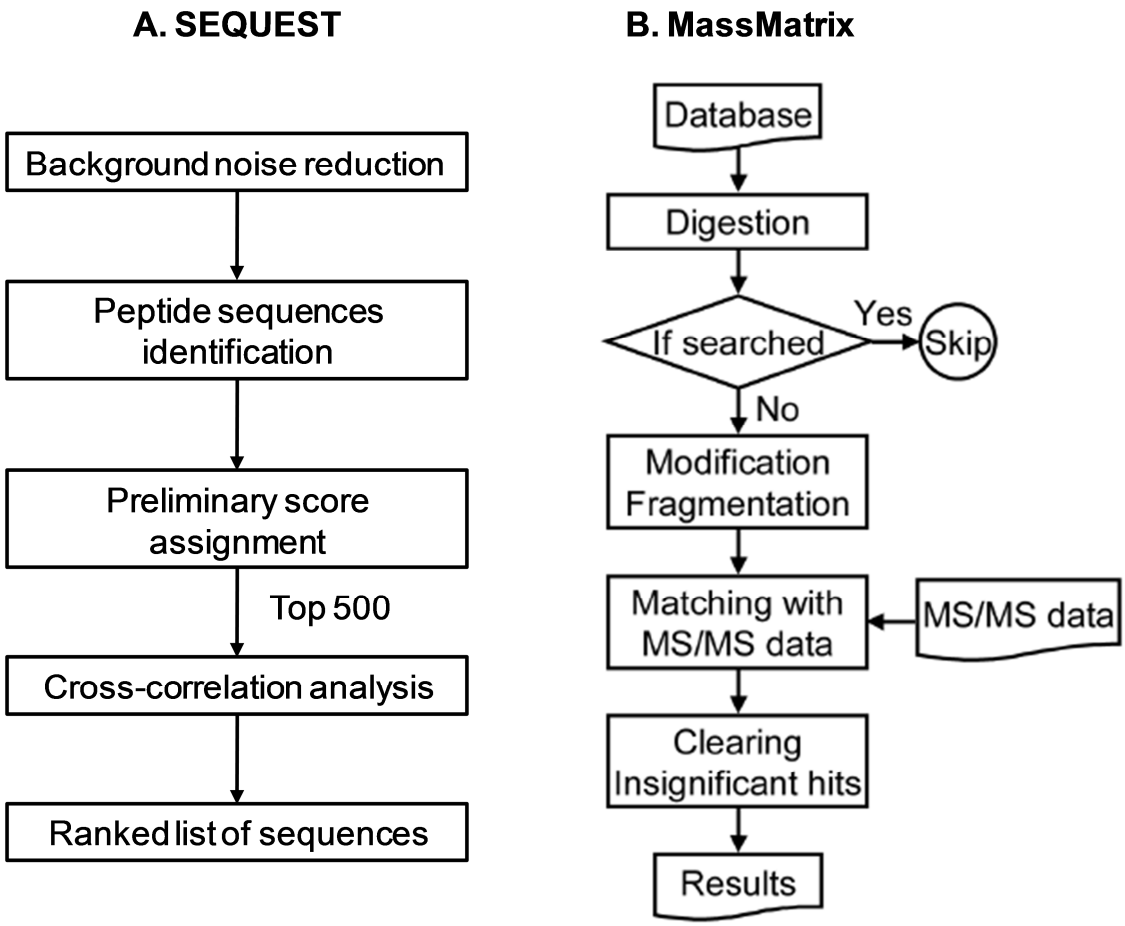

Figure 10. Data analysis flow diagrams for proteomics protein identification software A) SEQUEST and B) MassMatrix.

2 SCREENING FOR NATURAL CHEMOPREVENTION AGENTS THAT MODIFY HUMAN KEAP1

2.1 Introduction

Modification of the sensor protein Keap1 by electrophiles plays a critical role in directing Nrf2 accumulation in the nucleus and subsequent ARE activation [45, 59, 62]. Many ARE activators have been identified, some of which are abundant in edible plants including sulforaphane in broccoli sprouts [91], xanthohumol in hops [92], isoliquiritigenin in licorice [93], and quercetin in green and black tea [94]. Although there is no common structure among these activators, Talalay and coworkers [35, 51, 52] have categorized them into 10 distinct classes and found that most are electrophiles with reactivity toward sulfhydryl groups. Because of the significant role of Keap1 in chemoprevention, there is keen interest in discovering new compounds that modify this protein and ultimately activate the ARE.

Previously, we reported a screening method to discover natural products, either individual compounds or constituents of complex mixtures, that covalently modify Keap1 [66]. This assay begins with MALDI-TOF MS measurement to determine whether any of the test compounds covalently bind to Keap1 and increase its mass. If the active compound is a constituent of a complex mixture such as a botanical extract, the mixture is incubated with glutathione (GSH), and precursor ion tandem mass spectrometry is used to detect GSH conjugates followed by product ion tandem mass spectrometry to obtain structural information. However, some ARE activators such as sulforaphane are not detected using this method. Although incubation of Keap1 with sulforaphane at a molar ratio of 1:15 resulted in an average of 9 molecules of sulforaphane attached per molecule

of Keap1 (based on absorbance spectrophotometry) [63], MALDI-TOF MS did not detect any modification of Keap1. The most probable explanation for this observation is that sulforaphane dissociated from Keap1 during MALDI.

Therefore, a new mass spectrometry-based screening method was developed as part of this dissertation to enable the detection of compounds that reversibly modify Keap1 like sulforaphane. This new method is based on reaction of electrophiles with Keap1 followed by exchange with β-mercaptoethanol (BME) and then analysis using high resolution accurate mass measurement. This approach was inspired by Freeman and coworkers [95], who used a similar method for detection and quantification of reversibly adducted electrophiles in plasma, organelles, cells and tissue homogenates [95].This strategy is effective for the detection and identification of compounds that form reversible adducts with Keap1 including those that cannot be detected using MALDI-TOF MS.

2.2 Experimental section

2.2.1 Protein preparation and material

Recombinant human Keap1 protein was expressed and purified as described previously [63]. The protein (100 μM) was stored in 50 mM Tris-HCl buffer (pH 8.0), 2 mM Tris[2-carboxyethyl]phosphine hydrochloride (TCEP) (Thermo Fisher Scientific; Rockford, IL), 250 mM sodium chloride and 20% glycerol (v/v). Isoliquiritigenin, naringenin, Tris-HCl, sodium chloride, glycerol, formic acid, dimethyl sulfoxide and β-mercaptoethanol (BME) were purchased from Sigma-Aldrich (St. Louis, MO). Sulforaphane was purchased from ICN Biomedicals (Costa Mesa, CA), and micro Bio-Spin 6 columns were purchased from Bio-Rad (Hercules, CA). Deionized water was

prepared using a Milli-Q purification system (Millipore, Bedford, MA). Methanol (HPLC grade) was purchased from Thermo Fisher (Hanover Park, IL), Cocoa nibs were provided by Hershey Foods (Hershey, PA).

2.2.2 Modification of Keap1 and BME exchange

A 10 mM stock solution of isoliquiritigenin was prepared in dimethyl sulfoxide (DMSO). Keap1 (10 µM) was incubated with isoliquiritigenin at molar ratios from 1:0.5 to 1:5 (Keap1/isoliquiritigenin) in 100 µL 20 mM Tris-HCl buffer (pH 8.0). The reaction was carried out at room temperature for 2 h. In control experiments, 20 mM Tris-HCl buffer (pH 8.0) was substituted for human Keap1. Modified Keap1 was separated from free isoliquiritigenin using a micro Bio-Spin 6 size exclusion column. The fraction containing modified Keap1 was incubated for 1 h with 0.2 M BME at room temperature to trap isoliquiritigenin as it dissociated from Keap1. The incubation mixture was evaporated to dryness and reconstituted in 10% aqueous methanol containing 250 nM naringenin as an internal standard prior to analysis using LC-MS-MS with selected reaction monitoring.

To evaluate the selectivity of the screening assay, a methanolic extract of cocoa nibs was prepared as described previously [96]. The extract (10 mg/mL) was spiked with sulforaphane (20 µM final concentration) and incubated with Keap1 (10 µM) or 100 µL Tris-HCl buffer (pH 8.0) for 2 h. Size exclusion chromatography and exchange with BME was carried out as described for isoliquiritigenin. Since it was unknown if the cocoa extract contained compounds in addition to sulforaphane that could reversibly modify Keap1, a Shimadzu high resolution LC-IT-TOF mass spectrometer was used to screen for

all possible BME adducts. Positive and negative ion electrospray mass spectra were acquired over the mass range of *m/z* 100-800.

LC-MS chromatograms of the experiment (with Keap1) and control (without Keap1) were compared using Shimadzu MetID Solution software to identify peaks corresponding to BME adducts. Peaks enhanced in the chromatogram of the Keap1 incubation but not in the control incubation were expected to be BME adducts. Identification of BME adducts was carried out using LC-MS/MS product ion analysis with accurate mass measurement and comparison with standards. A sulforaphane-BME standard was prepared by incubating sulforaphane and BME at a ratio of 1:10 (sulforaphane/BME).

2.2.3 MALDI-TOF mass spectrometry

Positive ion MALDI-TOF mass spectra of intact Keap1 were acquired using an Applied Biosystems (Foster, CA) Voyager DEPRO mass spectrometer. A 1 μL aliquot of the Keap1 solution was mixed with 1 μL matrix solution which contained sinapinic acid (10 mg/mL) in acetonitrile/water (1:1, v/v) acidified with 0.1% (v/v) trifluoroacetic acid. A 1 μL aliquot of the mixture was then spotted on the MALDI-TOF sample stage and air dried before analysis. For each sample, 300 laser shots were acquired in linear mode and signal averaged over the range *m/z* 65,000-80,000.

2.2.4 LC-MS-MS analysis of BME-adducted isoliquiritigenin

Levels of isoliquiritigenin and isoliquiritigenin-BME were analyzed using negative ion electrospray on a Thermo (San Jose, CA) Surveyor HPLC system interfaced

to a Thermo TSQ Quantum triple quadrupole mass spectrometer. Isoliquiritigenin and its BME adduct were separated using a YMC C_{18} reverse phase column (2.0 mm × 50 mm, 5 µm, 120Å) using a 6 min linear gradient from 10% to 100% methanol with a counter solvent of 0.1 % formic acid in water at a flow rate of 0.2 mL/min. Argon was used as the collision gas for collision-induced dissociation at 23 eV for isoliquiritigenin, 20 eV for its BME adduct, and 21 eV for naringenin (internal standard). Selected reaction monitoring (SRM) was used to monitor the transition from the deprotonated molecule of each analyte to its most abundant product ion. Specifically, isoliquiritigenin and naringenin were measured using the SRM transitions of *m/z* 255 to *m/z* 119 and *m/z* 271 to *m/z* 150.5, respectively. The SRM transition of *m/z* 333 to *m/z* 255, corresponding to elimination of BME from the deprotonated molecule, was used to measure BME-isoliquiritigenin. Product ion tandem mass spectra of isoliquiritigenin and sulforaphane and their BME adducts are shown in Figure 11. These tandem mass spectra were used for the selection of product ions for SRM and for confirmation of chemical structures.

2.2.5 LC-IT-TOF MS analysis of BME-adducted sulforaphane in cocoa nibs crude extract

After incubation of the modified Keap1 and control with BME, samples were analyzed using a high mass accuracy Shimadzu (Kyoto, Japan) IT-TOF hybrid mass spectrometer. The same HPLC separation conditions were used as for isoliquiritigenin, except that a 15-min linear gradient was used from 10% to 100% methanol using a Shimadzu Prominence HPLC system. Positive and negative ion electrospray mass spectra were acquired using polarity switching over the mass range of *m/z* 100-800.

2.2.6 Data processing using Shimadzu MetID Solution software

The LC-MS chromatograms of both experiment and control were processed using Shimadzu MetID Solution software to identify peaks corresponding to adducts with BME. Background subtraction was allowed, and peak integration was performed on the peaks with at least 10 sec width and 500/min slope. Ion retention time within 0.1 min, and peak area difference within 50% between experiment and control were set to be determined as the same peak. New or enhanced peaks due to Keap1 modification in the experiment data file compared with control were identified based on automated data processing and confirmation by manual inspection. The elemental compositions of BME-adducts (within 5 ppm) were determined using a formula predictor based on high resolution accurate mass measurements.

2.3 Results and discussion

2.3.1 Comparison of the new screening method with our previously developed MALDI-TOF MS-based assay

2.3.2 LC- MS-MS analysis of BME-adducted isoliquiritigenin

Isoliquiritigenin (2,4,4'-trihydroxychalcone) (Figure 11A) is an example of a chemoprevention agent containing a Michael acceptor which is common to many ARE activators [97]. The α,β-unsaturated carbonyl group inisoliquiritigenin has been shown to modify specific cysteine residues of Keap1 in vitro [57]. Since Michael addition reactions are reversible (see also section 3.3.2), the equilibrium of their reaction with Keap1 cysteines can be shifted by addition of another thiol nucleophile at a high concentration to

form a new thioether adduct with isoliquiritigenin [95]. Although several thiol-based nucleophiles should be suitable such as BME, dithiothreitol (DTT) and TCEP, BME was selected for this study due to its small size and therefore minimal steric hindrance during reaction with electrophiles like isoliquiritigenin.

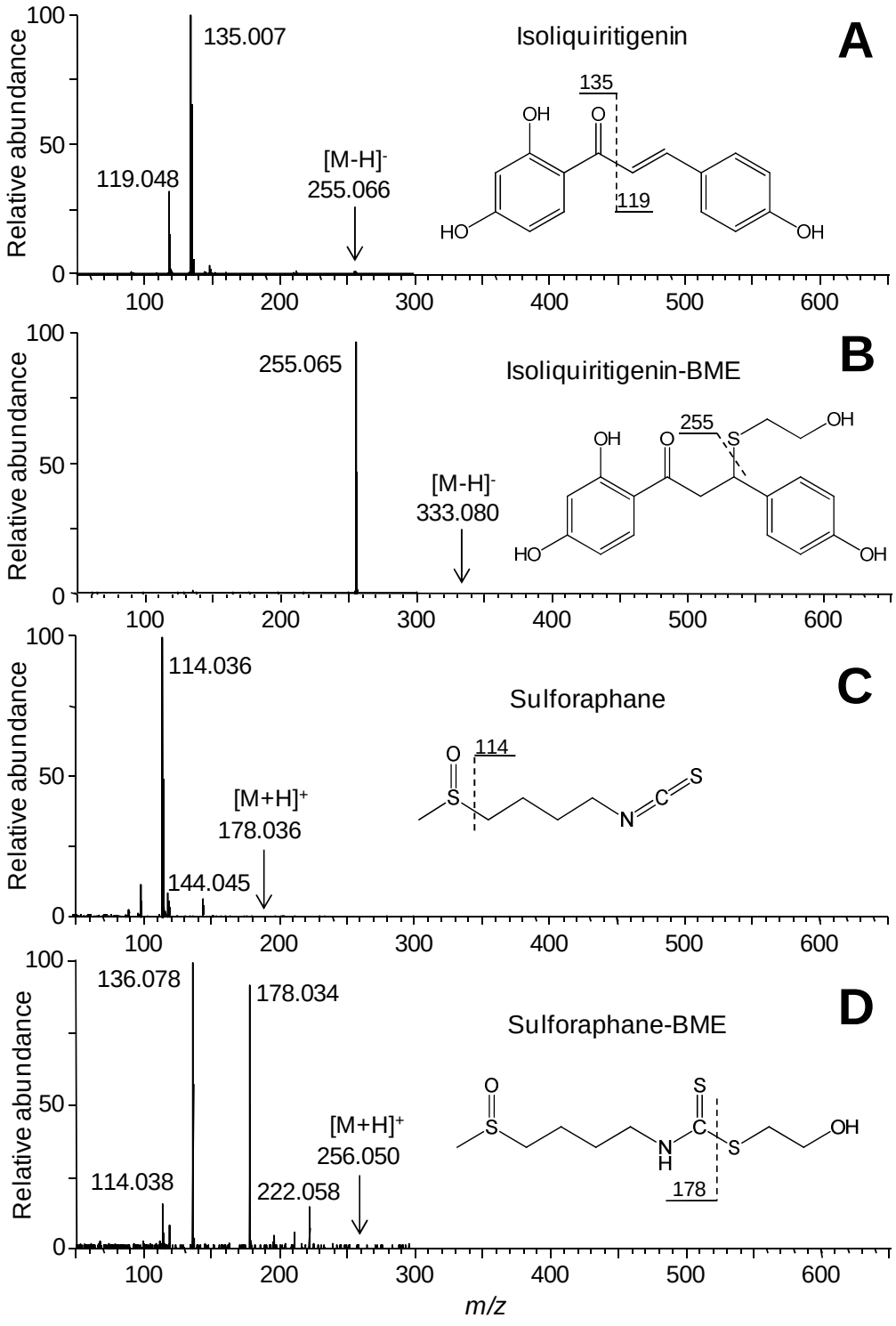

Figure 11. Chemical structures and electrospray product ion tandem mass spectra of the natural chemoprevention agents used in this study and their corresponding adducts with BME. A) isoliquiritigenin; B) isoliquiritigenin-BME adducts; C) sulforaphane; and D) sulforaphane-BME adduct.

The first step was to establish the feasibility of using BME to trap reversibly-bound electrophiles as they dissociated from Keap1 and to detect these electrophile-BME adducts by using LC-MS-MS. Keap1 was incubated with isoliquiritigenin, passed over a size exclusion column to remove free isoliquiritigenin, and the recovered covalently modified protein was treated with BME. Levels of isoliquiritigenin and isoliquiritigenin-BME were monitored by LC-MS-MS. Initially, LC-MS-MS with constant neutral loss scanning of the neutral molecule BME from the deprotonated molecules was used as a general approach to detect thioether adducts of BME [98]. Since constant neutral loss scanning was not sensitive enough for measuring low levels of isoliquiritigenin-BME (data not shown), this approach was not pursued. Instead, LC-MS-MS with collision-induced dissociation and SRM was used to measure isoliquiritigenin-BME to establish feasibility.

An isoliquiritigenin-BME adduct was detected after Keap1 was incubated with isoliquiritigenin followed by BME (Figure 12). As expected, no isoliquiritigenin or its BME adduct were detected in control incubations from which Keap1 had been omitted. This indicates that the isoliquiritigenin-BME adduct detected using LC-MS-MS (Figure 12B) was formed by reaction of BME with isoliquiritigenin that had been released from Keap1. These results establish a proof-of-concept that BME may be used to capture electrophiles released from Keap1. There was no free isoliquiritigenin carried over from the Keap1 (or buffer control) incubation during gel filtration. In addition, the amount of BME-isoliquiritigenin adduct increased in proportion to increasing molar ratios of [isoliquiritigenin]/[Keap1] (Figure 13B). This is consistent with past observations that the

number of Keap1 cysteines modified by isoliquiritigenin is related to the concentration of isoliquiritigenin in the incubation [57].

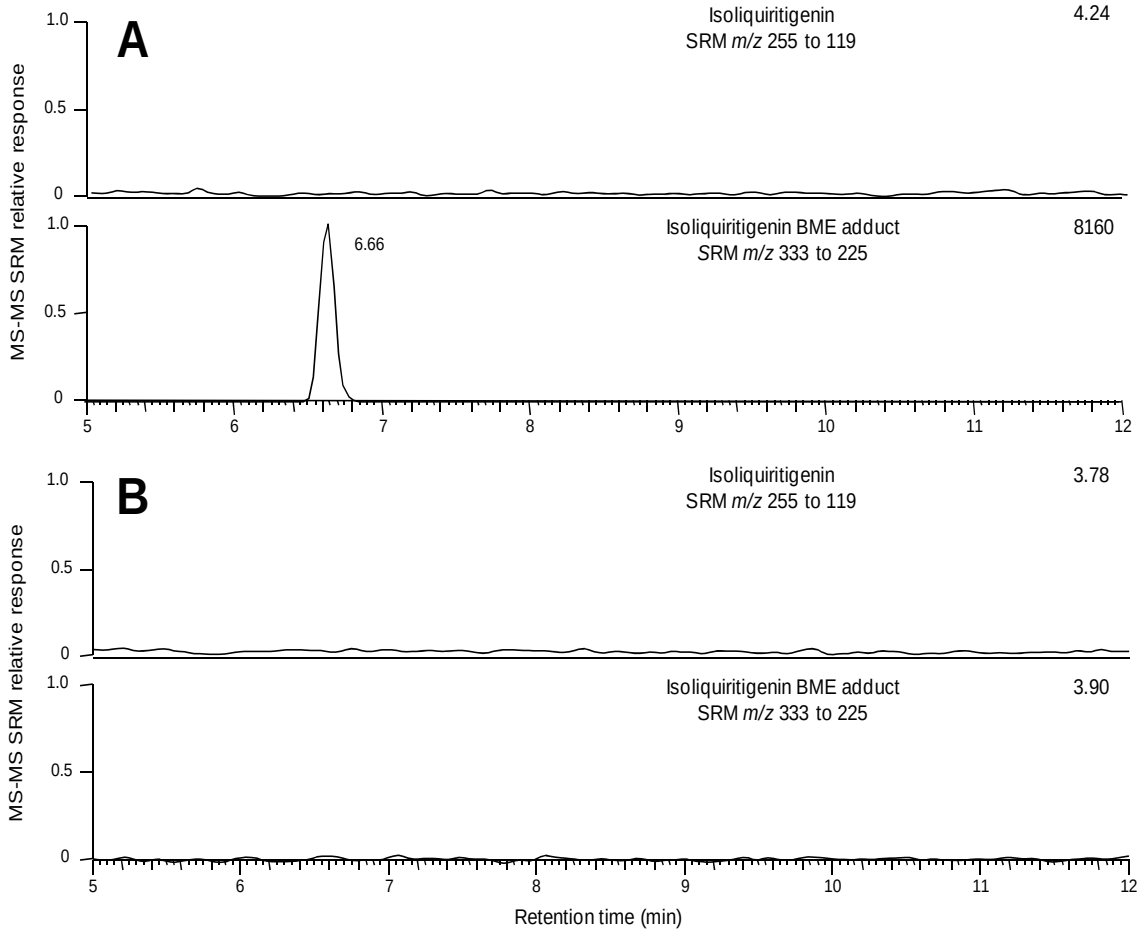

Figure 12. Computer-reconstructed mass chromatograms for negative ion electrospray LC-MS-MS analysis of isoliquiritigenin-BME adducts formed from isoliquiritigenin that had modified Keap1 and was then exchanged by incubation with BME. Selected reaction monitoring (SRM) of *m/z* 255 to *m/z* 119 was used to monitor isoliquiritigenin, and SRM of *m/z* 333 to *m/z* 225 was used to monitor isoliquiritigenin-BME. A) Isoliquiritigenin was incubated with Keap1 at a 2:1 molar ratio followed by gel filtration and BME exchange. B) Control incubation using Tris-HCl buffer but no Keap1. The relative MS-MS SRM responses are shown on the y-axis (normalized to the peak at 6.66 min in part A, and the absolute MS-MS responses (in arbitrary units) are shown in the upper right of each chromatogram.

2.3.2.1 MALDI-TOF mass spectrometry of Keap1-isoliquiritigenin adducts

Our previous MALDI-TOF MS-based assay is most effective for the detection of compounds that cause a mass shift in a significant number of Keap1 molecules. For example, MALDI-TOF MS-based screening can detect a mass shift of Keap1 due to reaction with isoliquiritigenin, but at least a 20-fold excess of isoliquiritigenin over Keap1 is required so that at least three molecules isoliquiritigenin become bound to Keap1 (Figure 13A). The 858 Da increase in the mass of Keap1 indicated that an average of 3.3 isoliquiritigenin molecules were covalently attached to each molecule of Keap1. Using the new approach of gel filtration followed by LC-MS-MS, isoliquiritigenin modification of Keap1 was detected sensitively and quantitatively at a molar ratio of 1:1. As long as a compound modifies Keap1 and can be trapped by BME, it can be detected by LC-MS-MS. This new approach, which is more sensitive and more quantitative than the previous MALDI TOF MS-based assay, is limited only by the detection limit of the LC-MS-MS system. In this application, the BME exchange method was approximately 20-fold more sensitive than the MALDI TOF-MS screening method.

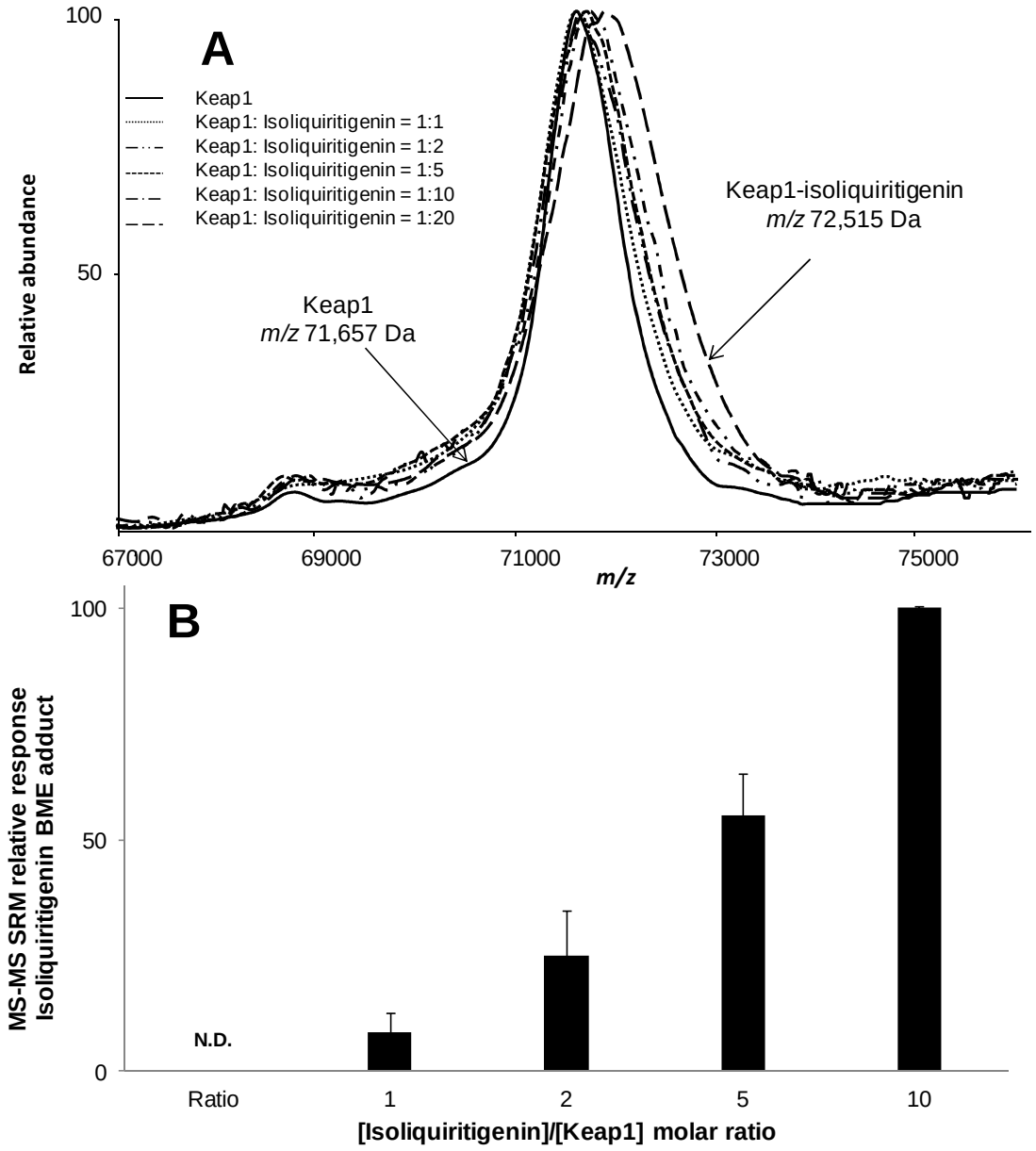

Figure 13. Detection of Keap1 modification by isoliquiritigenin. A) Positive ion MALDI TOF mass spectra of Keap1 after incubation with isoliquiritigenin at molar ratios of 1:1, 1:2, 1:5, 1:10, and 1:20 [Keap1/isoliquiritigenin] or with Tris-HCl buffer as control (solide line). The mass of Keap1 increased due to covalent attachment of isoliquiritigenin molecules to Keap1 cysteine sulfhydryl groups. B) Negative ion electrospray LC-MS-MS with SRM of isoliquiritigenin-BME adducts. The concentration of isoliquiritigenin-BME adducts increased in proportion to the molar ratio of isoliquiritigenin/Keap1. No isoliquiritigenin-BME adduct was detected in the control experiment that contained no Keap1 (N.D. = none detected).

2.3.3 Screening of complex mixtures for Keap1 modifiers using BME and LC-MS

To investigate the potential of the new Keap1/BME assay for screening mixtures such as botanical extracts for compounds that react to form covalent adducts with Keap1, sulforaphane (R-1-isothiocyanato-4-methylsulfinylbutane) (Figure 11A) was selected as a model compound, and a cocoa extract was used as a test matrix. Sulforaphane is a potent ARE activator from cruciferous vegetables [99] that is being evaluated for safety and efficacy in clinical trials [100-102]. Since modification of Keap1 cysteines by sulforaphane could not be detected in our previous MALDI-TOF MS assay, the utility of the new approach using BME trapping and LC-MS analysis was investigated by testing a cocoa extract spiked with sulforaphane (0.2% of total weight).

Instead of using LC-MS-MS with SRM transitions for detection of isoliquiritigenin-BME, LC-MS with a high resolution IT-TOF mass spectrometer was used in developing the general screening procedure. Unlike scanning instruments like quadrupole mass spectrometers that typically record up to a few mass spectra per second, the TOF analyzer can record thousands of mass spectra per second. Therefore, TOF-based mass spectrometers can be used to obtain high quality LC-MS chromatograms while recording entire mass spectra. Comparing experiment and control LC-MS data containing thousands of mass spectra to find BME adducts in incubations with Keap1 can be labor intensive if each pair of chromatograms is searched manually, one *m/z* value at a time. Therefore, this task was automated using software originally designed to find drug metabolites (Shimadzu Met-ID Solution software). The software automatically searched all possible computer-reconstructed mass chromatograms to find peaks enhanced in the experiment compared with the control.

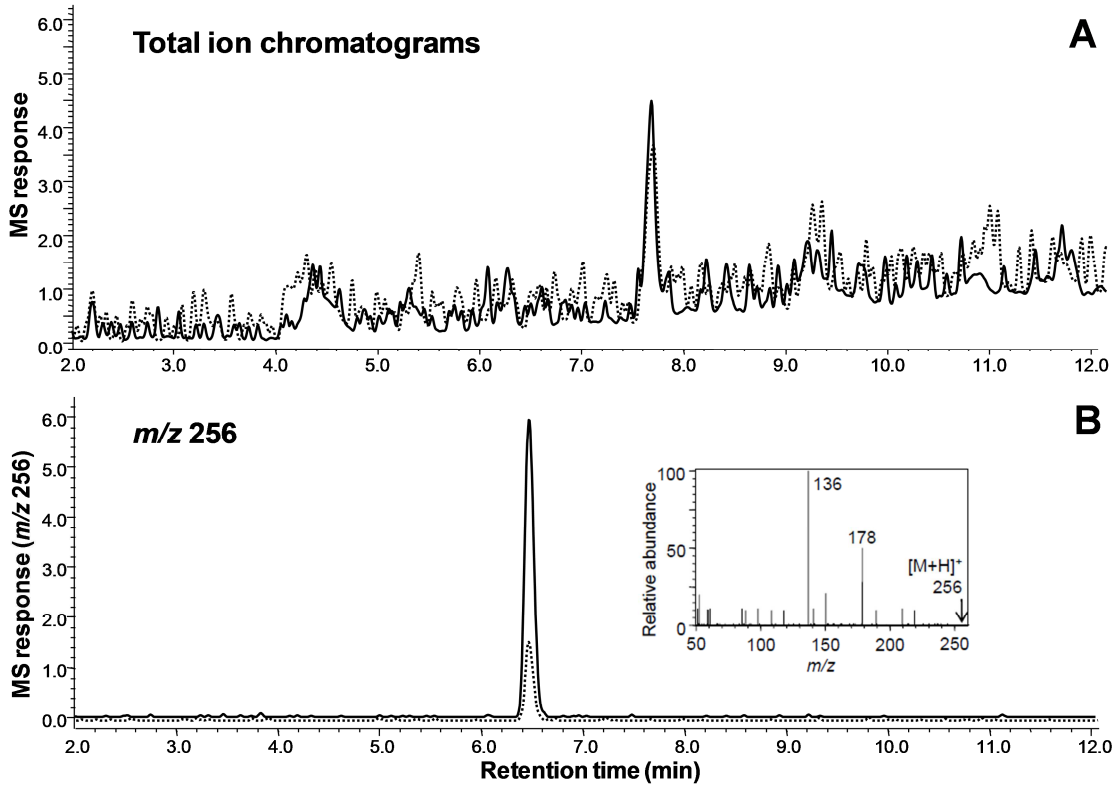

Figure 14. Electrospray LC-IT-TOF MS analysis of a cocoa nibs methanolic extract spiked with sulforaphane (0.2% by weight) and incubated with Keap1 (solid line) or buffer (dashed line), followed by gel filtration to isolate the protein and then treatment with BME to trap reversibly bound electrophiles such as sulforaphane. A) Total ion chromatograms of experiment (solid line) and control (dashed line). B) Computer-reconstructed mass chromatograms showing the detection of a sulforaphane-BME adduct of *m/z* 256 eluting at 6.5 min that was enhanced in the experiment (solid line) compared with the control (dashed line). The positive ion tandem mass spectrum shown in the insert identifies this peak as sulforaphane-BME (see standard in Figure 11).

Positive ion electrospray and negative ion electrospray LC-MS data files of the incubations of the cocoa extract containing sulforaphane with Keap1 and without Keap1 were compared, and peaks that were enhanced in one chromatogram relative to the other were identified. Only one enhanced peak was detected in the cocoa/sulforaphane experiment during positive ion electrospray LC-MS. The peak was observed at a retention time of 6.5 min and was enhanced 4-fold in the experiment relative to the

control (Figure 14). Accurate mass measurement indicated that this peak corresponded to a protonated molecule of *m/z* 256.0498. There are four formulae within 5 ppm of this measured mass (TABLE I), and the elemental composition of $C_8H_{17}NO_2S_3$ (ΔM 1.56 ppm) is the only formula that contains at least one sulfur, one oxygen and at least two carbon atoms contributed by the BME moiety. Therefore, this formula probably corresponded to an adduct between BME and sulforaphane (Figure 11D). Observation of a fragment ion of *m/z* 178 corresponding to loss of BME and a base peak of *m/z* 136 during positive ion electrospray tandem mass spectrometry (Figure 14B, insert) were also consistent with a BME adduct. Finally, the adduct was identified as sulforaphane-BME by comparing the retention time and fragmentation patterns with an authentic standard (Figure 11).

TABLE I

ELEMENTAL COMPOSITIONS WITHIN 5 PPM OF THE MEASURED MASS OF M/Z 256.0498 FOR THE PEAK ELUTING AT 6.5 MIN IN THE KEAP1/BME LC-MS SCREENING EXPERIMENT SHOWN IN FIGURE 14

Rank	Score	Formula	Ion	Meas. *m/z*	Pred. *m/z*	Diff (ppm)	Iso Score	DBE
1	61.45	$C_8H_9N_5O_3S$	$[M+H]^+$	256.0498	256.0499	-0.39	61.45	7.0
2	61.19	$CH_9N_{11}OS_2$	$[M+H]^+$	256.0498	256.0506	-3.12	64.61	3.0
3	50.86	$C_8H_{17}NO_2S_3$	$[M+H]^+$	256.0498	256.0494	1.56	51.58	1.0
4	44.78	$C_{16}H_5N_3O$	$[M+H]^+$	256.0498	256.0505	-2.73	46.81	16.0

Since the Keap1 modification experiment shown in Figure 14 used cocoa spiked with sulforaphane, detection and identification of the final sulforphane-BME adduct was a simple process. In case an unknown adduct is detected as an enhanced peak in the experiment compared with the control by automatic software analysis, a dereplication

strategy would be used. Positive and negative ion MS^2 and MS^3 analyses would be used to provide structural information regarding the elctrophilic molecule that had reacted with BME and Keap1. The elemental composition, retention time and fragmentation patterns would be compared with standards prepared by reaction of BME with known constituents of the sample or literature values for these compounds obtained using natural products databases such as the NAPRALERT database [103].

This new assay is designed to detect electrophiles that reversibly bind to Keap1 such as the natural products sulforaphane and isoliquiritigenin but is not appropriate for compounds that form irreversible adducts with Keap1 such as the synthetic electrophile *N*-iodoacetyl-*N*-biotinylhexylenediamine (IAB). However, reversible Keap1 modifiers might be superior chemotherapeutic agents, since they tend to display less cytotoxicity than irreversible modifiers, which might also irreversibly bind to DNA and other important biological molecules [104]. Also, reversible binding to Keap1 might produce an appropriate chemoprevention signaling response (instead of hyperactivation) while allowing Keap1 to be reused within the cell instead of requiring degradation and energy-consuming re-synthesis [98].

2.4 Summary

A new screening assay has been developed to screen compounds and complex mixtures such as botanical extracts for potential chemoprevention agents that form covalent but reversible adducts with Keap1. This assay is based on the detection of adducts of BME with electrophiles that were reversibly bound to Keap1 using LC-MS with automated peak detection software and high resolution accurate mass measurement. Compounds such as sulforaphane can be detected using this new screening approach that

are missed by our MALDI MS-based screening assay due to its facile dissociation from Keap1. In addition, this strategy combines identification and characterization of chemoprevention agents in a single mass spectrometry step, whereas our previous assay used MALDI MS for detection followed by LC-MS/MS characterization and identification.

3 CYSTEINE MODIFICATION PATTERNS OF HUMAN KEAP1 BY ELECTROPHILIC NATURAL PRODUCTS

3.1 Introduction

Found in cruciferous vegetables such as broccoli, sulforaphane (R-1-isothiocyanato-4-methylsulfinylbutane) (Figure 15) has been investigated as a chemopreventive agent using cell culture, animal models and in clinical trials [105-110]. Sulforaphane exerts its chemopreventive effects at least in part through the Nrf2-Keap1 signaling pathway with efficacy in the high nanomolar range [100-102]. Kobayashi *et al.* [62] found that induction of ARE-regulated genes in zebrafish by sulforaphane is highly dependent on C151 of Keap1 and have categorized sulforaphane as a class 1 ARE activator. This is consistent with Zhang *et al*. [45] who reported that NIH3T3 cells expressing Keap1 C151S were not responsive to sulforaphane. However, LC-MS/MS measurements by Hong *et al.* [67] indicated that sulforaphane modified Keap1 primarily in the Kelch domain instead of at C151; and LC-MS/MS measurements carried out by Ahn *et al.* [111] did not show direct binding of a sulforaphane analog to C151 of Keap1, although mutation of C151 reduced overall labeling of Keap1 by the analog.

On the basis of these contradictory results regarding Keap1 C151 and sulforaphane, we investigated whether the apparent inability of C151 to react with sulforaphane, as reported by Hong *et al*. [67] was a methodological artifact due to the reversible binding of sulforaphane, an isothiocyanate, to thiols (Figure 15). To address this question, we compared the Keap1 modification pattern by sulforaphane in vitro using two sample preparation methods. One method is that used previously to map cysteines of Keap1 that form stable adducts with electrophiles such as IAB and the natural products

xanthohumol, isoliquiritigenin and 10-shogaol [56, 57], and includes derivatization of unreacted cysteine residues with iodoacetamide. The other method omits iodoacetamide treatment and is designed to account for the reversible nature of sulforaphane adducts.

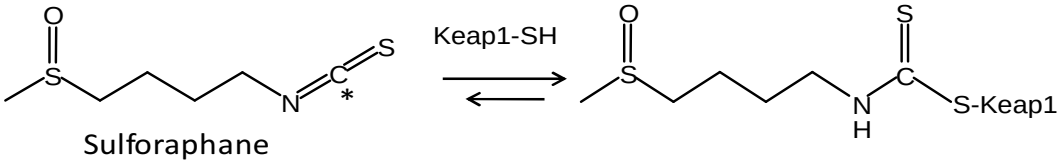

Figure 15. Reversible reaction of sulforaphane with Keap1 cysteine sulfhydryl groups. The asterisk indicates the isothiocyanate electrophilic carbon.

Since the *α,β*-unsaturated carbonyl group is commonly found in ARE activators, and Michael addition reactions are reversible, the sample preparation method used to map modified cysteines by ARE activators which contain a Michael acceptor groups is important to obtain correct modification pattern. In this investigation, reversibility of six ARE activators with *α,β*-unsaturated carbonyl groups were studied to facilitate the sample preparation method selection, and the six ARE activators were classified in terms of their reversibility.

In addition, cyclopentenone prostaglandins, prostaglandin A_2 (PGA_2) and 15-deoxy-$\Delta^{12,14}$-prostaglandin J_2 (15d-PGJ_2), are a class of endogenous electrophile that plays a regulation role in the inflammation process by exploiting the Nrf2-mediated transcriptional pathway [112, 113]. Kobayashi *et al.* [62] have categorized these two electrophiles into a separate class different from the natural chemopreventive agents like isoliquiritigenin or sulforaphane in the “cysteine code”. The alkylation pattern of these

two electrophiles has not been reported in detail and was one of the subjects of this investigation.

3.2 Experimental section

3.2.1 Materials

Sulforaphane was purchased from ICN Biomedicals, Inc. (Costa Mesa, CA), and recombinant human Keap1 was expressed and purified as described previously [63]. Isoliquiritigenin was purchased from Sigma-Aldrich (St. Louis, MO). Prostaglandin A_2 (PGA_2) and 15-deoxy-$\Delta^{12,14}$-prostaglandin J_2 (15d-PGJ_2) were purchased from Cayman Chemical (Ann Arbor, MI). Xanthohumol was isolated and provided by Dr. Luke R. Chadwick and Dr. Guido F. Pauli of the University of Illinois at Chicago. 1-[2-Cyano-3-12-dioxooleana-1,9(11)-dien-28-oyl]imidazole (CDDO-Im) was a generous gift from Dr. Michael B. Sporn of the Dartmouth Medical School.

3.2.2 Covalent modification of Keap1

Keap1 (10 µM) was incubated with sulforaphane at molar ratios of 1:0.5, 1:1, 1:2, 1:5, or 1:10 (Keap1/sulforaphane) in 100 µL 20 mM Tris-HCl buffer (pH 8.0) for 2 h at room temperature. Similar incubation with PGA_2, 15d-PGJ_2 and isoliquiritigenin were carried out at molar ratios of 1:1, 1:2 or 1:5 (Keap1/electrophile). The reaction was quenched by adding 1 mM dithiothreitol (DTT) followed by incubation for an additional 15 min. Samples were either analyzed immediately or (for sulforaphane molar ratios of 1:0.5 and 1:10 only; for the other three electrophiles molar ratios of 1:2 only) incubated with 3 mM iodoacetamide for 45 min in the dark followed by addition of 5 mM DTT to

remove the excess iodoacetamide before analysis. Mass spectrometry grade trypsin (Promega; Madison, WI) was added to each sample at a trypsin/Keap1 ratio of 1:50 (w/w) and incubated at 37 °C for 1.5 h. The tryptic peptides were analyzed using LC-MS/MS as described below to determine sites of modification by sulforaphane, PGA_2, 15d-PGJ_2, and isoliquiritigenin.

3.2.3 Reversibility of Keap1-electrophile adducts

Human Keap1 (10 µM) was treated with sulforaphane, isoliquiritigenin, xanthohumol, PGA_2, 15d-PGJ_2, or CDDO-Im at a molar ratio of 1:2 (Keap1/electrophile) in 100 µL 20 mM Tris-HCl buffer (pH 8.0) for 2 h at room temperature. Unbound electrophile was separated from the Keap1-electrophile adducts using a micro Bio-Spin 6 gel filtration column (Bio-Rad; Hercules, CA). The Keap1-electrophile adducts from the gel filtration column were diluted 20-fold with 20 mM Tris-HCl buffer (pH 8.0) containing 3 mM iodoacetamide to test the reversibility of electrophile modification of Keap1 or else with buffer containing no iodoacetamide and incubated for 5 h at room temperature (24 h for sulforaphane and 3h for CDDO-Im). Aliquots of 10 µL each were removed from the incubations at different time points to evaluate the reversibility of Keap1 modification by each electrophile. Each aliquot was mixed with 10 µL 500 nM naringenin in 30% methanol as an internal standard and analyzed immediately using LC-MS/MS. In a separate experiment, the maximum amount of electrophile bound to Keap1 was determined by measuring the reduction in electrophile concentration during a 2-h incubation of sulforaphane (initial concentration of 20 µM) with 10 µM Keap1. The amount of electrophile released from Keap1 at each shorter time point was calculated by

comparing the amount of free electrophile present in the incubation solution with the total electrophile bound to Keap1during the incubation.

3.2.4 DTT quenching time optimization

Human Keap1 (10 µM) was incubated with sulforaphane at a molar ratio of 1:2 (Keap1/sulforaphane) in 100 µL 20 mM Tris-HCl buffer (pH 8.0). The reaction was carried out at room temperature for 2 h and quenched by adding 1 mM DTT. To determine optimum quenching time while minimizing the loss of Keap1-sulforaphane adducts, sulforaphane concentration was monitored at 5, 15, 30, 45, and 60 min using LC-MS/MS as described below.

3.2.5 LC-MS/MS analysis using LTQ-FT ICR and TSQ Quantum mass spectrometers

Keap1 peptide digests were analyzed on a Thermo (San Jose, CA) hybrid LTQ-FT ICR mass spectrometer equipped with a Dionex (Auburn, CA) microcapillary HPLC system. Reversed phase microcapillary HPLC was carried out using an Agilent Zorbax C_{18} column (3.5 µm, 75 µm i.d.× 150 mm) and an LC Packings C_{18} PepMap precolumn cartridge (5 µm, 0.3 mm i.d. × 5 mm). The solvent system consisted of a 60 min linear gradient from 5% to 45% solvent B and then from 45 to 80% solvent B over 15 min (solvent A: 95:4.9:0.1; and solvent B: 4.9:95:0.1, water/acetonitrile/formic acid, v/v/v) at a flow rate of 250 nL/min. Positive ion electrospray tandem mass spectra were acquired in a data-dependent mode in which each MS scan was followed by five MS/MS scans using a normalized collision energy of 35%. Dynamic exclusion was enabled to minimize redundant spectral acquisitions.

All LC-MS/MS data were processed using two different search programs to improve confidence levels of identification, BioWorks 3.3.1 (Thermo) based on the SEQUEST algorithm, and MassMatrix [86, 87, 114, 115],. The mass accuracy for precursor ions was set to 10 ppm with up to 2 missed cleavages allowed. Modification was permitted to allow for the detection of the following (using sulforaphane as an example): methionine oxidation (+15.9949 Da), asparagine/glutamine deamidation (+0.9840 Da), cysteine carbamidomethylation (+57.0214 Da) and sulforaphane adducts (+177.0282 Da). Only peptides with modifications found in both search programs were nominated as potential matches, and the Keap1 modification sites were further validated by manual inspection of the tandem mass spectra. The X_{corr} and ΔC_n scores of the peptide matches from Bioworks were evaluated as described by Peng *et al*. [84], and pp, pp2 and pptag scores from MassMatrix were statistically significant with p values < 0.05 [86].

Sulforaphane released from Keap1-sulforaphane adducts was measured using positive ion electrospray tandem mass spectrometry with collision-induced dissociation and SRM on a Thermo TSQ Quantum triple quadrupole mass spectrometer equipped with a Surveyor HPLC system. Sulforaphane and naringenin (internal standard) were separated using a YMC C_{18} reverse phase column (5 µm, 2.0 mm × 50 mm, 120Å) with a 6 min linear gradient from 30% to 100% methanol and a co-solvent of 0.1% formic acid in water at a flow rate of 0.2 mL/min. Argon was used as the collision gas for collision-induced dissociation at 11 V for sulforaphane and 21 V for naringenin. During SRM, sulforaphane was measured using the ion transitions of *m/z* 178 to 114, and naringenin was measured using negative ion electrospray and the SRM ion transition of *m/z* 271 to 150.5. Isoliquiritigenin, xanthohumol, PGA_2, or 15d-PGJ_2 released from Keap1-

electrophile adducts was measured using negative ion electrospray tandem mass spectrometry and the same gradient HPLC mobile phase. CDDO-Im and naringenin were separated using a 0.8 min linear gradient from 70% to 100% acetonitrile with a co-solvent of 0.1% formic acid in water at a flow rate of 0.4 mL/min.

3.3 Results and discussion

3.3.1 Modification of Keap1 cysteine residues by sulforaphane

3.3.1.1 Release of sulforaphane from Keap1-sulforaphane adducts

On the basis of the lack of detection of Keap1 C151-sulforaphane adducts by Hong *et al.* [67] and the reversibility of such adducts, we wanted to ascertain if C151-sulforaphane adducts could be detected when adduct stability was maximized during sample preparation. The effect of iodoacetamide competition and sample processing time on the formation and stabilization of Keap1-sulforaphane adducts was assessed by removing unreacted sulforaphane from the reaction mixture using gel filtration chromatography followed by dilution into buffer or buffer containing 3 mM iodoacetamide. The decrease in Keap1-sulforaphane adduct concentration by the dissociation of free sulforaphane from the adduct was determined by the observation of an increase in free sulforaphane in the incubation buffer (Figure 16). The concentration of free sulforaphane increased steadily over time and reached a stable concentration after 3 h. At that time, 70% of the sulforaphane had been released from the Keap1-sulforaphane adducts indicating that equilibrium had apparently been reached between adduct formation and dissappearance.

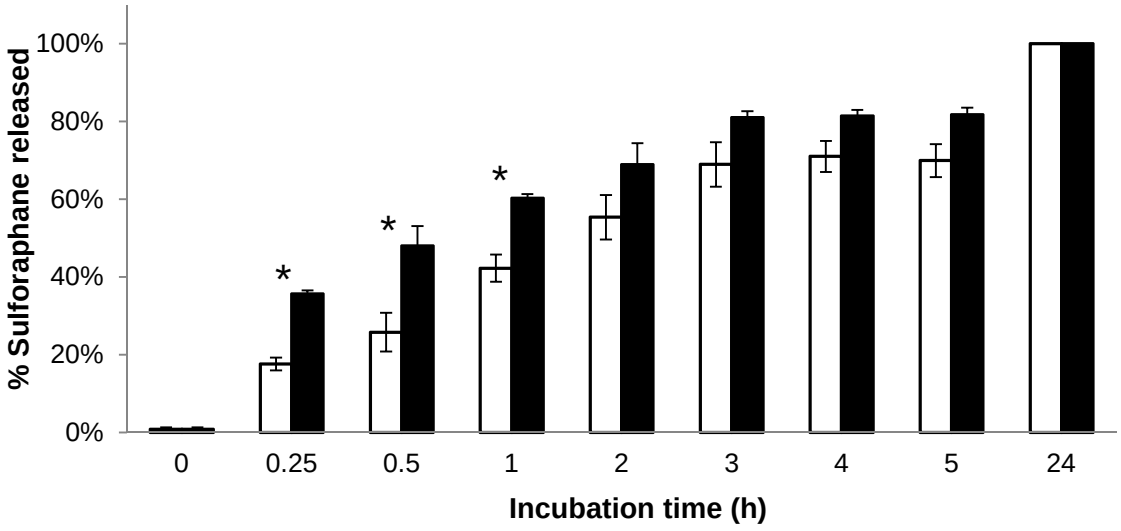

Figure 16. Sulforaphane released from Keap1-sulforaphane adducts during incubation with 20 mM Tris buffer (empty bars) or Tris buffer containing 3 mM iodoacetamide (solid bars). Total sulforaphane bound to Keap1 (100%) was determined by measuring the reduction in sulforaphane concentration during a 2 h incubation with Keap1. Free sulforaphane was measured using LC-MS/MS. Data are expressed as the mean ± SD of triplicate experiments. Statistically significant differences ($p \leq 0.05$) are denoted by "*".

When iodoacetamide was added to the dilution buffer, the extent of adduct disappearance increased so that approximately 50% of sulforaphane was released during the first 30 min of the reaction instead of only 25% as observed in the incubation without iodoacetamide. Iodoacetamide derivatization of free cysteines effectively blocked, i.e., competed against, free sulforaphane from reacting with Keap1. The loss of Keap1-sulforaphane adducts was 80% complete after 3 h, and no Keap1-sulforaphane adducts were present after 24 h (Figure 16).

3.3.1.2 DTT quenching time optimization

To minimize the loss of Keap1-sulforaphane adducts during sample preparation, DTT quenching time was optimized as shown in Figure 17. More than 5 min but no

longer than 15 min was needed to quench excess sulforaphane using DTT. By shortening the quenching time from 30 min used in our previous protocol [57] to 15 min, by eliminating iodoacetamide treatment and by digesting with trypsin for 1.5 h (instead of up to 3 h), the total sample preparation time was reduced to less than 2 h.

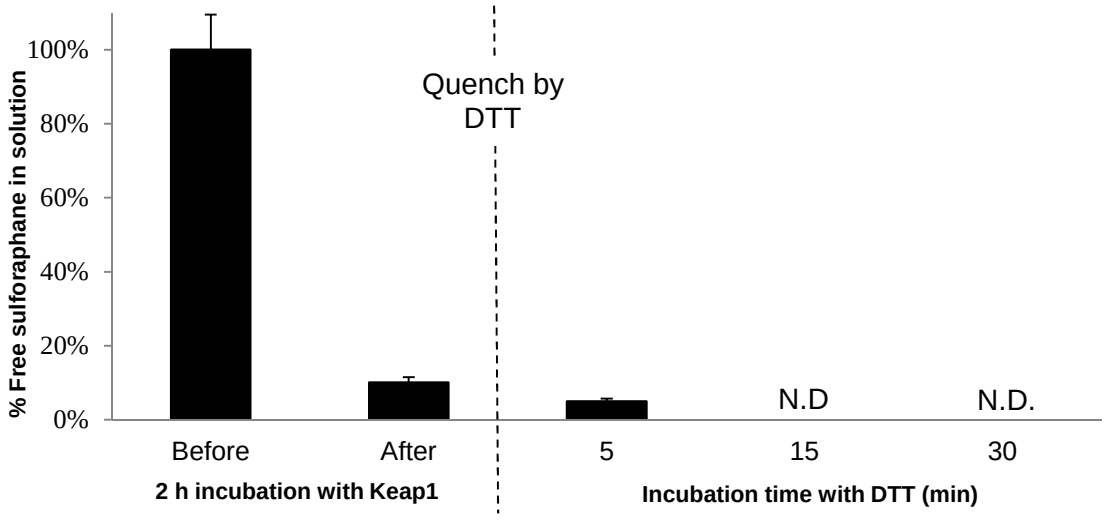

Figure 17. DTT quench time optimization. Sulforaphane was incubated with Keap1 for 2 h and quenched with 1 mM DTT. The minimum quench time needed to remove free sulforaphane (15 min) was obtained by monitoring free sulforaphane in solution using LC-MS/MS. Data are expressed as the mean ± SD of triplicate experiments and normalized to the initial amount of sulforaphane in the solution. (N.D. = none detected)

3.3.1.3 Effect of iodoacetamide treatment on Keap1 cysteine modification pattern by sulforaphane

We then examined the Keap1 modification pattern obtained using LC-MS/MS following this streamlined sample preparation procedure. During peptide mapping and sequencing using high resolution LC-MS/MS, the protein sequence coverage was at least 90%, and all 27 cysteines were detected and identified among the tryptic peptides. As expected, fewer modified cysteine residues were detected in Keap1-sulforaphane samples

that had been treated with iodoacetamide than in samples prepared using the streamlined protocol (TABLE II). Treatment with iodoacetamide also resulted in an apparently different modification pattern compared with that of samples that were untreated. Significantly, no labeling of C151 by sulforaphane was detected in samples treated with iodoacetamide; instead, C151 was observed to be derivatized only by iodoacetamide in these samples (Figure 18C). However, in samples that were not treated with iodoacetamide, labeling of C151 was detected at both high (1:10) and low (1:0.5) ratios of Keap1 to sulforaphane (Figure 18B). Sulforaphane labeling at C241, C273, C288, and C319 in the central linker domain, C395, C406, and C434 in the Kelch domain, and at C613, C622 and C624 in the C-terminal domain was also detected only in the samples that were not treated with iodoacetamide (TABLE II).

In the iodoacetamide-treated Keap1 that had been incubated with sulforaphane at a ratio of 1:0.5, sulforaphane adducts were detected only at C38, C226, and C368 (TABLE II). These three sites of sulforaphane binding were detected in all Keap1 samples incubated with sulforaphane regardless of iodoacetamide treatment or the ratio of Keap1 to sulforaphane. Sulforaphane adducts at C77 and C489 were detected in all samples except the lowest Keap1 to sulforaphane ratio (1:0.5) in iodoacetamide-treated samples. Several other sites of sulforaphane attachment including C23, C171, C196, C513, C518, and C583 were observed in both the iodoacetamide-treated and untreated samples but only at the highest sulforaphane to Keap1 ratio of 10:1.

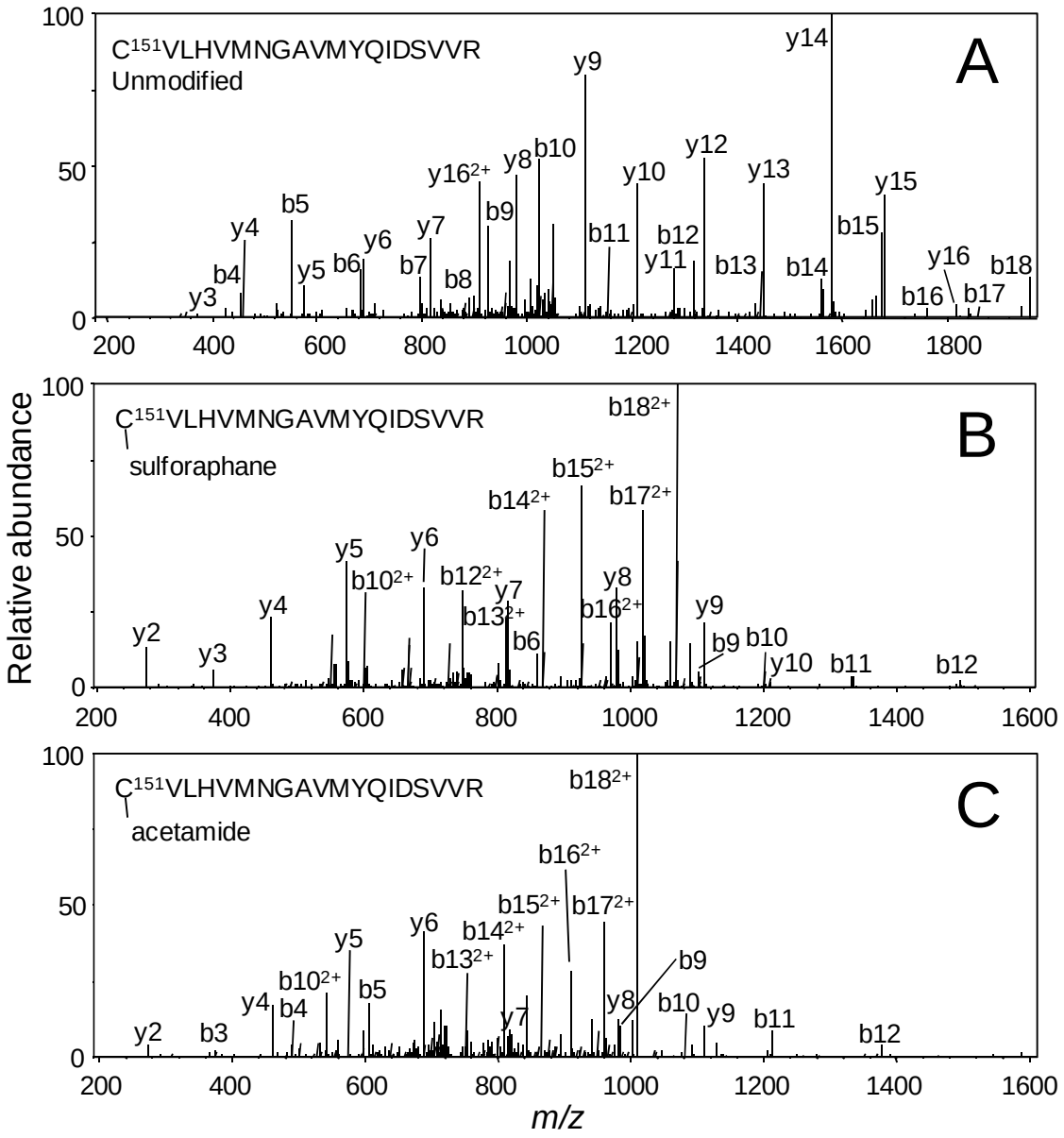

Figure 18. Product ion tandem mass spectra of Keap1 peptide 151 to 168 obtained during data-dependent LC-MS/MS analysis of tryptic digests of Keap1. Data were acquired using high resolution accurate mass measurement, and mass assignments were within 10 ppm of the theoretical values. Keap1 samples were prepared identically except as follows: A) Control that had not been treated with sulforaphane or iodoacetamide. The $[M+2H]^{2+}$ ion (corresponding to a neutral mass of 2,133.04 u) was used as the precursor for product ion tandem mass spectrometry; B) Keap1 incubated with sulforaphane but not iodoacetamide. The abundant $[M+3H]^{3+}$ ion (corresponding to a neutral mass of 2,310.07 u) was used as the precursor ion for MS/MS, and an adduct with sulforaphane was detected; C) Keap1 incubated with sulforaphane followed by derivatization with iodoacetamide. The $[M+3H]^{3+}$ ion (corresponding to a neutral mass of 2,190.06 u) was selected for MS/MS. Instead of sulforaphane, iodoacetamide was found to have reacted with the peptide.

TABLE II

DETECTION OF CYSTEINE RESIDUES IN HUMAN KEAP1 MODIFIED BY SULFORAPHANE WITH AND WITHOUT IODOACETAMIDE TREATMENT

		No iodoacetamide treatment		Iodoacetamide treatment	
Domain	Cysteine	0.5[a]	10	0.5	10
N-terminal	C13				
	C14				
	C23		1,2,3[b]		2,3
	C38	1,2,3	1,2,3	1,2,3	1,2,3
BTB	C77	1,3	1,2,3		1,2
	C151	1,2,3	1,2,3		
	C171		1,2,3		1,2,3
Central	C196		1,2,3		1
linker	C226	1,2	1,2,3	2,3	1,2
	C241		1,2,3		
	C249				
	C257				
	C273		1,2,3		
	C288		1,3		
	C297				
	C319	1,3	1,2,3		
Kelch	C368	1,2,3	1,2,3	1,2,3	1,2,3
	C395		1		
	C406	3	1,2,3		
	C434	1,3	1,2,3		
	C489	1,2,3	1,2,3		1,2,3
	C513		1,2,3		1,2,3
	C518		1,2,3		1
	C583		1,3		1,2,3
C-terminal	C613	1,3	1,2,3		
	C622		2,3		
	C624		2,3		

[a] Sulforaphane was incubated with Keap1 at a molar ratio of 0.5:1 or 10:1 (sulforaphane/Keap1).

[b] Triplicate experiments were performed. The numbers indicate the experiments in which sulforaphane-modified peptides were detected by using LC-MS/MS.

To determine the relative reactivities of the 27 Keap1 cysteines towards sulforaphane, a titration-like process was used that included five ratios of sulforaphane to

Keap1 ranging from 0.5:1 to 10:1 and no iodoacetamide treatment (TABLE III). The number of modified Keap1 cysteines increased as the relative sulforaphane concentration was increased, and 22 out of 27 cysteines could be modified by sulforaphane. All of the cysteines in the Kelch, BTB and C-terminal domains (but not all in the *N*-terminal and central linker domains) were modified at the highest ratio of sulforaphane to Keap1. The four most readily modified cysteines of human Keap1 by sulforaphane were C38 in the *N*-terminal domain, C151 in the BTB domain, and C368 and C489 in the Kelch domain. The five cysteines that did not react with sulforaphane were C13 and C14 in the *N*-terminal domain, and C249, C257 and C297 in the central linker domain. The 27 Keap1 cysteines were placed into 7 groups according to their reactivity towards sulforaphane (TABLE III). Covalent binding of sulforaphane to C406, which belongs to the third most readily modified cysteine residues in Keap1, has not been reported previously.

TABLE III

ORDER OF REACTIVITY OF KEAP1 CYSTEINE RESIDUES TOWARDS SULFORAPHANE MEASURED USING HIGH RESOLUTION LC-MS/MS

		[Sulforaphane]/[Keap1]				
Domain	Cysteine	0.5	1	2	5	10
N-terminal	C13					
	C14					
	C23		2[a]	2,3	1,2,3	1,2,3
	C38	1,2,3	1,2,3	1,2,3	1,2,3	1,2,3
BTB	C77	1,3	2,3	1,2,3	1,2,3	1,2,3
	C151	1,2,3	1,2,3	1,2,3	1,2,3	1,2,3
	C171					1,2,3
Central	C196			1	2,3	1,2,3
linker	C226	1,2	1,2,3	1,2,3	1,2,3	1,2,3
	C241				1,3	1,2,3
	C249					
	C257					
	C273			3	1,3	1,2,3
	C288					1,3
	C297					
	C319	1,3	1,2,3	1,2,3	1,2,3	1,2,3
Kelch	C368	1,2,3	1,2,3	1,2,3	1,2,3	1,2,3
	C395			2,3	1,3	1
	C406	3	2,3	2	1,2,3	1,2,3
	C434	1,3	1,2,3	1,2,3	1,2,3	1,2,3
	C489	1,2,3	1,2,3	1,2,3	1,2,3	1,2,3
	C513		2,3	1,2,3	1,2,3	1,2,3
	C518			1,2,3	1,3	1,2,3
	C583				1,3	1,3
C-terminal	C613	1,3	2,3	1,2,3	1,2,3	1,2,3
	C622					2,3
	C624					2,3

Cysteine reactivity[b]

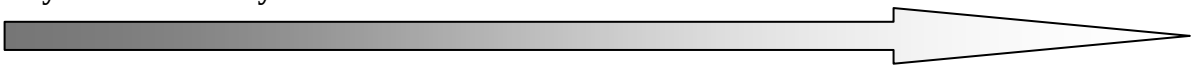

High **Low**

38, 151, 368, 489	77, 226, 319, 434	406, 513, 613	23, 395, 518	196, 241, 273, 583	171,288, 622,624

[a] The numbers indicate the experiments out of three identical replicates in which sulforaphane-modified cysteines were detected by using LC-MS/MS.

[b] The order of the Keap1 cysteine reactivity based on triplicate data.

Previously studies have probed the in vitro modification of Keap1 cysteines by sulforaphane and its analogues [67, 111], but the results are inconsistent with in vivo observations that demonstrate the importance of C151 in sensing sulforaphane [35, 55, 59, 62, 65, 111]. While investigating these conflicting C151 data for sulforaphane, we found that omitting derivatization with iodoacetamide from the sample preparation procedure and shortening the overall procedure time prior to LC-MS/MS analysis allowed the detection of C151 as one of the most readily modified cysteine residues of Keap1 towards sulforaphane (TABLE II). The other most readily modified cysteine residues were C38, C368 and C489. Our modified analytical procedure resulted in an in vitro "cysteine code" for sulforaphane that is consistent with in vivo observations and reconciles previous conflicting data.

It is important to note that we have shown in a previous study that the Keap1 protein preparation we used in the MS studies presented here is fully capable of binding to Cul3 and Nrf2, which are its in vivo binding partners [116]. Furthermore, the Cul3-Rbx1-Keap1 complex is functionally active and can catalyze the ubiquitination of Nrf2, which is the process by which Keap1 regulates cellular levels of Nrf2 in vivo. Since our recombinant human Keap1 has the appropriate tertiary and quaternary protein structure to bind to and form a complex with Cul3 and Nrf2, this is in a biologically suitable and relevant conformation for reaction with sulforaphane.

The ARE is activated in response to the modification of Keap1 C151 by an increased amount of Nrf2, a result of decreased Keap1-mediated Nrf2 ubiquiritination, and degradation [47, 59]. This decrease in Nrf2 ubiquitination appears to arise from a diminished interaction between Keap1 and Cul3 upon the modification of C151, as

shown by coimmunoprecipitation experiments in cells for both Keap1 C151W [59] and for sulforaphane [47], as well as for IAB using purified Keap1 and Cul3 [65]. Another model for the activation of Nrf2 upon modification of Keap1 cysteines is the disruption of the Keap1-Nrf2 interaction. However, we have seen using isothermal titration calorimetry that modification of Keap1 cysteines including C151 by IAB does not alter the affinity of Keap1 and Nrf2 [63]. In addition, we find that modification of Keap1 cysteines by sulforaphane does not alter its ability to bind Nrf2, as determined by native electrophoretic mobility shift assays.

The eight most readily modified Keap1 cysteine residues towards sulforaphane (C38, C151, C368, C489, C77, C226, C319, and C434; belonging to the 1^{st} and 2^{nd} most readily modified groups in TABLE III) have also been reported to be modified by other electrophilic ARE activators [56-58, 63, 117]. Reaction of sulforaphane with C406 is reported here for the first time, and reactions with C23, C241, C319, C406, and C622 were not reported previously by Hong *et al*. [67]. Although C273 and C288 have been reported to be functionally important [35, 45, 55], these cysteine residues were not readily modified by sulforaphane and appear in the 5^{th} and 6^{th} groups, respectively, in terms of cysteine reactivity (TABLE III).

The electrophilic isothiocyanate group of sulforaphane and its analogs reacts rapidly but reversibly with Keap1 cysteine sulfhydryl groups to form dithiocarbamates [52]. Since iodoacetamide covalently modifies cysteine sulfhydyl groups through S_N2 reactions to form stable thioethers, treatment of Keap1-sulforaphane adducts with iodoacetamide will result in time-dependent loss of sulforaphane (initially from the most highly modified cysteine residues) and subsequent derivatization of these cysteine sites

by iodoacetamide. Natural product ARE activators including xanthohumol, isoliquiritigenin and 10-shogaol have been reported to modify Keap1 preferentially at C151, C241, C273, C288, C319, C434, and C613 [57]. However, these cysteine residues have only been detected previously as targets of sulforaphane when iodoacetamide treatment was not used during sample preparation. This suggests that the binding of sulforaphane to these sites can go undetected due to the inherent reversibility and loss of sulforaphane during sample processing. In contrast, binding of sulforaphane to C38, C226 and C368 of Keap1 has been detected despite treatment with iodoacetamide, which suggests that these cysteine residues are less reversible and form more stable adducts with sulforaphane.

Iodoacetamide derivatization of Keap1 has been used to block unreacted cysteine residues so that they cannot react with each other to form disulfide bonds or continue to react with excess sulforaphane during subsequent sample preparation. Since iodoacetamide derivatization was eliminated from our protocol, DTT was used to consume unreacted sulforaphane. Therefore, it is unlikely that significant additional reaction could occur between sulforaphane and cysteines during sample processing. Since at least 90% protein coverage was obtained using LC-MS/MS, disulfide bond formation did not interfere with peptide mapping or sequencing and was not a concern using our new method.

Located in the *N*-terminal domain of Keap1 and a target of sulforaphane, C38 is conserved across most species with the exception of the Keap1a isoform in zebrafish [62]. Strongly reactive towards sulforaphane, C38 is only weakly reactive towards other ARE activators including xanthohumol [57]. Sensitive to *S*-glutathionylation in vitro,

C23 can also form a disulfide bond with C38 under in vitro conditions of oxidative stress [117], suggesting the C23-C38 disulfide bond formation might reduce Keap1 repression of Nrf2. However, a C23Y mutant has been found in breast cancer that results in inhibition of Keap1-directed ubiquitination of Nrf2 [118]. Interestingly, a C23A-C38A double mutation did not affect the repressor activity of Keap1 [35]. Further studies will be needed to explain the physiological significance of C38 and C23 in Keap1 function and potential regulation through C38 modification by sulforaphane.

Sensitive to both sulforaphane modification and S-glutathionylation [117], C368 is located inside the inner barrel of the propeller of the Kelch domain which is the Nrf2-binding region on Keap1. An energy minimization study indicated that modification at C368 by glutathione could interfere with the Keap1 binding of Nrf2 by inducing a conformational change of the protein [117]. Although we did not observe any disruption of the interaction of Keap1 and Nrf2 when using an electrophoretic mobility shift assay after 9 Keap1 cysteines including C368 were modified by sulforaphane [63], modification at C368 might reduce the affinity between Keap1 and Nrf2 to a degree that is undetectable at the protein concentration used in the assay. Another cysteine residue in the Kelch domain, C489 reacts strongly with sulforaphane and has been reported to form adducts with xanthohumol, isoliquiritigenin, 10-shogoal, and *N*-ethylmaleimide [52, 57], but the biological importance of adduct formation at C489 remains uncertain.

3.3.2 Reversibility and optimization of sample preparation

The reversibility of binding of Keap1 of five Michael acceptor that are also ARE activators, including isoliquiritigenin, xanthohumol, CDDO-Im, PGA_2, 15d-PGJ_2, and

sulforaphane (described in section 3.3.1.1) were investigated in vitro with two purposes. First, the reversibility of protein-electrophile adducts and the effect of iodoacetamide treatment on these adducts was investigated in order to select a suitable sample preparation method. Second, information on the reversibility binding to Keap1 of these known ARE activators might be valuable for the interpretation of data for their chemoprevention effect.

3.3.2.1 Reversibility of binding and sites of modification of Keap1 by the natural products isoliquiritigenin and xanthuhumol

Isoliquiritigenin (2,4,4'-trihydroxychalcone) (Figure 18A) is a constituent of licorice (*Glycyrrhiza glabra*), tonka bean *Dipteryx odorata* (Aubl.) Willd, and shallot (*Allium ascalonicum*) [93, 119]. It has potential as a chemopreventive agent due to induction of phase 2 enzymes that protect cells against reactive, toxic, and potentially carcinogenic species [97]. Xanthohumol (Figure 18B) is a prenylflavonoid derived from the female flowers of the hop plant (*Humulus lupulus* L.) and has been reported to be a cancer chemopreventive agent both in vitro and in vivo [92, 120]. Both isoliquiritigenin and xanthohumol have been reported to form adducts with Keap1 in vitro. The most reactive sites on Keap1 towards isoliquiritigenin are C151 and C226; and the most reactive Keap1 sites towards xanthohumol are the cysteine residues C151, C319 and C613 [57].

The procedures used to assess the reversibility Keap1-sulforaphane adducts were applied again to study the reversibility of Keap1-isoliquiritigenin and Keap1-xanthohumol adducts as well as the effect of iodoacetamide. Approximately 10% of isoliquiritigenin had been released from the Keap1-isoliquiritigenin adducts after 30 min

as shown in Figure 20. The concentration of free isoliquiritigenin increased slowly over time and reached a stable concentration after 3 h, where 20% of isoliquiritigenin had been dissociated from the adducts. Unlike the Keap1-sulforaphane adduct, Keap1-isoliquiritigenin showed the same initial rate of dissociation with or without the addition of iodoacetamide. Keap1-xanthohumol showed a completely different dissociation profile from that of Keap1-isoliquiritigenin or Keap1-sulforaphane. No free xanthohumol was detected during incubation of the Keap1-xanthohumol complex with or without iodoacetamide for up to 5 h (data not shown). High resolution LC-MS/MS analysis showed that three Keap1 cysteines (C151, C319, and C613) were modified by xanthohumol within 5 h, but no modified cysteines were detected after 24 h. This suggests that xanthohumol has a much slower rate of dissociation from Keap1.

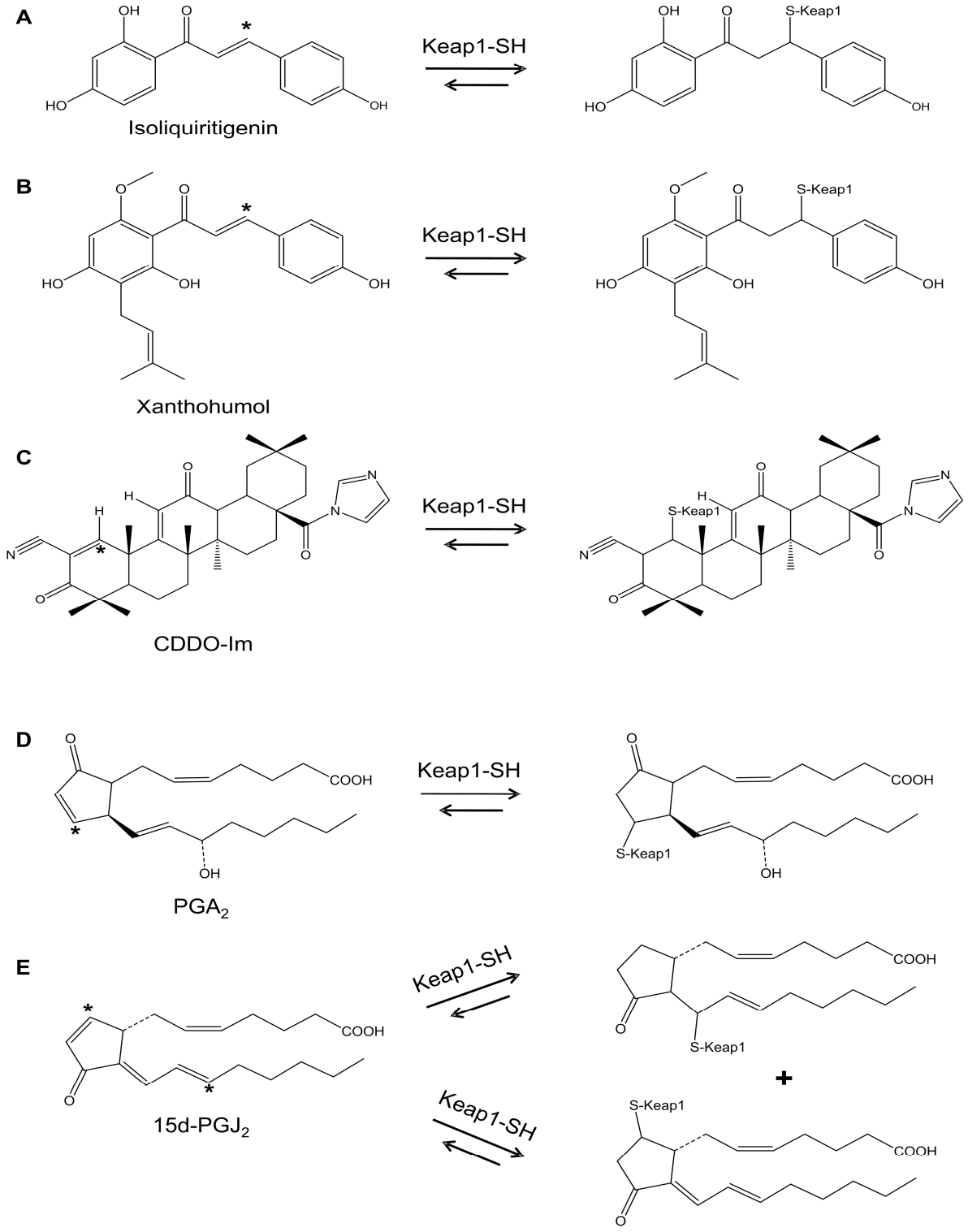

Figure 19. Reversible reaction of five ARE activators with Keap1 cysteine sulfhydryl groups. The asterisk indicates the electrophilic carbon. A) isoliquiritigenin, B) xanthohumol, C) 1-[2-cyano-3-,12-dioxooleana-1,9(11)-dien-28-oyl]imidazole (CDDO-Im), D) prostaglandin A_2 (PGA_2), and E) 15-deoxy-$\Delta^{12,14}$-prostaglandin J_2 (15d-PGJ_2).

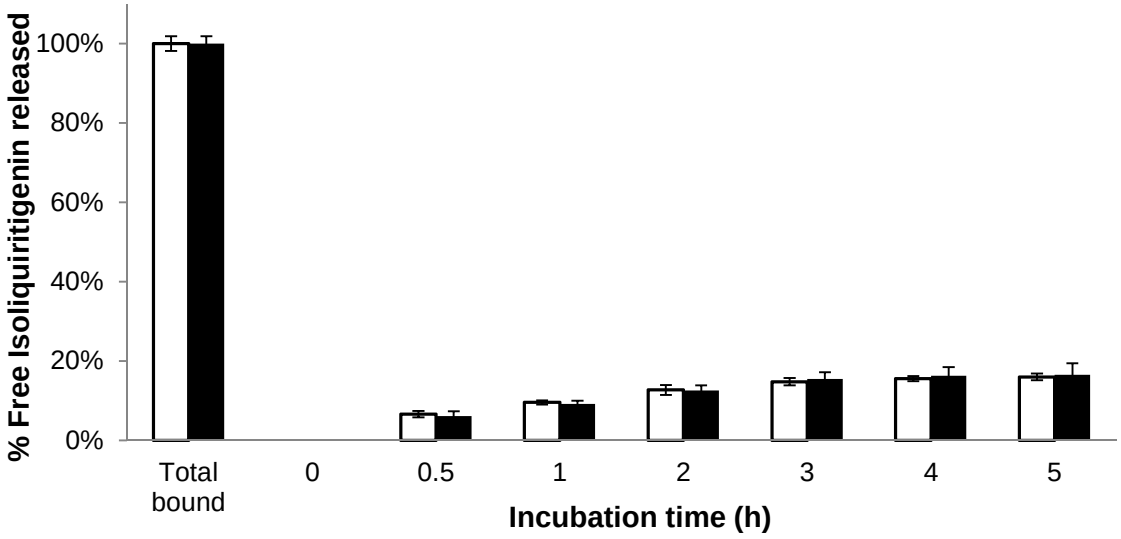

Figure 20. Isoliquiritigenin released from Keap1-isoliquiritigenin adducts during incubation with 20 mM Tris buffer (empty bars) or Tris buffer containing 3 mM iodoacetamide (solid bars). The total isoliquiritigenin bound to Keap1 (100%) was determined by measuring the reduction in isoliquiritigenin concentration during a 2 h incubation with Keap1. Free isoliquiritigenin was measured using LC-MS/MS. Data are expressed as the mean ± SD of triplicate experiments.

3.3.2.2 Reversibility of Keap1-CDDO-Im adducts

CDDO-Im is the most potent ARE activator described to date, and activation of the Nrf2 pathway is believed to be mediated by Michael addition reaction of CDDO-Im with nucleophilic cysteine sulfhydryl groups on Keap1 [102]. Recently, it has been reported that modification of C151 by CDDO-Im is important for activation of the ARE in cells [59].

The initial dissociation rate of Keap1-CDDO-Im adducts was very fast and reached an equilibrium within 10 min (Figure 21). At equilibrium, approximately 40% of CDDO-Im had been released from the Keap1-CDDO-Im complexes. No time points were acquired within the first 5 min due to the time constraints of sampling and analysis. When

iodoacetamide was added to the dilution buffer, the rate of dissociation of the adducts increased during the first 5 min; whereas, less CDDO-Im (30-35%) was detected released compared to the one without iodoacetamide addition after reaching the equilibrium. It is possible that some impurity in the CDDO-Im standard reacted with iodoacetamide, which accounted for the disappearance of CDDO-Im after the equilibrium.

The dissociation of Keap1-CDDO-Im adducts begins during gel filtration and continues during the dissociation step. For rapidly dissociating complexes such as this, substantial amounts of CDDO-Im probably dissociated during gel filtration and were not recovered. According to the concentration of free CDDO-Im measured in buffer after 10 min of the isolated Keap1-CDDO-Im adducts and thereafter, approximately 40% of CDDO-Im was released into solution. If substantial quantities of CDDO-Im were lost during gel filtration, then essentially all remaining CDDO-Im might have been released from Keap1 after dilution and incubation for only 10 min.

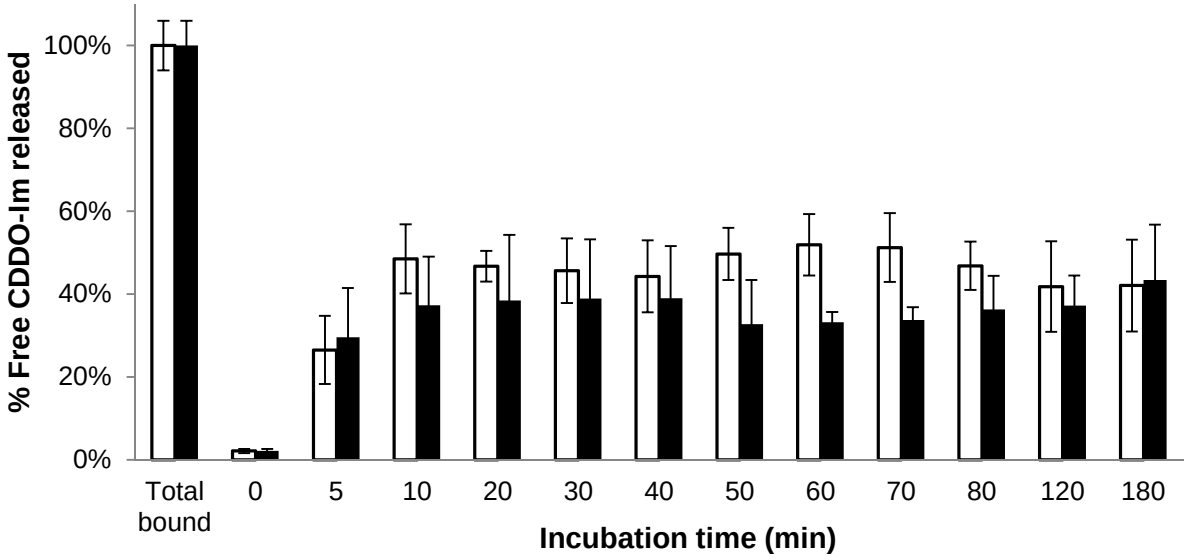

Figure 21. CDDO-Im released from Keap1-CDDO-Im adducts during incubation with 20 mM Tris buffer (empty bars) or Tris buffer containing 3 mM iodoacetamide (solid bars). The total CDDO-Im bound to Keap1 (100%) was determined by measuring the reduction in CDDO-Im concentration during a 2 h incubation with Keap1. Free CDDO-Im was measured using LC-MS/MS. Data are expressed as the mean ± SD of triplicate experiments. No statistically significant differences between samples treated or not treated with iodoacetamide.

3.3.2.3 Reversibility of Keap1 adducts with prostaglandins PGA_2 and 15d-PGJ_2

PGA_2 and 15d-PGJ_2 are lipid oxidation products that accumulate in cells and tissues during acute inflammation. They have profound effects on redox status by activating Keap1/Nrf2 cascades [121]. The presence of an α,β-unsaturated cyclopentane ring makes PGA_2 and 15-PGJ_2 electrophilic and susceptible to Michael addition reactions with the sulfhydryl group of cysteine residues (Figure 18D, 18E). Yamamoto *et al.* [62] reported that both Keap1a and Keap1b in zebrafish embryos have a sensor site for PGA_2 and 15d-PGJ_2, which is different from most of the other ARE activators such as

sulforaphane and tBHQ that only respond to Keap1b containing a reactive analogous C151.

The reversibility of Keap1-PGA_2 adduct was investigated using the same procedures that were used for sulforaphane including gel filtration, dilution and iodoacetamide derivatization. The reversibility profile of Keap1-PGA_2 (Figure 22) is similar to that of isoliquiritigenin (Figure 20). Approximately 10% of the total PGA_2 that was originally bound to Keap1 was released and measured in the dilution buffer after 30 min. By 2 h, an equilibrium had been reached between adduct formation and dissociation at which time, 20% of the original bound PGA_2 was free in solution. With inclusion of iodoacetamide in the dilution buffer, there were no statistically significant differences between samples treated or not treated with iodoacetamide.

Although structurally similar to PGA_2, 15d-PGJ_2 formed adducts with Keap1 that were irreversible during the first 5 h, whether or not iodoacetamide was added to the dilution buffer (data not shown). This indicates that although PGA_2 and 15d-PGJ_2 have been categorized into the same class due to C151 independence [62], it is still possible that they activate the Keap-Nrf2 pathway differentially and lead to distinct biological effects due to different rate of dissociation from Keap1. Additional studies are needed to investigate these potentially different mechanisms of action.

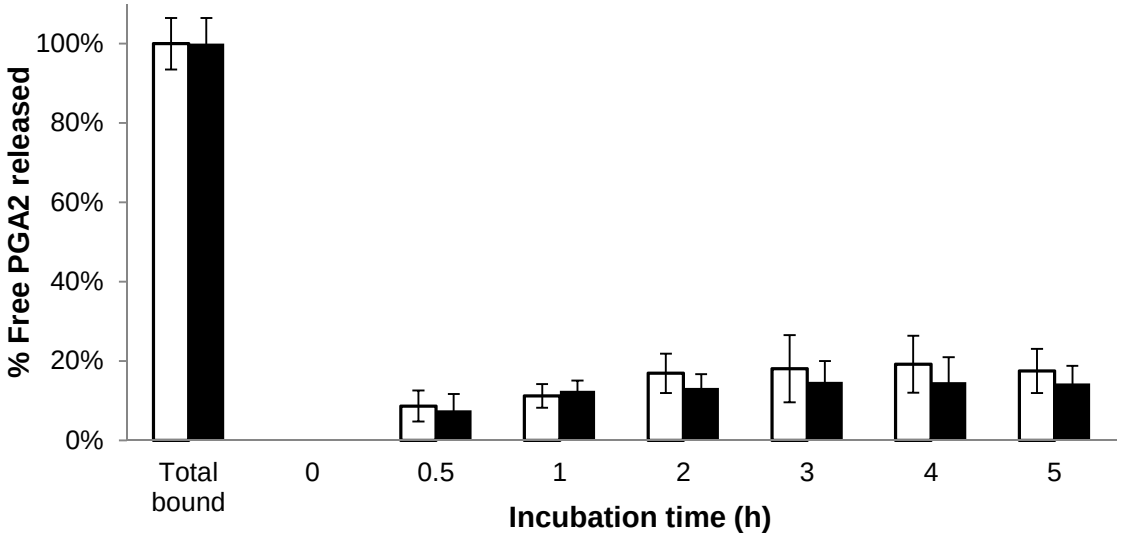

Figure 22. PGA_2 released from Keap1-PGA_2 adducts during incubation with 20 mM Tris buffer (empty bars) or Tris buffer containing 3 mM iodoacetamide (solid bars). The total PGA_2 bound to Keap1 (100%) was determined by measuring the reduction in PGA_2 concentration during a 2 h incubation with Keap1. Free PGA_2 was measured using LC-MS/MS. Data are expressed as the mean ± SD of triplicate experiments. No statistically significant differences between samples treated or not treated with iodoacetamide.

3.3.2.4 Effect of reversibility on mapping of modified Keap1

Base on the previous binding studies, six ARE activators could be ranked order according to their reversibility as follows: CDDO-Im > sulforaphane > PGA_2 > isoliquiritigenin > xanthohumol = 15d-PGJ_2 (Figure 23).

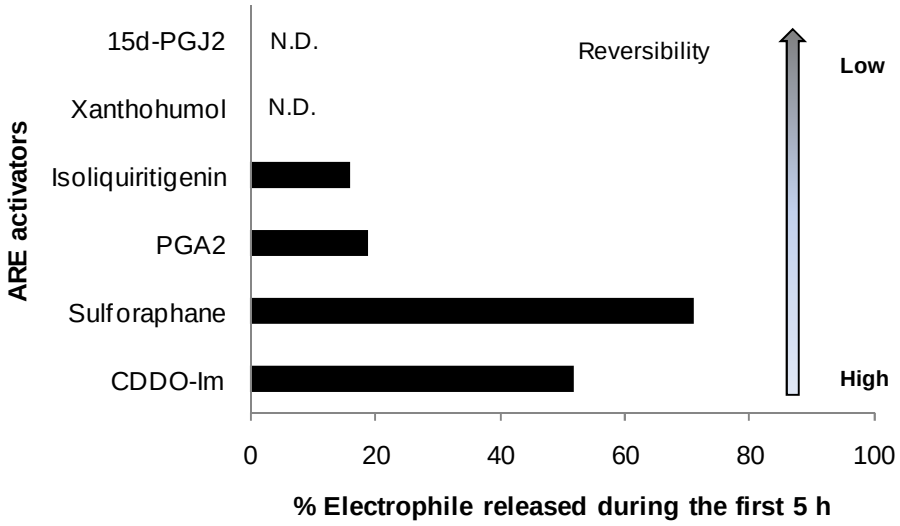

Figure 23. Reversibility of six ARE activators. The solid bar represents the maximum percentage of each electrophile released from Keap1-electrophile complex during the first 5 h incubation. N.D. represents the complex did not dissociate within the first 5 h, which indicated that the compound form stable adduct with Keap1.

Previously, we showed that a revised sample preparation method should be used when mapping Keap1 modification pattern by sulforaphane, due to its reversible reaction with Keap1 cysteines. To determine whether reversible Keap1 modifiers other than sulforaphane should be investigated using this streamlined procedure, the more slowly dissociating Keap1 modifier PGA_2 and isoliquiritigenin were used. These compounds were incubated with Keap1 using the method with and the new method excluding iodoacetamide, and the Keap1 adducts were compared using LC-MS/MS.

More than 90% of Keap1 sequence coverage was obtained while mapping PGA_2 and isoliquiritigenin modification using either method. As shown in TABLE IV, there were only minor differences in Keap1 modification by PGA_2 using iodoacetamid or the new sample preparation procedure excluding iodoacetamide. There were also minor

differences in Keap1 modification by isoliquiritigenin using either method. C434 was found to be modified by PGA_2 only when iodoacetamide was omitted, and C38 was found to be modified by isoliquiritigenin only using the sample preparation without iodoacetamide. However, these two cysteines were found to be modified using either method when the molar ratio of Keap1/electrophile was increased from 1:2 to 1:5 (data not shown). Although most sites of Keap1 modification by slowly dissociating compounds like isoliquiritigenin and PGA_2 (10-20% dissociation over 5 h) can be detected using LC-MS/MS following either sample preparation method, the fact that one additional modified cysteine can be detected for each electrophile indicates that iodoacetamide treatment should be avoided even for these compounds.

At a molar ratio of 1:20 (Keap1/CDDO-Im), CDDO-Im was incubated with Keap1 and then prepared using the iodoacetamide method and the streamlined method excluding iodoacetamide. No modified Keap1 peptides could be detected (data not shown). Considering that the dissociation rate of Keap1-CDDO-Im adducts was faster than Keap1-sulforaphane adducts, it appears that all CDDO-Im had dissociated from Keap1 by the end of either sample preparation procedure for peptide mapping. However, when Keap1 that had been in incubated with CDDO-Im was analyzed directly using MALDI-TOF MS without iodoacetamide treatment or trypsinization, Keap1 increased in mass (Figure 24). Therefore, the sample preparation procedure that had been optimized for Keap1-sulforaphane adducts appears to permit too much dissociation to occur for adducts that are less stable.

TABLE IV

DETEATION OF CYSTEINE RESIDUES IN HUMAN KEAP1 MODIFIED BY PGA_2 OR ISOLIQUIRITIGENIN WITH AND WITHOUT IODOACETAMIDE TREATMENT

		PGA_2[a]		Isoliquiritigenin	
Domain	Cysteine	No IA[b]	IA	No IA	IA
N-terminal	C13				
	C14				
	C23			1[c],3	1,2,3
	C38	1	1,2	2,3	
BTB	C77				
	C151			1,2,3	1,2,3
	C171				
Central	C196				
linker	C226	1,2,3	1,2,3	1,2,3	1,2,3
	C241				
	C249	1	1		
	C257				
	C273	2,3	2,3		
	C288				
	C297				
	C319	1,2,3	1,2,3	1,2,3	1,2,3
Kelch	C368	1,2,3	1,3		
	C395				
	C406				
	C434	1,3			
	C489				
	C513	2,3	3		
	C518	2,3	3		
	C583				
C-terminal	C613			1,2,3	2
	C622				
	C624				

[a] PGA_2 or isoliquiritigenin was incubated with Keap1 at a molar ratio of 2:1 (electrophile/Keap1).

[b] IA = iodoacetamide treatment.

[c] Triplicate experiments were performed. The numbers indicate the experiments in which PGA_2 or isoliquiritigenin-modified peptides were detected by using LC-MS/MS.

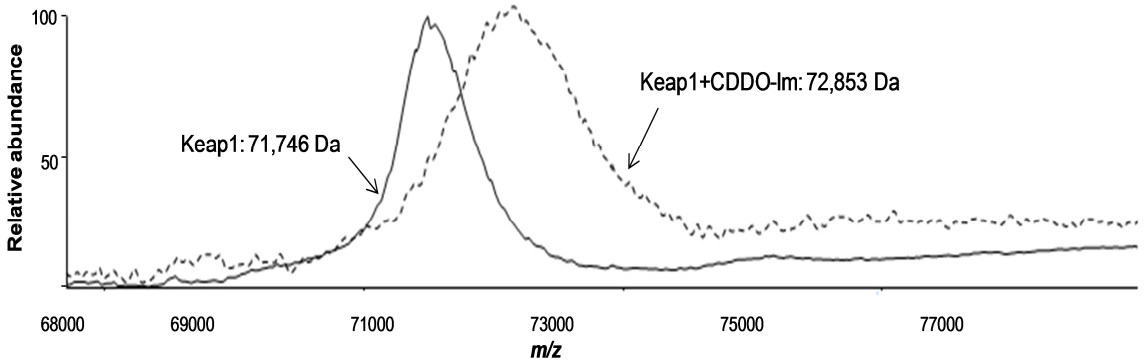

Figure 24. Positive ion MALDI-TOF mass spectra of Keap1 after incubation with CDDO-Im at molar ratio of 20:1 (CDDO-Im/Keap1). The solid line indicates Keap1 incubation with buffer (control) (*m/z* 71,746). The dashed line represents Keap1 incubated with CDDO-Im (*m/z* 72,853).

3.3.3 Modification sites of human Keap1 treated by 15d-PGJ_2 and PGA_2

15d-PGJ_2, a cyclopentenone prostaglandin, exerts cytoprotective effects that are mainly mediated through the Nrf2 pathway [112]. It has been reported by several independent studies that 15d-PGJ_2 targets Keap1 cysteines other than C151 [54, 122, 123]. Yamamoto *et al*. [62] showed that ARE activation by 15d-PGJ_2 and also PGA_2 were largely independent of C151 in zebrafish embryos transfected with mouse Keap1 C151S. Similarly, our group found that ARE activation by 15d-PGJ_2 in human cells is much less dependent on Keap1 C151 than that of sulforaphane or CDDO-Im [59].

Park *et al*. [124] reported that C257 and C273 were modified by 15d-PGJ_2 in HEK293T cells transfected with mouse Keap1. Yamamoto *et al*. [62] showed that C273 and C288 in mouse Keap1 were modified by 15d-PGJ_2, and that C273, C297, and C489 were modified by PGA_2. However, no human Keap1 modification by 15d-PGJ_2 pattern has been investigated, and the modification of Keap1 by PGA_2 reported in the previous section was the first such study. Considering the unique features of the interaction of

these compounds with mouse Keap1, additional studies of their modification of human Keap1 might provide insights into their mechanisms of action.

A titration-like process was used that included 3 ratios of PGA_2 or 15d-PGJ_2 to Keap1 ranging from 1:1 to 1:5 (Keap1/electrophile) with no iodoacetamide treatment to determine the relative reactivity of the human Keap1 cysteines towards these two ARE activators (TABLE V). With protein coverage over 90%, all 27 Keap1 cysteines were detected as either modified by electrophiles or unmodified. As expected, more cysteines became modified as the concentration of electrophile was increased. Consistent with the in vivo results, PGA_2 and 15d-PGJ_2 displayed a distinctly different pattern of Keap1 modification than previously studied ARE activators such as sulforaphane and isoliquiritigenin. Both PGA_2 and 15d-PGJ_2 modified human Keap1 more readily in the central linker domain followed by the Kelch domain, rather than BTB domain, where C151 is located. Specifically, C151 was not detected as modified, in agreement with previous results reported by others in the cell and zebrafish studies [62, 123]. However, the sensor cysteines of human Keap1 that were modified by PGA_2 and 15d-PGJ_2 were slightly different from those reported using mouse Keap1.

The five most readily modified human Keap1 cysteine residues by PGA_2 were C226, C319, C273, C368, and C434; whereas the five most readily modified cysteine residues by 15d-PGJ_2 were C241, C249, C273, C513, and C518. Freeman *et al*. [125] carried out kinetic studies and found that the reactivities of some cysteine residues towards IAB are significantly different in human and mouse Keap1. Thus, the difference between our findings and these other studies might be due to the species differences. Although 15d-PGJ_2 and PGA_2 modified Keap1 at different sites, C273 was one of the

most reactive Keap1 sites towards both electrophiles. Therefore, C273 might be a common sensor for these two non-C151 dependent ARE activators. The tandem mass spectra of the peptide ions containing C273 residues that been covalently modified by PGA_2 or 15d-PGJ_2 are shown in Figure 25.

TABLE V

ORDER OF REACTIITY OF KEAP1 CYSTEINE RESIDUES TOWARDS PGA_2 OR 15d-PGJ_2 MEASURED USING HIGH RESOLUTION LC-MS/MS

		[PGA_2]/[Keap1]			[15d-PGJ_2]/[Keap1]		
Domain	Cysteine	1	2	5	1	2	5
N-terminal	C13						
	C14						
	C23						1,2
	C38	1[a]	1	1,3			1,2
BTB	C77						
	C151						2,3
	C171						
Central	C196						
linker	C226	1,2,3	1,2,3	1,2,3		2	1,2,3
	C241				1,2,3	1,2,3	1,2,3
	C249		1	1,3	1,2,3	1,2,3	1,2,3
	C257						
	C273	2	2,3	1,2,3	1,2	1,2,3	1,2,3
	C288				1	1	1,2
	C297				2		
	C319	1,2	1,2,3	1,2,3		2	2,3
Kelch	C368	3	1,2,3	1,2,3		3	2,3
	C395						
	C406						
	C434	1	1,3	1,2,3			2,3
	C489			2,3			3
	C513		2,3	1,2,3	1,3	1,2,3	1,2,3
	C518		2,3	1,2,3	1,3	1,2,3	1,2,3
	C583						
C-terminal	C613			1,3			2,3
	C622						
	C624						

[a] The numbers represent the experiments out of three identical replicates in which PGA_2 or 15-PGJ_2 modified cysteines were detected by using LC-MS/MS.

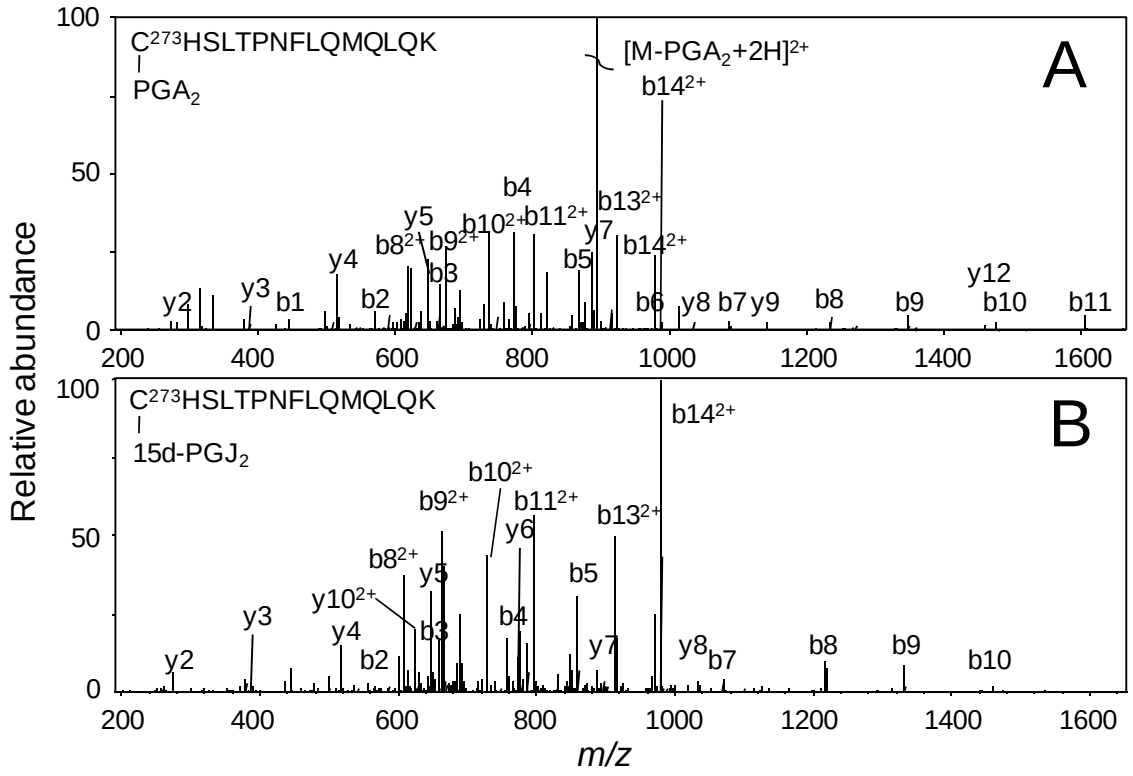

Figure 25. Product ion tandem mass spectra of Keap1 peptide 273 to 287 obtained during data-dependent LC-MS/MS analysis of a tryptic digest of Keap1 that had been incubated with A) PGA_2 ($[M+3H]^{3+}$ ion corresponding to a neutral mass of 2121.10 was used as the precursor ion); or B) 15d-PGJ_2 ($[M+3H]^{3+}$ ion corresponding to a neutral mass of 2103.09 was selected for MS/MS). Data were acquired using high resolution accurate mass measurement, and mass assignments were within 10 ppm of the theoretical values. Keap1 samples were prepared identically.

3.4 Summary

The reaction of Keap1 cysteine sulfhydryl groups with sulforaphane is a highly reversible process. After Keap1 has formed adducts with sulforaphane, treatment with iodoacetamide causes competition between iodoacetamide and the free-sulforaphane that was formed via dissociation from the Keap1-sulforaphane adduct. Iodoacetamide has been routinely used to block unmodified cysteines and prevent disulfide bond formation during tryptic digestion and mass spectrometric analysis. However, we have

demonstrated that the use of iodoacetamide can obscure results and interpretation since highly reversible, cysteine-sulforaphane adducts at sites such as C151 can readily dissociate and be outcompeted by iodoacetamide thereby making the cysteine-sulforaphane adducts undetectable. By shortening the DTT quenching time, eliminating treatment with iodoacetamide, and minimizing tryptic digestion time, sample preparation is shortened so that even the most reversible cysteine-sulforaphane modified residues such as C151-sulforaphane can be detected. In addition, our methodology shows that one can routinely obtain at least 90% amino acid coverage and detection of all 27 cysteines of Keap1. This approach revealed a Keap1 modification pattern that is considerably different from those reported previously or obtained during this investigation using iodoacetamide in the protocol. Notably, C151 was determined to be one of four cysteine residues preferentially modified by sulforaphane, and these chemical mapping results are consistent with in vivo observations reported by multiple investigators. Future mapping studies of electrophiles that reversibly react with Keap1 cysteine sulfhydryl groups should also minimize sample preparation time and avoid unnecessary derivatization with iodoacetamide.

Electrophiles that react with Keap1 through Michael addition belong to a common classes of ARE activators. The relative rates of reversibility of five Michael additions acceptors that are also ARE activators were investigated including isoliquiritigenin, xanthohumol, CDDO-Im, $PGA_{2,}$ and 15d-PGJ_2. The order of dissociation from Keap1 of these five Michael addition acceptors as well as sulforaphane was CDDO-Im > sulforaphane > PGA_2 > isoliquiritigenin > xanthohumol = 15d-PGJ_2. Because Michael addition products are reversible, LC-MS/MS based mapping studies of tryptic peptides of

modified Keap1 must be carried out quickly. A streamlined procedure that eliminates iodoacetamide treatment was found to be essential for the detection of sulforaphane adducts with C151 of Keap1. Compounds that formed slightly less reversible adducts with Keap1 such as PGA_2 and isoliquiritigenin also benefitted from the modified procedure. However, Michael addition acceptors such as CDDO-Im that form much less stable adducts with Keap1 than does sulforaphane dissociated too quickly for any sites of Keap1 modification to be detected using even the modified sample processing procedure.

Finally, the sites of human Keap1 modification by the potent ARE activators PGA_2 and 15d-PGJ_2, were identified. Previously, binding of these compounds had been investigated only using mouse Keap1. Our in vitro data agreed well with previous in vivo observations of mouse Keap1 that indicated PGA_2 and 15d-PGJ_2 modify sites other than C151.

4 EFFECT OF CUL3 ON CYSTEINE MODIFICATION OF WILD-TYPE HUMAN KEAP1 AND KEAP1 C151W MUTANT BY ISOLIQUIRITIGENIN

4.1 Introduction

Keap1 serves as a redox-regulated substrate adaptor protein for Cul3. Since the original Nrf2-Keap1 dissociation model was challenged both in vitro [63] and in vivo [47, 126], disruption of the Nrf2 ubiquitination pathway facilitated by the Cul3-based E3-ligase ubiquitination complex has attracted attention. Zhang *et al*. [47] have found that the Keap1 C151S mutant was significantly resistant to downregulation of Keap1-dependent ubiquitination of Nrf2 by both tBHQ and sulforaphane in the presence of Cul3. They proposed that modification of Keap1 C151 by electrophiles such as tBHQ or sulforaphane reduces the ability of Keap1 to associate with Cul3, targeting less Nrf2 for ubiquitination and degradation and leading to more Nrf2 in the nucleus.

Studies by Gao *et al.* [64] using coimmunoprecipitation and Rachakonda *et al.* [65] using CD spectroscopy demonstrated that the secondary structure of wild-type Keap1 protein changes and is accompanied by dissociation of the Keap1 and Cul3 complex after exposure to oxidized eicosapentaenoic acid, a major component of fish oil [64], or IAB [65]. In contrast, a C151S mutant of Keap1 was resistant to IAB-induced structural change and did not dissociate from Cul3. In order to find out whether modification of other Keap1 cysteines in addition to C151 is required to alter the Keap1-Cul3 interaction, Eggler *et al*. [59] mutated Keap1 C151 to the amino acid with the largest partial molar volume, tryptophan, to mimic the steric modification of C151 by electrophilic molecules. Remarkably, transfected Keap1 C151W was largely unable to facilitate Nrf2 ubiquitination, resulting in a level of Nrf2 that was similar to that observed

in the absence of overexpressed Keap1. In addition, immunoblot analysis indicated that modification of C151 to a tryptophan destabilized Keap1-Cul3 interaction but did not alter the affinity of mutant Keap1 for Nrf2. Considering the large amount of IAB (molar ratio Keap1/IAB = 1:135) used by Rachakonda *et al.* [65], it is questionable whether IAB at a physiologically relevant level would produce similar conformational changes in Keap1 and disrupt the interaction between Keap1 and Cul3.

To help clarify how Keap1 modification at C151 can disrupt Keap1-Cul3 interaction, peptide mapping studies were carried out using isoliquiritigenin as a Keap1 C151-dependent natural product ARE activator [57]. LC-MS/MS was used to probe for conformational changes that altered cysteine modification on Keap1 and Cul3 before and after binding. Alteration in cysteine accessibility to electrophiles has been used previously as a tool to detect protein conformational changes [127, 128]. The Keap1 cysteine modification pattern in wild type Keap1 and the C151W mutant as well the Cul3 cysteine modification pattern were determined during Keap1 Cul3 binding.

4.2 Experimental section

4.2.1 Protein preparation and materials

Recombinant human wild-type (wt) Keap1, Keap1 C151W mutant and Cul3 proteins were provided by Dr. Aimee Eggler and Dr. Evan Small of the University of Illinois at Chicago. The details of cloning, expression, and purification were described elsewhere [47, 59, 63]. The proteins were stored at a concentration of 250 μM in 50 mM Tris-HCl buffer (pH 8.0) containing 2 mM TCEP, 250 mM sodium chloride and 20% glycerol (v/v).

4.2.2 Reaction of isoliquiritigenin with wt Keap1 and Keap1 C151W

Human wt Keap1 or Keap1 C151W (10 µM) were preincubated for 30 min with Cul3 at molar ratio of 2:1 (Keap1/Cul3) and then incubated with isoliquiritigenin at molar ratios of 1:2, 1:5 and 1:20 (Keap1/isoliquiritigenin) in 100 µL 20 mM Tris-HCl buffer (pH 8.0) for 2 h at room temperature. As a control, Cul3 (5 µM) was incubated with isoliquiritigenin at molar ratios of 1:4 and 1:10 (Cul3/isoliquiritigenin). A comparison reaction was carried out in a reverse order by incubating wt Keap1 (10 µM) that had been preincubated with isoliquiritigenin at molar ratios of 1:2 and 1:5 (Keap1/isoliquiritigenin) for 2 h with Cul3 for 2 h at a molar ratio of 2:1 (Keap1/Cul3). Reaction products of the 1:20 molar ratio incubation were analyzed using MALDI-TOF MS immediately after incubation and the other reactions were quenched by adding 1 mM DTT and incubating for an additional 15 min. Iodoacetamide (3 mM) was then added to block any remaining free cysteine residues. After incubating for 45 min in the dark, an additional 5 mM DTT was added to remove excess iodoacetamide before tryptic digestion. Mass spectrometry grade trypsin (Promega; Madison, WI) was added to each sample at a trypsin/Keap1 ratio of 1:50 (w/w) and incubated at 37 °C for 1.5 h. The tryptic peptides were analyzed using LC-MS/MS as described below to determine the sites of covalent attachment of isoliquiritigenin.

4.2.3 MALDI-TOF mass spectrometry

Aliquots (1.0 µL) of each Keap1 reaction solution were mixed with 1.0 µL aliquots of a matrix solution consisting of sinapic acid in acetonitrile/water/trifluoroacetic acid (50:49.9:0.1, v/v/v) at a concentration of 10 mg/mL. Immediately before analysis, 1

µL of each mixture was spotted onto the MALDI sample plate and air-dried. Positive ion MALDI-TOF mass spectra were acquired over the range of *m/z* 65,000-80,000, operating in a linear mode.

4.2.4 High resolution Nano LC-MS/MS

To identify the cysteine modification sites on wt Keap1, Cul3 and the Keap1 151W mutant, analyses were carried out using a Thermo LTQ-FT ICR mass spectrometer equipped with a Dionex microcapillary HPLC system. Tryptic peptides were concentrated on a LC Packings C_{18} PepMap precolumn cartridge (5 µm, 0.3 mm x 5 mm) and separated on an Agilent Zorbax C_{18} reverse phase column (3.5 µm, 75 µm x 150 mm). The solvent system consisted of a 35 min linear gradient from 5% to 45% solvent B and then from 45% to 80% solvent B over 15 min (solvent A: 95:4.9:0.1; and solvent B: 4.9:95:0.1, water/acetonitrile/formic acid, v/v/v) at a flow rate or 250 nL/min. Positive ion electrospray mass spectra were acquired on a LTQ-FT ICR hybrid mass spectrometer in data-dependent MS/MS mode in which the five most abundant peptide ions in each mass spectrum were selected for CID using a normalized collision energy of 35%. All LC-MS/MS data were processed using Bioworks 3.3.1 and MassMatrix with searching parameters described previously, followed by manual validation of each modification site.

4.3 Results and discussion

4.3.1 Effect of Cul3 binding on cysteine modification of human wt Keap1 by isoliquiritigenin

4.3.1.1 MALDI-TOF MS

Incubation of Keap1 with isoliquiritigenin at a molar ratio of 1:20 resulted in an average increase in mass of Keap1 of 909 Da due to multiple Michael acceptor additions (Figure 26A). The presence of Cul3 as a binding partner of Keap1 resulted in a smaller increase in average mass of Keap1 of 792 Da (Figure 26B). The smaller mass increase indicates that Cul3 binding prevents modification of some cysteine residues of Keap1 by isoliquiritigenin. However, this experiment did not address which cysteine(s) of Keap1 or Cul3 were affected when Cul3 bound to Keap1.

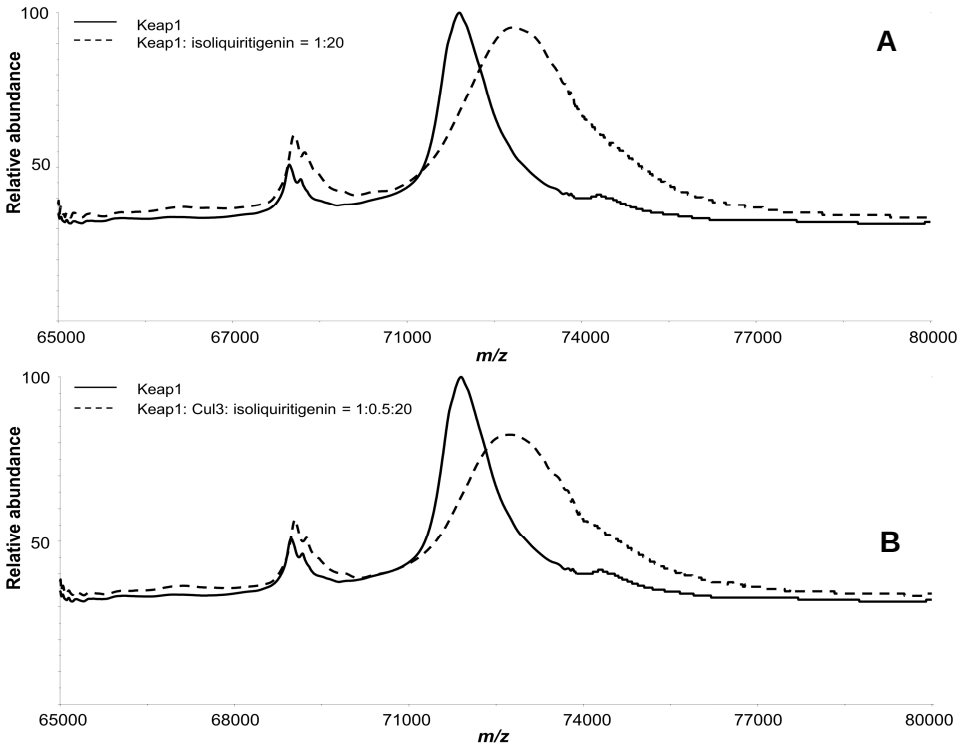

Figure 26. Positive ion MALDI-TOF mass spectra of Keap1 after incubation with A) isoliquiritigenin; and B) isoliquiritigenin in the presence of Cul3. The solid lines indicate Keap1 incubation with buffer (control) (*m/z* 71,978). The dashed line in A) represents Keap1 incubated with isoliquiritigenin (*m/z* 72,887) and in B) represents Keap1 incubated with isoliquiritigenin after preincubation with Cul3 (*m/z* 72,770).

4.3.1.2 LC-MS/MS analysis

To address this question of which cysteine residues of the Keap1-Cul3 complex are modified by isoliquiritigenin, tryptic digestion and LC-MS/MS analysis was used to identify specific modified sites. Routinely, 90% and 60% of the Keap1 and Cul3 protein sequence, respectively, were covered by MS/MS analysis of the tryptic digest using the LTQ-FT ICR mass spectrometer. All the Keap1 and most of the Cul3 cysteine-containing tryptic peptides were detected, except C156, C251 and C522 of Cul3. Cysteine residues on both Keap1 and Cul3 were found to have reacted with isoliquiritigenin. Examples of

MS/MS sequencing of Keap1 and Cul3 peptides modified by isoliquiritigenin are shown in Figure 27.

Among the 27 cysteines of human Keap1, the cysteine residues most readily modified by isoliquiritigenin were C23, C151, C226, C319 and C613 (TABLE VI). The most readily modified of the 10 cysteine residues of Cul3 were C187 and C636. TABLE VI shows that the binding of Cul3 to Keap1 reduced modification of Keap1 by isoliquiritigenin at C226 and enhanced modification at C196. When Cul3 was bound to Keap1, C187 of Cul3 was no longer modified by isoliquiritigenin. Notably, the most reactive residue of Keap1 C151 [57], was still identified as one of the top two reactive sites in the presence of Cul3, as determined by the number of time the peptide was detected in triplicate experiments. This is consistent with the hypothesis that C151 of Keap1 functions a sensor for electrophiles in the ARE activation pathway.

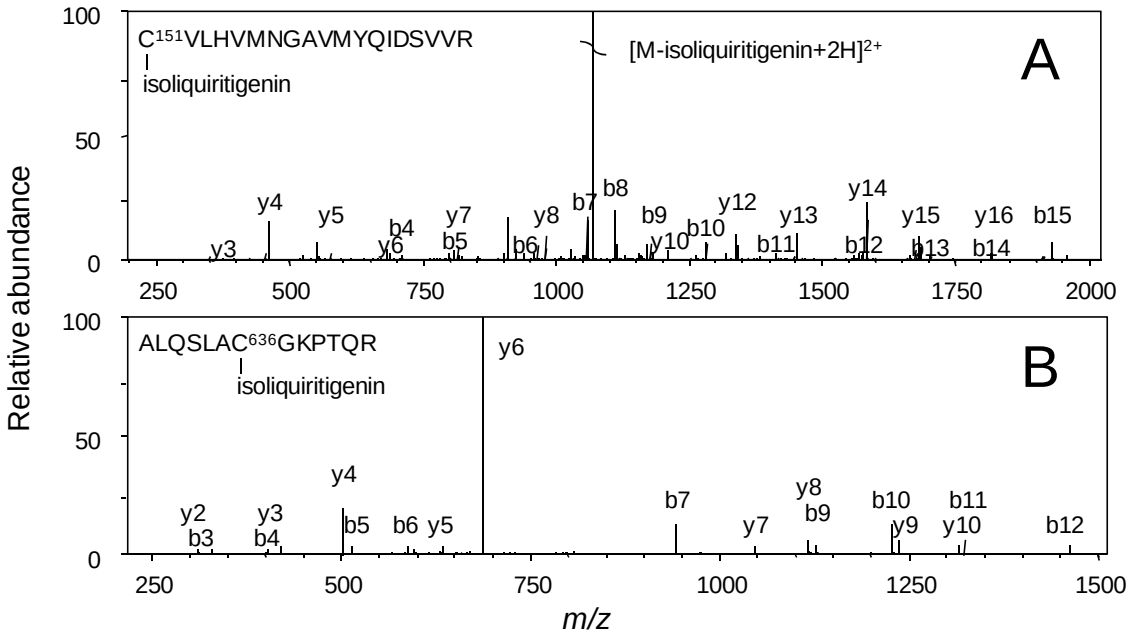

Figure 27. Product ion tandem mass spectra of tryptic peptides of Keap1 and Cul3 after incubation with the Michael addition acceptor isoliquiritigenin obtained during data-dependent LC-MS/MS analysis using high resolution accurate mass measurement. Mass assignments were within 10 ppm of the theoretical values. The samples were prepared identically except as follows: A) Keap1 peptide 151 to 168. The abundant $[M+2H]^{2+}$ ion (corresponding to a neutral mass of 2389.13) was used as the precursor ion for MS/MS; and B) Cul3 peptide 630 to 642 incubated with isoliquiritigenin. The $[M+2H]^{2+}$ ion (corresponding to a neutral mass of 1627.79) was selected for product ion MS/MS.

4.3.2 Effect of Cul3 binding on the cysteine modification pattern of human Keap1 C151W mutant by isoliquiritigenin

Based on the fact that a variety of ARE activators depend on Keap1 C151 to fully activate the ARE and the high reactivity of C151 towards many activators [56, 57, 62], Eggler *et al.* [59] mutated C151 to tryptophan, the amino acid with the largest partial molar volume, to mimic the modification of C151 by electrophiles. In MDA-MB-231 cells, the elevated ARE level showed that C151W mutation causes Keap1 to lose its ability to repress Nrf2. Remarkably, no disruption of Keap1-Nrf2 interaction by the

Keap1 C151W mutation was detected; whereas, the interaction with Cul3 was destabilized [59]. Since C151 is located in the Keap1 BTB dimerization domain, which interacts with Cul3, modification at C151 might cause a Keap1 conformational change specifically affecting the interaction with Cul3 instead of altering binding to Nrf2.

Isoliquiritigenin was used as a model compound to probe changes in Keap1 modification as a result of C151W mutation. LC-MS/MS analysis of Keap1 C151W and wt Keap1 showed similar cysteine modification patterns by isoliquiritigenin (TABLE VI). With the addition of Cul3, modification of Keap1 by isoliquiritigenin was enhanced at C38 and C196. Similar to wt Keap1, C187 of Cul3 was not modified by isoliquiritigenin when Cul3 was bound to Keap1 C151W. This implies that C187 of Cul3 might be located in the Keap1 and Cul3 binding interface so that modification of C187 by isoliquiritigenin is blocked when the two proteins are bound to each other.

Interestingly, C636 on Cul3 was not modified by isoliquiritigenin when Cul3 was bound to Keap1 C151W. However, C636 was modified by isoliquiritigenin in the presence of wt Keap1 (TABLE VI). A possible explanation for the different reactivity of wt and mutant Keap1 bound to Cul3 might be that C151W mutation represents Keap1 100% modified by isoliquiritigenin at C151 before binding to Cul3, which simulates the stimulated condition by activators in cells; whereas wt Keap1 represents 0% modification before binding, which simulates the basal condition. The differential modification of Cul3 C636 implies a Keap1-Cul3 conformational change for the C151W mutant, either by concealing C636 or lowering its activity.

TABLE VI

CYSTEINE RESIDUES IN HUMAN WT KEAP1, KEAP1 C151W MUTANT AND CUL3 MODIFIED BY ISOLIQUIRITIGENIN

Conditions		Modified cysteines			
Preincubation	Addition	Keap1[a]	Cul3[c]	Keap1[b]	Cul3[d]
Keap1 wt	isoliquiritigenin	C23[1,2,3][f], C151[1,2,3], C226[1,2,3], C319[1,2,3], C613[2]		C23[1,2,3], C38[2,3], C151[1,2,3], C226[1,2,3], C319[1,2,3], C613[2]	
Keap1 C151W	isoliquiritigenin	C23[2,3], C226[1,2,3], C319[1,2,3], C613[1]		C23[1,2,3], C38[2,3], C226[1,2,3], C319[1,2,3], C434[3], C613[2,3]	
Cul3	isoliquiritigenin		C187[1,3], C636[1,2,3]		C187[1,2,3], C636[1,2,3]
Keap1 wt + Cul3[e]	isoliquiritigenin	C23[2], C38[3], C151[1,2,3], C196[1,2], C319[1,2,3], C613[1]	C636[1,2,3]	C23[1,2,3], C38[2,3], C151[1,2,3], C196[1,2,3], C226[1,2,3], C319[1,2,3], C368[3], C613[2,3]	C636[1,2,3]
Keap1 C151W + Cul3[e]	isoliquiritigenin	C23[1,3], C38[2,3], C226[1,3], C319[1,2,3]	None detected	C23[1,2,3], C38[1,3], C196[2], C226[1,2,3], C319[1,2,3], C434[3], C613[1,2,3]	None detected
Keap1 wt + isoliquiritigenin	Cul3[e]	C23[3], C38[3], C151[1,2,3], C319[3]	None detected	C23[1,3], C38[3], C151[1,2,3], C196[1,3], C226[1,3], C319[1,3], C368[1,3], C395[1], C613[3]	None detected

[a] Molar ratio isoliquiritigenin/Keap1 = 2

[b] Molar ratio isoliquiritigenin/Keap1 = 5

[c] Molar ratio isoliquiritigenin/Cul3 = 4

[d] Molar ratio isoliquiritigenin/Cul3 = 10

[e] Keap1 wt or mutant was incubated with Cul3 at a molar ratio of 2:1.

[f] Triplicate experiments were performed. The numbers indicate the experiments in which isoliquiritigenin-modified peptides were detected by using LC-MS/MS.

If modification at Keap1 C151 prevents modification of C636 of Cul3 bound to Keap1, then a question arises about the sample in which Keap1 and Cul3 are preincubated, followed by isoliquiritigenin addition. In this sample, why is C636 still

detected as modified, even though C151 is shown to be modified? One explanation for the detection of Cul3 C636 modification in this wt Keap1 experiment is that only a small percentage of Keap1 was modified at Keap1 C151 and bound to Cul3, and the majority of Keap1 was unmodified at C151. A second explanation is that Cul3 prebound to Keap1 blocks the conformational change in Keap1 triggered by C151 modification, allowing modification of C636. A third explanation is kinetics, that Cul3 C636 had already been modified by the time the conformational change of Keap1 happened after C151 modification, and thus C636 modification was detected after tryptic digestion. If all the exposed cysteines including Keap1 C151 and Cul3 C636 have an equal opportunity to be modified by isoliquiritigenin, the first scenario is unlikely. However, we do not know what percentage of Keap1 was modified at C151, and the experiment did not address whether the extent of modification was sufficient to result in a conformational change of Keap1 and the sequential alteration of Cul3 interaction.

To address this question further, we premodified Keap1 with isoliquiritigenin followed by binding to Cul3. In order to rule out the possibility that modified Cul3 C636 would not be detected due to insufficient isoliquiritigenin in the reaction, we used LC-MS-MS to measure the isoliquiritigenin concentration in the solution (as described in 2.2.4) before Cul3 addition to ensure that excess isoliquiritigenin was available. Modification of Cul3 C636 was not detected when ~ 26% of the original isoliquiritigenin was still free in solution before Cul3 addition. The simplest explanation is that C151 was modified in the majority of Keap1 molecules prior to Cul3 addition, preventing C636 modification, ruling out the possibility that only a small percentage of Keap1 was modified at C151 in the previous experiment. This also indicates that the binding rate of

Cul3 to Keap1 is much faster than the rate of reaction of isoliquiritigenin with C636. It is unknown whether the Keap1 conformational change induced by C151 modification is slower than the reaction of C636 with isoliquiritigenin, or whether Cul3 binding blocks this conformational change. However, modification by isoliquiritigenin at a 1:2 ratio (Keap1/isoliquiritigenin) is sufficient to induce the conformational change in the Keap1-Cul3 interaction thereby concealing Cul3 C636.

Although a change in binding affinity cannot be ruled out, Keap1 and Cul3 definitely bind even after modification of Keap1 C151, which is contrary to a previous study reporting that Keap1 and Cul3 do not bind after modification of C151 [65]. We propose that modification of C151 of Keap1 generates a conformational change that extends to the Cul3 protein in the Keap1-Cul3 complex. This hypothesis is consistent with the observation that certain activators, including IAB and tBHQ, not only cause decreased ubiquitination of Nrf2 but also increase Cul3-dependent ubiquitination of Keap1 [47, 58]. This increased ubiquitination of Keap1 is only possible if in the cellular environment Keap1 and Cul3 are associated.

Most previous studies have focused on the oxidative stress sensor properties of Keap1, and no studies have reported the identification of any key cysteine residues on Cul3 yet. In this investigation, Cul3 C636 was identified for the first time as a reactive cysteine. It is notable that besides indicating a Keap1-Cul3 structural alteration, modification of Cul3 C636 might play a sensor role in ARE activation. Further detailed investigation is needed to determine the role of Cul3 C636 in the ARE activation pathway.

4.4 Summary

Modification of Keap1 C151 has been proposed to disrupt Nrf2 ubiquitination by inducing Keap1 conformational changes and destabilizing the Keap1-Cul3 interaction. The large amount of eletrophile used in these studies raises the question of whether a more physiological concentration of electrophile would have the same effect. To address this concern, we used the well-studied natural ARE activator isoliquiritigenin to investigate changes in Keap1 modification upon binding to Cul3.

The pattern of modification of Keap1 by isoliquiritigenin has been reported by our group previously [56]. However, whether conformational changes of Keap1 or Cul3 occur during the activation of the ARE were unclear. By comparing Keap1 modification by isoliquiritigenin with or without binding to Cul3, we found that the reactivity of two cysteine residues of Keap1, C226 and C196 were altered upon binding of Keap1 to Cul3. However, the key sensor cysteine of Keap1, C151, still showed high reactivity after Cul3 binding. Isoliquiritigenin modified wt Keap1 and the Keap1 C151W mutant in a similar manner in the absence of Cul3. With the addition of Cul3, the reactivity of C38 and C196 of Keap1 mutant were enhanced. C187 of Cul3 was no longer modified by isoliquiritigenin, when Cul3 was bound to wt Keap1 or Keap1 C151W. This indicates the C187 of Cul3 moght be protected within the Keap1-Cul3 complex.

Cul3 C636 was identified as a site that is reproducibly modified by isoliquiritigenin when incubated with Cul3 alone or Cul3 with wt Keap1. However, Cul3 C636 does not react with isoliquiritigenin when Cul3 is bound to Keap1 C151W, which implies that a Keap1-Cul3 conformational change occurs due to Keap1 C151 modification (such as mutation of cysteine to tryptophan). By preincubating wt Keap1

with isoliquiritigenin before allowing Keap1 to bind to Cul3, it was confirmed that C636 of Cul3 is prevented from reacting with isoliquiritigenin. This was probably due to a conformational change that might also shut down Nrf2 ubiquitination and cause Keap1 ubiquitination.

5 MAPPING THREE-DIMENSIONAL STRUCTURES OF THE KEAP1-CUL3 COMPLEX BY CHEMICAL CROSS-LINKING AND MASS SPECTROMETRY

5.1 Introduction

Understanding of the three-dimensional structure of proteins as well as protein-protein interactions plays a crucial role in comprehending the molecular mechanisms underlying biological processes. To date, x-ray crystallography and nuclear magnetic resonance (NMR) spectroscopy are two primary strategies offering high-resolution structural characterization of protein and protein complexes. However, both techniques require a large amount of material, are intrinsically time-consuming and in many cases, not feasible, if the protein does not form crystals that diffract well or is too large for NMR.

Chemical cross-linking of proteins has long been used to map protein-protein interactions. With the recent improvements in instrument sensitivity, mass accuracy, peptide fragmentation, and database searching, cross-linking in combination with mass spectrometry has emerged as an indispensable tool for structural characterization of protein and protein-protein interactions [129-131]. Although the structural information is low-resolution in its nature, this alternative approach has great potential to overcome some of the inherent limitations of X-ray crystallography and NMR. MS analysis is applicable to identify exact interaction sites in protein complexes with a relatively small amount of material, fast analysis speed and automated data process. In addition, since the identification of cross-links is based on the peptide level, the mass range of the protein

complex is theoretically unlimited. Furthermore, the wide range of specificities for cross-linkers toward functional groups and spacer length offer diverse options for experimental design [132], which can provide important supplemental information to X-ray or NMR structural data and can provide low-resolution structural information when X-ray or NMR methods are not possible. However, despite the apparent advantages, identification and correct assignment of the cross-linked peptides by MS can be hampered by the complexity of the peptide mixtures containing predominantly non-cross-linked peptides. Moreover, most of the commercialized database searching software such as SEQUEST and Mascot do not have an option to deal with cross-linking data. Manual inspection becomes an essential tool in cross-linking study. Indeed, this laborious and low-throughput data analysis and validation has often been likened to "*finding a needle in a hay stack"* [133].

As discussed in the previous section, modification of C151 of Keap1 appears to alter the interaction between Keap1 and Cul3 by a conformational change upon exposure to chemopreventive compounds such as isoliquiritigenin. However, there are some exceptions to this partial molar volume dependent model such as the Keap1 C151-independent activator 15d-PGJ_2. To understand the molecular mechanisms underlying the interaction of Keap1 and Cul3 precisely, three-dimensional structure analysis is essential. Due to the difficulty in crystallizing the full-length dimeric Keap1 [134] and the large size of both proteins, no three-dimensional structure of Keap1 or Cul3 has been solved to date.

Here, we investigated the structure of a Keap1 dimer and Cul3 complex using cross-linking coupled with mass spectrometry. The Keap1 and Cul3 complex was

subjected to the cross-linking reaction followed by enzymatic digestion and mass spectrometric analysis. Homobifunctional cross-linkers were used to crosslink Keap1 and Cul3 protein by targeting primary amines on the proteins. The structural information yielded from this strategy is low resolution, but the identification of intra- and intermolecular cross-linked peptides will be valuable to gain insight into how the proteins fold, and which residues are exposed on the surface and may involved in the Keap1 and Cul3 interaction. In addition, these data will be useful to facilitate protein-protein docking models and guide X-ray analysis with the ultimate goal of elucidating the role of the Keap1 and Cul3 complex in the molecular mechanism.

5.2 Experimental Section

5.2.1 Materials

Recombinant human Keap1 and Cul3 proteins were provided by Dr. Eggler and Dr. Small of the University of Illinois at Chicago. The details of cloning, expression, and purification were reported elsewhere [47, 63]. The proteins were stored at a concentration of 250 μM in 50 mM Tris-HCl buffer (pH 8.0) containing 2 mM TCEP, 250 mM sodium chloride and 20% glycerol (v/v). Cross-linking reagent bis(sulfosuccinimidyl) suberate (BS^3) was purchased from Thermo Fisher Scientific (Rockford, IL). A bio-Silect 250 size exclusion column was purchased from Bio-Rad (Hercules, CA). Centricon 20 devices [30,000 molecular weight cut-off (MWCO)] were purchased from Millipore (Bedford, MA). Mass spectrometry-grade trypsin and chymotrypsin were purchased from Promega (Madison, WI). Glutaraldehyde solution (25 wt. % in H_2O) and other reagents were purchased from Sigma-Aldrich (Milwaukee, WI and St. Louis, MO).

5.2.2 Chemical cross-linking method optimization using glutaraldehyde

The protein storage buffer of both Keap1 and Cul3 was exchanged with cross-link buffer 20 mM HEPES (pH 8.0) containing 2 mM TCEP and 150 mM sodium chloride using a Centricon 20 device by performing three sequential 180-fold dilutions according to the manufacturer's instructions. Keap1-Cul3 complex (250 μM) was made by incubating Keap1 (500 μM) and Cul3 (250 μM) at a molar ratio of 2:1 at room temperature for 30 min. Different concentrations of Keap1-Cul3 complex ranging from 1 μM to 250 μM were treated with glutaraldehyde aqueous stock solution (25%) to produce a final glutaraldehyde concentration ranging from 0.01% to 5%.

5.2.3 Keap1-Cul3 complex cross-linking using glutaraldehyde

Recombinant human Keap1 and Cul3 proteins were dialyzed overnight into cross-link buffer. Keap1 (56.6 μM) was incubated with Cul3 (28.3 μM) at a molar ratio of 2:1 ([Keap1]/[Cul3]) in the cross-link buffer at room temperature for 30 min. The Keap1-Cul3 complex was separated by a Bio-Silect 250-5 size exclusion column on a Pharmacia AKTA FPLC system (Amersham Biosciences; Piscataway, NJ) at a flow rate of 0.5 mL/min. Freshly prepared glutaraldehyde aqueous stock solution (5%) was added to 3 μM Keap1-Cul3 complex to produce a final concentration of 0.05% (w/v) in 100 μL of cross-link buffer. The reaction was carried out at room temperature for 20 min in the dark and quenched by the addition of 1M Tris-HCl (pH 8.0) to a final concentration of 50 mM for additional 15 min to ensure complete deactivation of the glutaraldehyde. The cross-linked Keap1-Cul3 complex was purified again with the size exclusion column to minimize the non-reacted reagent and non-specific cross-linked products.

The cross-linked complex was then reduced with 5 mM DTT for 30 min at room temperature, and cysteines were reacted with 10 mM iodoacetamide in dark for 45 min in 50 mM Tris-HCl (pH 8.0). Subsequently, 10 mM DTT was added to quench remaining iodoacetamide. Mass spectrometry-grade trypsin was added at a trypsin-to-protein complex ratio of 1:20 (w/w) and incubated at 37 ^{o}C overnight. The tryptic peptides were quenched by 10% of formic acid to pH 3 and stored at -20 ^{o}C before analyzing using LC-MS/MS as described below to identify intra- and intercross-linked peptides by glutaraldehyde.

5.2.4 Keap1-Cul3 complex cross-linking using bis[sulfosuccinimidyl] suberate (BS^3)

Recombinant human Keap1 and Cul3 proteins were dialyzed and incubated using the same procedure as glutaraldehyde treatment described above. After the Keap1-Cul3 complex was separated by the size exclusion column, fresh prepared homobifunctional cross-linking reagent BS^3 in cross-link buffer was added at a molar ratio of 30-fold excess of the 6 μM complex in a total volume of 100 μL reaction. The reaction was carried out at room temperature for 60 min in the dark and quenched by the addition of 1M Tris-HCl (pH 8.0) at a final concentration of 50 mM for 15 min. The cross-linked Keap1-Cul3 complex was purified again with the size exclusion column to minimize the non-reacted reagent and nonspecific cross-linked products.

The cross-linked complex was reduced and alkylated with DTT and iodoacetamide, respectively, as glutaraldehyde treatment described above. Mass spectrometry-grade trypsin was added at an enzyme-to-protein complex ratio of 1:50

(w/w) and incubated at 37 ^{o}C overnight. Half of the samples were quenched by 10% of formic acid to pH 3 and stored at -20 ^{o}C. For another half of the samples, chymotrypsin was used as a second digestion enzyme and incubated for another 8 h at the same enzyme-to-protein ratio as trypsin. The enzymatic peptides were quenched and stored before analyzing using LC-MS/MS described below to identify intra- and intercross-linked peptides by BS^3.

5.2.5 LC-MS/MS analysis of cross-linked peptides using LTQ-FT ICR mass spectrometer

The peptide mixture was analyzed on a Thermo Finnigan (San Jose, CA) hybrid LTQ-FT ICR mass spectrometer equipped with a Dionex (Auburn, CA) microcapillary HPLC system. Reversed phase microcapillary HPLC was carried out using an Agilent Zorbax C18 column (3.5 µm, 75 µm × 150 mm) and LC Packings C18 PepMap precolumn cartridge (5 µm, 0.3 × 5 mm). The solvent system consisted of a 60 min linear gradient from 5 to 45% solvent B and then from 45 to 80% solvent B over 15 min (solvent A: 95:4.9:0.1; and solvent B: 4.9:95:0.1, water/acetonitrile/formic acid, v/v/v) at a flow rate of 250 nL/min. Positive ion electrospray mass spectra were acquired in a data-dependent mode in which each MS scan was followed by five MS/MS scans using a normalized collision energy of 35%. Dynamic exclusion was enabled to minimize redundant spectral acquisitions.

5.2.6 LC-MS/MS analysis of cross-linked peptides using LTQ-Orbitrap Velos

The cross-linked peptides sample was analyzed on LTQ-Orbitrap Velos by Dr. Alexander Schillling with the similar separation condition we used on LTQ-FT ICR mass

spectrometer. Instead of acquiring five MS/MS scans after MS scan using collision induced dissociation cell (CID) with a normalized collision energy of 35% on LTQ-FT ICR mass spectrometer, he acquired ten most intense peptide ions using a higher-energy collisional dissociation cell (HCD) with a normalized collision energy of 15% on LTQ-Orbitrap Velos.

5.2.7 Database searching and parameters setting

The MS raw files were converted to mzXML files using MassMatrix data conversion tools. Isotope distributions for the precursor ions of the MS/MS spectra were deconvoluted to obtain the charge states and monoisotopic *m/z* values of the precursor ions during the automatic conversion [90]. Searches were conducted against a created database containing the sequences of human Keap1 and Cul3 only using MassMatrix [86, 87, 114, 115]. The mass accuracy for precursor and product ions was set to 10 ppm and 0.6 Da, respectively for FT ICR data, or 10 ppm and 0.01 Da, respectively for Orbitrap data. Trypsin was chosen as the digestion enzyme with up to 2 missed cleavages allowed for glutaraldehyde and with up to 4 missed cleavages allowed for BS^3 treated samples, as chymotrypsin was used as a second enzyme. Carbamidomethylation on cysteine (+57. 0214 Da) was set as a fixed modification and methionine oxidation (+15.9949 Da) was set as a variable modification.

For glutaraldehyde treatment, the chemical formula of the linker between two lysines is specified as C_5H_4 with a monoisotopic mass of 64.0313 Da. One additional variable modification for lysine was specified due to the dead-end induced by Tris-HCl buffer (+185.1052 Da) (Figure 28A). For BS^3 treatment, the chemical formula of the

linker between two lysines is specified as $C_8H_{10}O_2$ with a monoisotopic mass of 138.0681 Da. Two additional variable modifications for lysine were specified due to the dead-end induced by water (+156.0786 Da) and Tris-HCl buffer (+259.1420 Da) (Figure 28B). Cleavages by proteases at modified lysines by glutaraldehyde or BS^3 were excluded and the maximum number of cross-links allowed for each peptide was set to 2. The search result files were sent to a posthoc analysis program, XMapper to calculate an overall score and generate cross-link assignments using a heat map figure. The cross-linked peptide candidates identified by automated matching were validated by manual inspection of the tandem mass spectra.

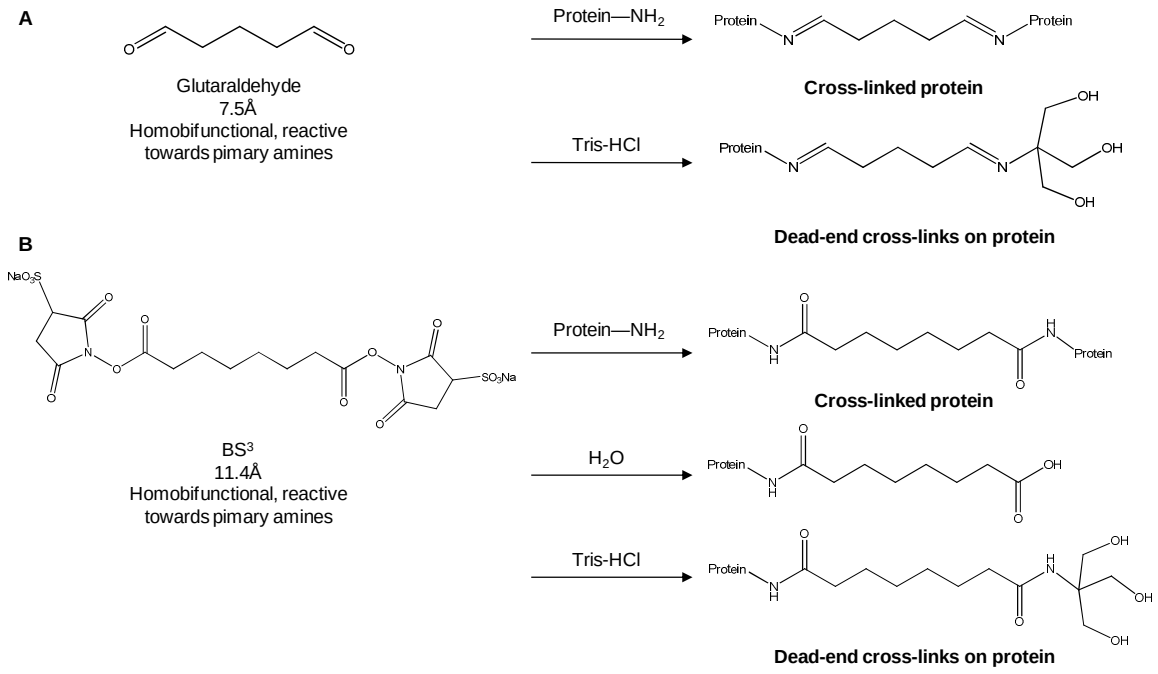

Figure 28. Structure of cross-linking reagent A) glutaraldehyde and B) BS^3, and the possible dead-end cross-links introduced by quenching reagent. The lengths shown are spacer arms of the cross-linking reagents.

5.3 Results and discussion

5.3.1 Identification of cross-linked peptides using glutaraldehyde

5.3.1.1 Method optimization

The cross-linking reaction prior to MS analysis is critical to the identification of cross-linked peptides and the following protein interaction mapping. During the reaction, the three-dimensional structure of the proteins cannot be disturbed, but on the other side, sufficient amounts of cross-linked peptides have to be generated to allow for subsequent mass spectrometric detection. Thus, the concentration of proteins and the amount of cross-linking reagent to be added were optimized in the first step.

Most proteins contain many lysine residues, usually exposed on the protein surface due to the polarity of the amine group. In addition, lysine residues are generally not involved in the catalytic site, which prevents protein conformational change and loss of biological activity by moderate cross-linking [135]. Glutaraldehyde, $CH_2(CH_2CHO)_2$, was selected due to its high reactivity and low cost in addition to its widely application in fast and efficient “freezing” interactions in tissues [136]. It is a homobifunctional reagent and it can bridge the ε-amino group of lysine side chains on the surface of the protein by forming Schiff bases [137].

Treatment with various amounts of glutaraldehyde of different concentration of the Keap1-Cul3 complex showed that either high concentration of protein complex or glutaraldehyde causes protein aggregation by size-exclusion chromatography (data not shown). Maintaining the protein complex concentration at less than 10 μM and 0.05% glutaraldehyde final concentration reduced the unwanted aggregation. In addition, to

minimize the nonspecific cross-linked products and high molecular mass aggregates, size-exclusion chromatography was applied before and after the cross-linking reaction to separate the Keap1-Cul3 complex and the cross-linked complex, respectively.

5.3.1.2 Cross-linked peptides identification

The sequence coverage of Keap1 and Cul3 proteins was 34% and 64%, respectively. A large amount of high charge state peptides were eluted after 60 min with high organic phase. Since the length of cross-linked peptides was enhanced by the cross-linker and the miscleavage site at the modified lysine residues, the low coverage for both proteins compared to previous alkylation studies is probably due to the incomplete digestion using trypsin only.

The potential cross-linked peptides were identified and mapped in the heat map using XMapper (as shown in Figure 29). A majority of the cross-links showed in the map are background cross-links with low scores in light blue or cyan. They were possibly formed on the proteins with structure altered during the cross-linking experiment, which are biologically irrelevant and represent the existence of noise in cross-linking determination [90]. As shown in Figure 29, two hits were identified with a score higher than 50 (cell in red), BK397-BK273 and BK711-BK11. Both hits are intramolecular cross-links on Cul3 protein, and BK397-BK273 was identified in duplicated experiments.

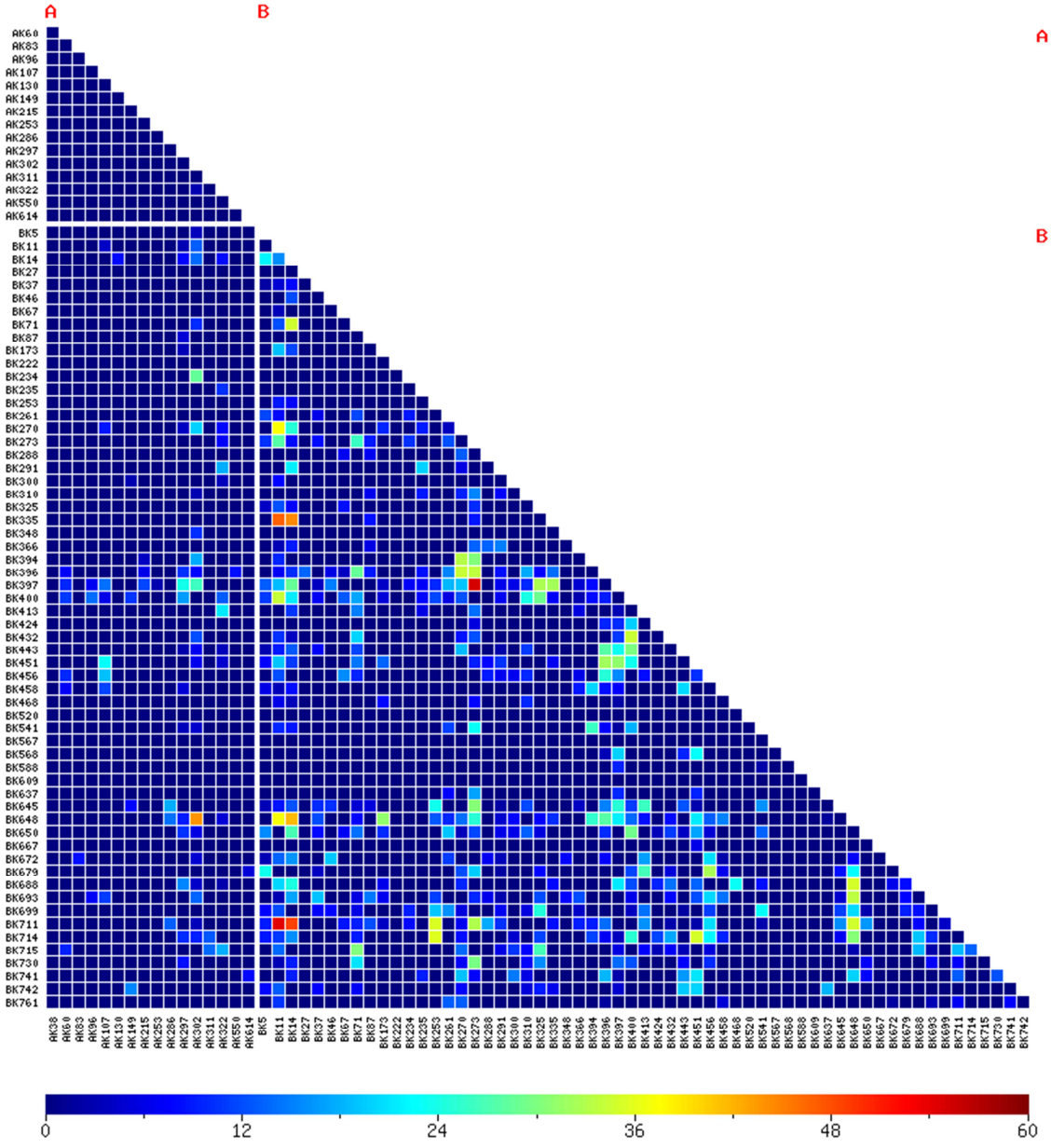

Figure 29. Cross-links in the glutaraldehyde cross-linked Keap1-Cul3 complex analyzed by LTQ-FT ICR MS followed by database searching using MassMatrix. Each cell in the heat map represents a cross-link between two lysine residues. “A” chain represents Keap1 protein and “B” chain represents Cul3 protein. Confidence of the identification of each cross-link is indicated by its score displayed in the scaled color heat map.

However, the scores of these two hits are not significantly higher than the background cross-links and neither intermolecular cross-links nor intramolecular cross-links from Keap1 protein were identified. These cross-linked peptides are probably undetected because glutaraldehyde is too short to crosslink the subunits of dimeric Keap1 or form intermolecular cross-links between Keap1 and Cul3 proteins with a spacer length of 7.5Å. A cross-linker containing a longer spacer arm may favor intermolecular cross-linking and have a better opportunity to interpret the interaction between Keap1 and Cul3. In addition, the number of lysine residues on the Keap1 surface is important for intramolecular cross-link formation. Keap1 protein (monomer) contains only 16 lysine residues (2.6% of the coverage), which are evenly distributed. Low content and the accessibility of lysine residues may also cause the low efficiency of forming intramolecular cross-links.

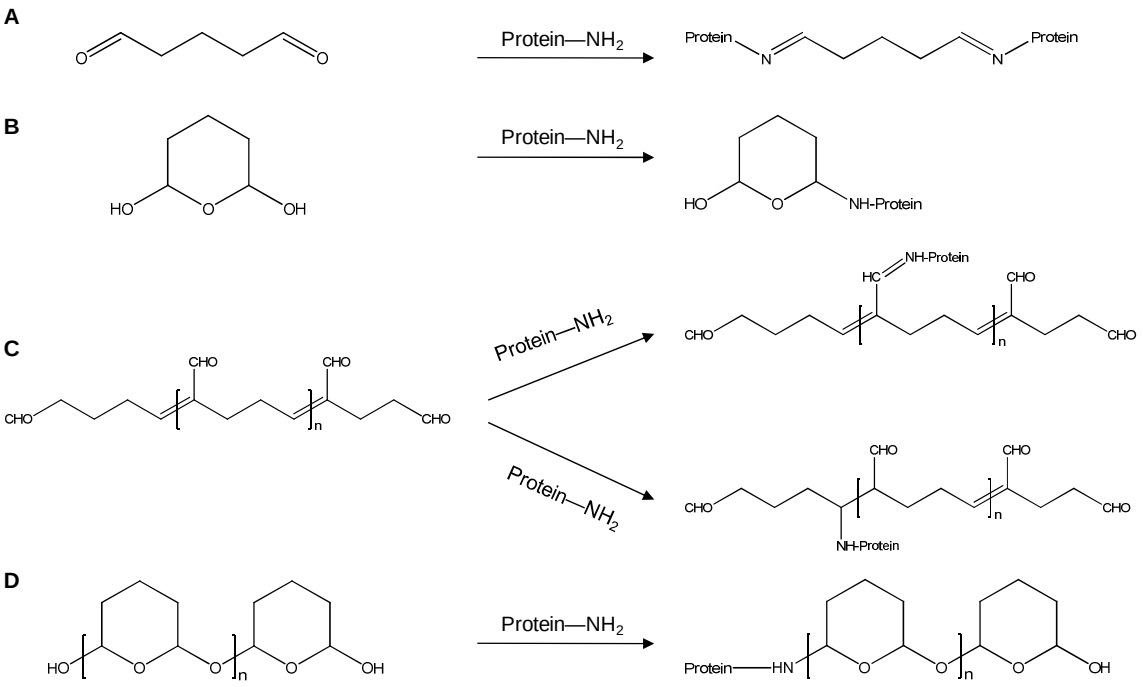

Figure 30. Possible forms of glutaraldehyde in aqueous solution and reactions with proteins. A) monomeric form, B) cyclic hemiacetal form, C) polymeric α,β-unsaturated form reacts with protein via aldol condensation (upper) or Michael addition (lower), and D) polymeric cyclic hemiacetal form.

Moreover, some studies indicated that glutaraldehyde produces high background during the process of cross-linking with proteins due to other reactions. Besides lysine, glutaraldehyde can react with other amino acids side chains such as cysteine and histidine due to its high reactivity. It has been demonstrated that in addition to the predominant monomeric form of glutaraldehyde (Figure 30A), other forms including cyclic hemiacetal of its hydrate (Figure 30B), polymeric α,β-unsaturated form (Figure 30C), and polymeric cyclic hemiacetal forms (Figure 30D) are present in aqueous solution [138]. All of these forms might participate differently in cross-linking reactions with proteins, in spite of the negligible quantity in the dilute solution [139]. Thus, the nonspecific reaction with amino acids and multiple forms of glutaraldehyde result in a broad range of conjugates, which

decreased the cross-linking efficiency and dramatically increased the complexity of database searching and identification.

5.3.2 Identification of cross-linked peptides using BS^3

A slightly longer cross-linker BS^3 (11.4 Å) was used next to crosslink the Keap1-Cul3 complex. BS^3 reacts with primary amines in lysine side chains and protein N-termini.

5.3.2.1 Enzyme digestion optimization

Chemically cross-linked peptides were classified into two types: interchain cross-links and intrachain cross-links. Peptides with more than two cross-links are difficult to characterize by tandem MS due to poor fragmentation and large size. Four possible types of cross-linked peptides were classified with up to two cross-links as shown in Figure 31. Type 1 peptides only have interchain cross-links; type 2 peptides only have intrachain cross-links; type 3 peptides are hybrids with both inter- and intrachain cross-links; and type 4 peptides have circular chains [87]. Only peptides with up to 2 cross-links were considered in MassMatrix. Therefore, manipulating the peptides within an appropriate size facilitates the cross-linking identification. Chymotrypsin was used as a second enzyme after trypsin for half of the samples in order to increase the digestion efficiency of long cross-linked peptides. The sequence coverage of Keap1 and Cul3 using trypsin were 67% and 72%, respectively. Chymotrypsin addition increased the coverage to 78% and 81%, respectively. In addition, more high score hits (score > 50) were identified with low background in the sample using two enzymes (Figure 32B) compared to the one

using trypsin only (Figure 32A). Thus, a second enzyme is essential for large complex cross-linking study such as Keap1-Cul3 complex.

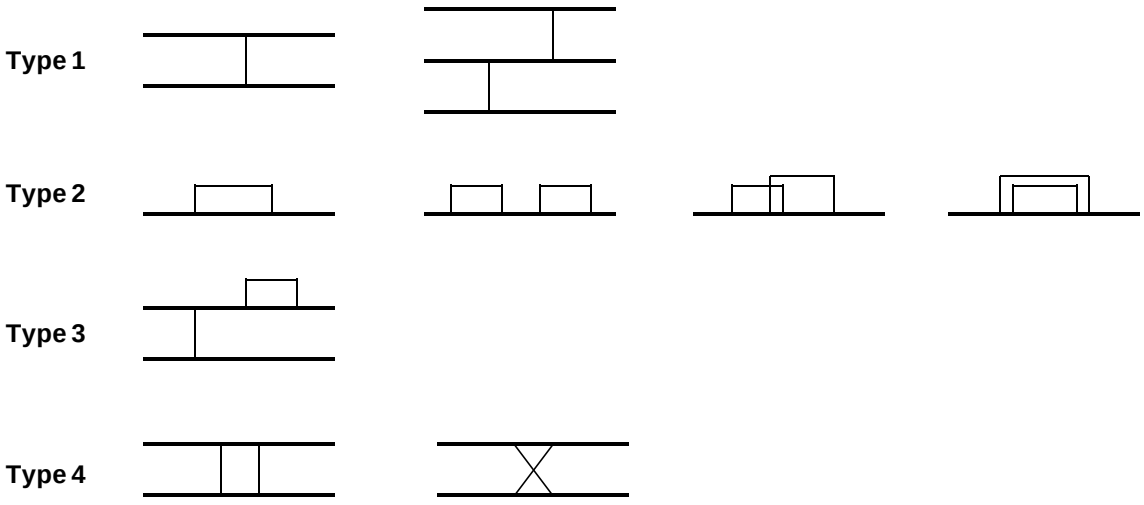

Figure 31. Four possible types of cross-linked peptides with up to two cross-links.

A

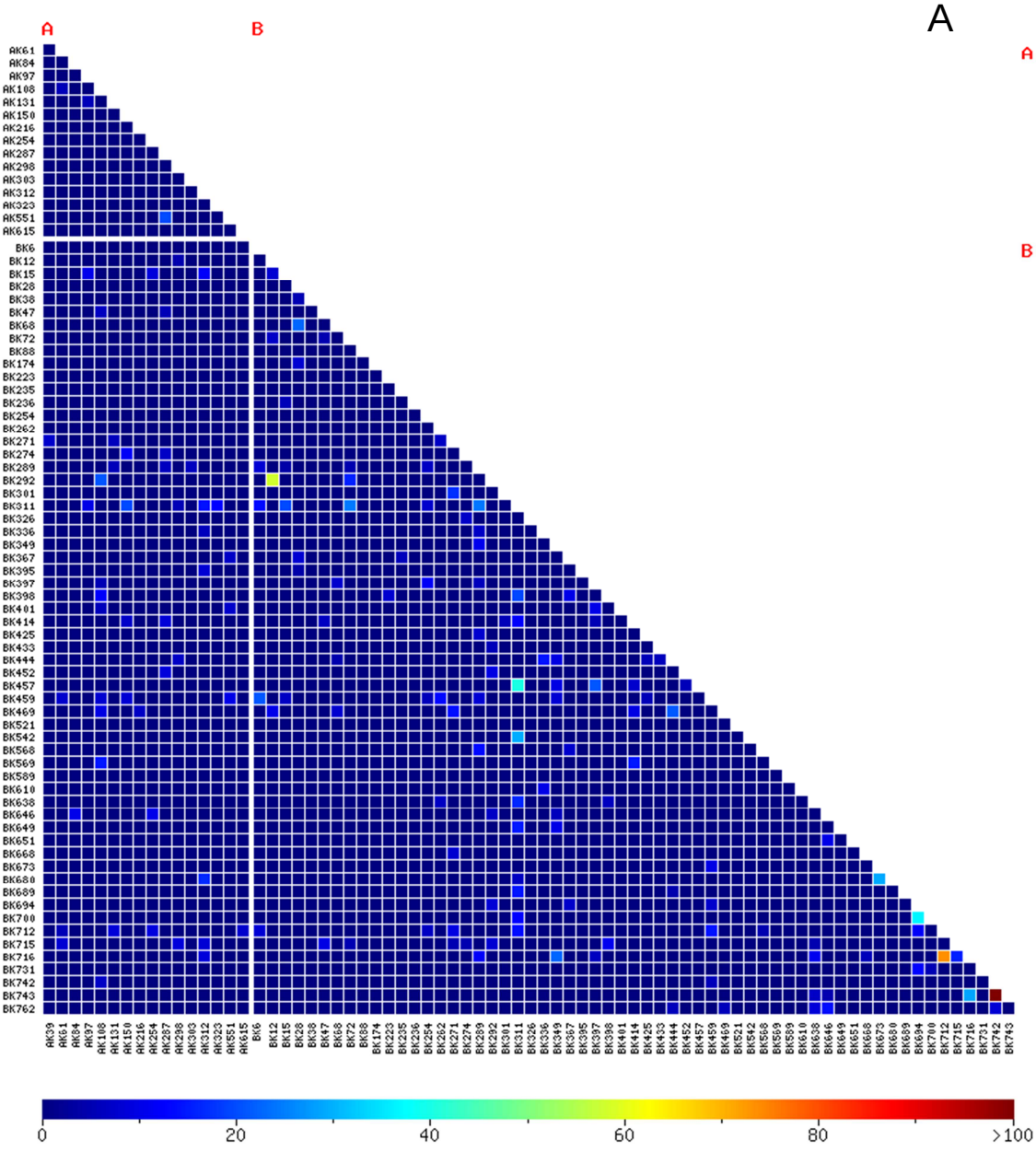
A
B
A
B
AK61
AK84
AK97
AK108
AK131
AK150
AK216
AK254
AK287
AK298
AK303
AK312
AK323
AK551
AK615
BK6
BK12
BK15
BK28
BK38
BK47
BK68
BK72
BK88
BK174
BK223
BK235
BK236
BK254
BK262
BK271
BK274
BK289
BK292
BK301
BK311
BK326
BK336
BK349
BK367
BK395
BK397
BK398
BK401
BK414
BK425
BK433
BK444
BK452
BK457
BK459
BK469
BK521
BK542
BK568
BK569
BK589
BK610
BK638
BK646
BK649
BK651
BK668
BK673
BK680
BK689
BK694
BK700
BK712
BK715
BK716
BK731
BK742
BK743
BK762
AK39
AK61
AK84
AK97
AK108
AK131
AK150
AK216
AK254
AK287
AK298
AK303
AK312
AK323
AK551
AK615
BK6
BK12
BK15
BK28
BK38
BK47
BK68
BK72
BK88
BK174
BK223
BK235
BK236
BK254
BK262
BK271
BK274
BK289
BK292
BK301
BK311
BK326
BK336
BK349
BK367
BK395
BK397
BK398
BK401
BK414
BK425
BK433
BK444
BK452
BK457
BK459
BK469
BK521
BK542
BK568
BK569
BK589
BK610
BK638
BK646
BK649
BK651
BK668
BK673
BK680
BK689
BK694
BK700
BK712
BK715
BK716
BK731
BK742
BK743
0
20
40
60
80
>100

B

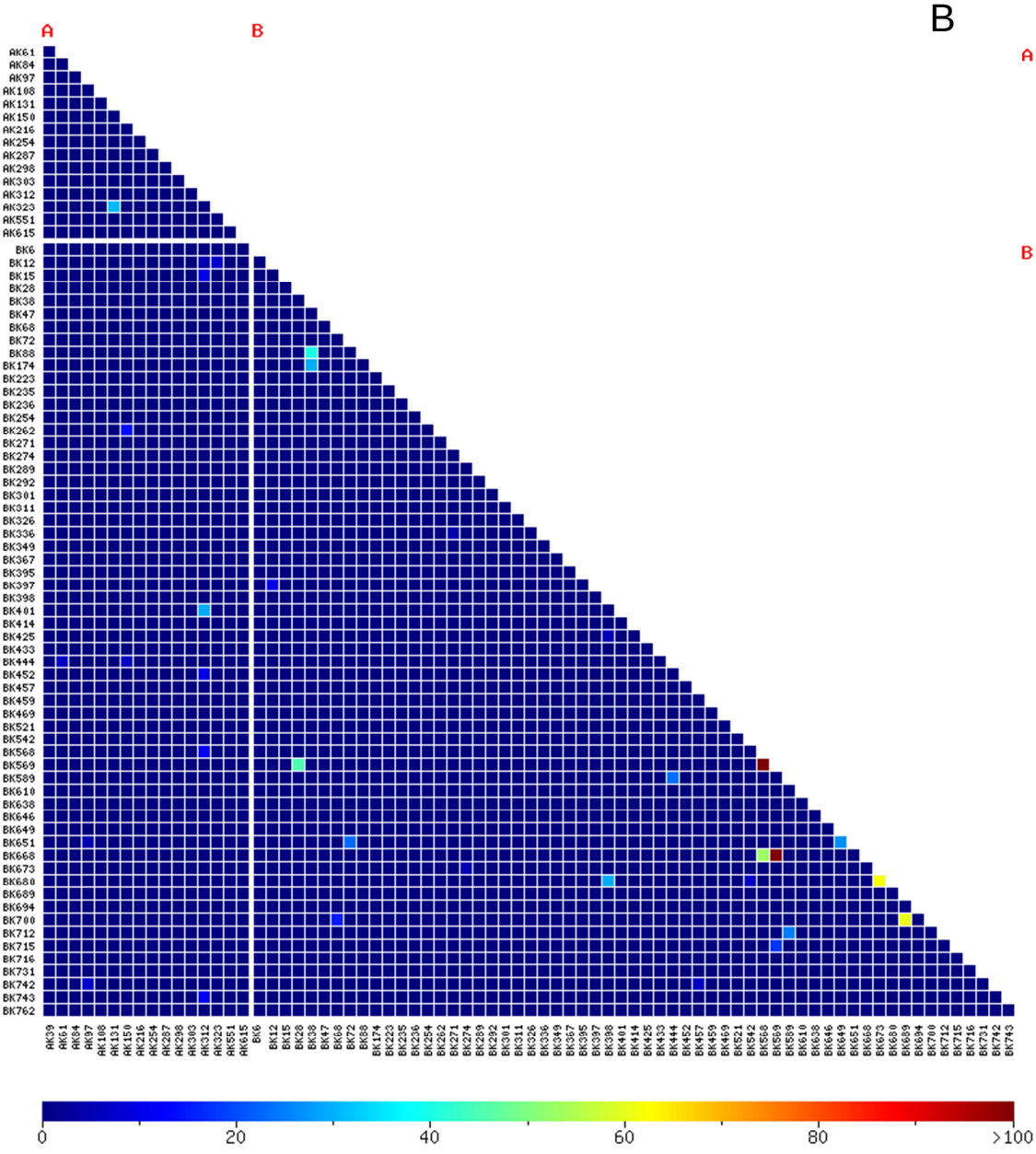
A
B
AK61
AK84
AK97
AK108
AK131
AK150
AK216
AK254
AK287
AK298
AK303
AK312
AK323
AK551
AK615
BK6
BK12
BK15
BK28
BK38
BK47
BK68
BK72
BK88
BK174
BK223
BK235
BK236
BK254
BK262
BK271
BK274
BK289
BK292
BK301
BK311
BK326
BK336
BK349
BK367
BK395
BK397
BK398
BK401
BK414
BK425
BK433
BK444
BK452
BK457
BK459
BK469
BK521
BK542
BK568
BK569
BK589
BK610
BK638
BK646
BK649
BK651
BK668
BK673
BK680
BK689
BK694
BK700
BK712
BK715
BK716
BK731
BK742
BK743
BK762
A
B
0
20
40
60
80
>100

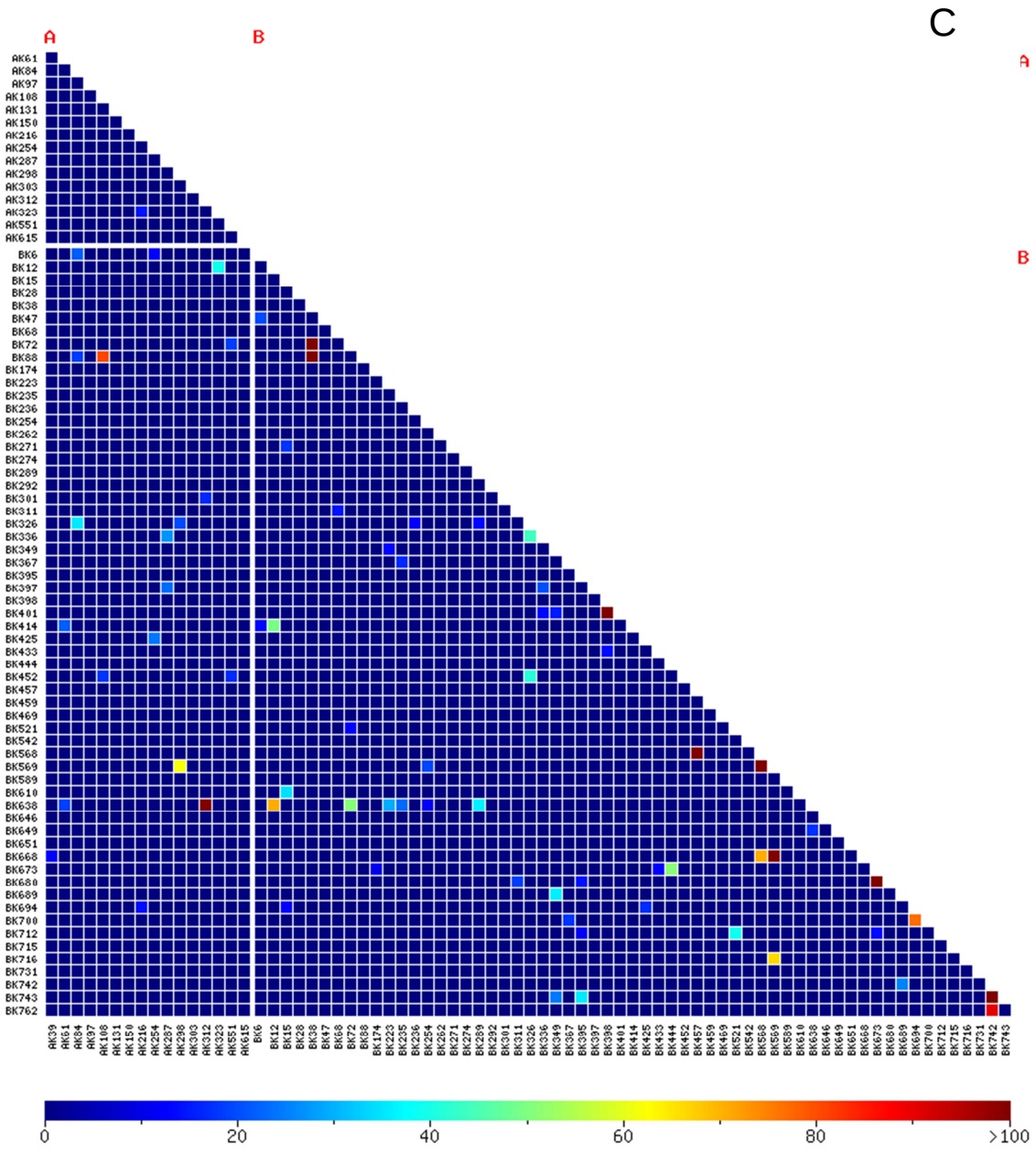

Figure 32. Digestion efficiency comparison of using trypsin alone and trypsin followed by chymotrypsin in BS^3 cross-linked Keap1-Cul3 complex analyzed by LTQ-FT ICR MS or LTQ-Orbitrap Velos. A) Trypsin alone and analyzed using LTQ-FT ICR MS, B) trypsin followed by chymotrypsin and analyzed using LTQ-FT ICR MS, and C) trypsin followed by chymotrypsin and analyzed using LTQ-Orbitrap Velos. Each cell in the heat map represents a cross-link between two lysine residues. “A” chain represents Keap1 protein and “B” chain represents Cul3 protein. Confidence of the identification of each cross-link is indicated by the scores displayed in the scaled color heat map.

5.3.2.2 BS^3 cross-linked peptides analysis using LTQ-FT ICR mass spectrometer

A protein-to-cross-linker ratio of 1:30 was used according to the suggestion of manufacturer's instructions. Compared to glutaraldehyde showed in Figure 29, BS^3 had relatively lower background cross-links with much higher scores for cross-links, which is easier to distinguish cross-linked peptides (Figure 32B). Thirteen peptides were detected with intra- or intercross-links with a cutoff score of 40. Six peptides were detected with a score higher than 50, including two with a score over 100 (as listed in TABLE VII).

The two cross-linked peptides with highest scores BK569-BK668 and BK568-BK569 are intramolecular cross-links in Cul3. Considering the length of BS^3 spacer (11.4 Å), the length of a lysine side chain, which is around 6-6.5 Å and an estimated coordinate error for mobile surface residues (1.5 Å) [140], the maximal distance of linkable lysine residues will be around 27.4 Å. Unfortunately, no three-dimensional structure of Cul3 is available to compare and validate whether these two cross-links fell below this range. One intramolecular cross-link in Keap1 was identified as AK131-AK323. K131 is in the BTB domain, which involves in Keap1 dimerization and Cul3 binding, and K323 is in the Kelch domain. Although the crystal structure of Keap1 Kelch domain is available [141], it is still hard to compare this cross-link without the whole protein structure. No cross-links were identified within Kelch domain. Instead of assuming the low efficiency of the cross-linking, it is possible that there are no lysine residues within a 27 Å range, or some big groups between two sites block the cross-links. One cross-link was identified between K312 in the Keap1 and K401 in the Cul3. K312 is within the Keap1 IVR domain, which associates with the N-terminal of Cul3 [48]. However, with a boundary score within 40-

50 and without the structure information, it is hard to confirm this cross-link as a true positive or background link.

In addition, twenty-two peptides were identified as dead-ends introduced by quenching reagent, including two from Keap1 and twenty from Cul3. This kind of modification does not provide any information on lysine distances within a protein or between Keap1 and Cul3 as cross-links do, but it indicates that these lysine residues are on the surface of a protein, accessible to reactive groups.

TABLE VII

IDENTIFIED CROSS-LINKS IN THE KEAP1-CUL3 COMPLEX USING BS^3 CROSS-LINKING REAGENT FOLLOWED BY LTQ-FT ICR MASS SPECTROMETER ANALYSIS

Cross-Link	Score	Type	Cross-Linked Peptide	
BK569-BK668[a]	>100	C-intra[b]	GPVKKEDGSEVGVGGAQVTGSNTR TVNDQFTSKL	[B565:588 B660:669][c]
BK568-BK569		C-intra	GPVKKEDGSEVGVGGAQVTGSNTR	[B565:588]
BK689-BK700	60-70	C-intra	VDDDRKHEIEAAIVR KETRQK	[B695:709 B689:694]
BK673-BK680		C-intra	VKIQTVAAKQGESDPER	[B672:688]
BK568-BK668	50-60	C-intra	TVNDQFTSKL GPVKK	[B660:669 B565:569]
BK28-BK569		C-intra	GPVKEDGSEVGVGGAQVTGSNTR DEKYVNSIW	[B565:588 B26:34]
BK38-BK88	40-50	C-intra	EVVTEHLINKVR KNAIQEIQR	[B79:90 B38:46]
BK38-BK174		C-intra	KNAIQEIQR ERKGEVVDR	[B38:46 B172:180]
AK131-AK323		K-intra	EQGMEVVSIEGIHPKVM HKPTQVMPCRAPKVGR	[A117:133 A311:326]
AK312-BK401 BK398-BK680		KC-inter C-intra	VKIQTVAAKQGESDPER KGVKGL HKPTQVMPCR	[B672:688 B398:403 A311:320]
BK649-BK651		C-intra	EPKSKEIENGHIF	[B647:659]
BK589-BK712		C-intra	KHILQVSTF IMKSR	[B589:597 B710:714]

a. AK represents lysine residue on Keap1 protein; BK represents lysine residue on Cul3 protein.

b. C-intra represents the intramolecular cross-linked peptide in Cul3 protein; KC-inter represents the intermolecular cross-linked peptide between Keap1 and Cul3 protein.

c. [A/Bxxx:xxx] represents the location of the peptide in the Keap1 or Cul3 protein sequences.

TABLE VIII

IDENTIFIED DEAD-ENDS IN THE KEAP1-CUL3 COMPLEX USING BS^3 CROSS-LINKING REAGENT FOLLOWED BY LTQ-FT ICR MASS SPECTROMETRY ANALYSIS

Lysine	Type	Lysine	Type
Keap1:		Cul3:	
K131	H_2O[a]	K569	H_2O/ Tris-HCl
K312	Tris-HCl	K589	H_2O/ Tris-HCl
Cul3:		K649	H_2O
K88	H_2O	K651	H_2O
K262	H_2O	K668	H_2O
K292	Tris-HCl	K673	H_2O
K395	Tris-HCl	K689	Tris-HCl
K397	Tris-HCl	K694	H_2O/ Tris-HCl
K398	H_2O/ Tris-HCl	K700	Tris-HCl
K401	H_2O/ Tris-HCl	K731	H_2O
K521	H_2O	K743	Tris-HCl
K568	H_2O/ Tris-HCl		

[a.] H_2O, Tris-HCl or H_2O/Tris-HCl indicates the dead-end introduced by quenching reagent H_2O, Tris-HCl or both, respectively.

5.3.2.3 BS^3 cross-linked peptides analysis using LTQ-Orbitrap Velos

The sequence coverage of Keap1 and Cul3 using LTQ-Orbitrap Velos was even better than using LTQ-FT ICR mass spectrometer, which is 82% and 87%, respectively. Thirty cross-linked peptides were identified with a cutoff score of 40 using LTQ-Orbitrap Velos (TABLE IX). Eighteen peptides had a score over 50, including nine over 100. Most of the cross-linked peptides identified by LTQ-FT ICR mass spectrometer were also identified by LTQ-Orbitrap Velos with a higher score.

Three intermolecular cross-links were detected with a score over 60. They are AK312-BK638 (>100), AK108-BK88 (80-90) and AK298-BK569 (60-70). Previously in 4.3.2, C636 in Cul3 was identified differentially alkylated by isoliquiritigenin in the present of wild-type Keap1 or Keap1 C151W mutant, which indicates the conformational

change of Keap1-Cul3 complex upon modification of C151 in Keap1. The identified cross-link between K312 in Keap1 and K638 in Cul3 offers an alternative explanation from a structure point of view. Since these two peptides fell below a distance of 27.4 Å range, it suggests that C636 might be located within the Keap1 and Cul3 interaction interface. Modification of C151 in Keap1 might alter the interaction with Cul3 such that C636 is no longer accessible to modification, perhaps physically blocked by Keap1. No similar cross-links or dead-ends were detected using LTQ-FT ICR mass spectrometer, since this peptide was not in the Cul3 sequence coverage.

AK298-BK569 is another noteworthy intermolecular cross-link identified. K298 was found to be the ubiquitination site on Keap1 with the treatment of ARE activator IAB [58]. Hong *et al*. proposed that ARE activator adduction on Keap1 triggers a switching of Cul3-dependent ubiquitination from Nrf2 to Keap1, which results in Nrf2 activation. However, not all of the ARE activators induce ubiquitination on Keap1. So far, only IAB, tBHQ [142], quercetin [94], ebselen [60] and falcarindiol [143] have been reported to induce a high molecular weight form of Keap1 in vitro or in vivo and K298 was identified as a target site with IAB. The cross-link we identified indicates that K298 in the wild-type Keap1 is accessible to ubiquitin and quite close to K569 on the Cul3. It is possible that the modification on Keap1 cysteines introduces a change in the Keap1 and Cul3 interaction, which results in the ubiquitin target switching from Nrf2 to Keap1. Since ARE activators have different alkylation patterns, they will cause different extents of interruption. Sulforaphane has been shown to not switch ubiquitination [142]. It is probable that modification by some activators such as sulforaphane causes K298 to be buried inside the structure and unable be modified by ubiquitin or the modification is not

sufficient to cause the shift of ubiquitin target from Nrf2 to Keap1, thus, no high molecular weight form of Keap1 was observed. Although this hypothesis requires further testing, it is interesting to note that K298 in Keap1 and K569 in Cul3 are quite close.

In addition, six and twenty-six peptides with dead-ends were identified in Keap1 and Cul3, respectively (TABLE X). Most of the dead-end peptides detected using LTQ-FT ICR mass spectrometer were also detected by LTQ-Orbitrap Velos.

TABLE IX

IDENTIFIED CROSS-LINKS IN THE KEAP1-CUL3 COMPLEX USING BS^3 CROSS-LINKING REAGENT FOLLOWED BY LTQ-ORBITRAP VELOS ANALYSIS

Cross-Link	Score	Type	Cross-Linked Peptide	
BK569-BK668	>100	C-intra	GPVKKEDGSEVGVGGAQVTGSNTR TVNDQFTSKL	[B565:588 B660:669]
BK568-BK569		C-intra	GPVKKEDGSEVGVGGAQVTGSNTR	[B565:588]
BK457-BK568		C-intra	YGPVKKEDGSEVGVGGAQVTGSNTR NMISKLK	[B564:588 B453:459]
BK398-BK401		C-intra	KGVKGLTEQEVETILDK	[B398:414]
BK673-BK680		C-intra	VKIQTVAAKQGESDPER	[B672:688]
BK742-BK743		C-intra	FLPSPVVIKKR	[B734:744]
BK38-BK72		C-intra	DLLKNAIQEIQR HGEKLY	[B35:46 B69:74]
BL38-BK88		C-intra	EVVTEHLINKVR DLLKNAIQEIQR	[B79:90 B35:46]
AK312-BK638		KC-inter	HKPTQVMPCRAPK ALQSLACGKPTQR	[A311:323 B630:642]
BK742-BK762	90-100	C-intra	FLPSPVVIKKR KVY	[B734:744 B762:764]
AK108-BK88	80-90	KC-inter	ASSSPVFKAMFTNGL EVVTEHLINKVR	[A101:115 B79:90]
BK694-BK700		C-intra	QKVDDDRKHEIEAAIVR	[B693:709]
BK568-BK668	70-80	C-intra	TVNDQFTSKL GPVKK	[B660:669 B565:569]
AK298-BK569	60-70	KC-inter	NATFYGPVKKEDGSEVGVGGAQVTGSNTR CKDY	[B560:588 A297:300]
BK569-BK716		C-intra	GPVKKEDGSEVGVGGAQVTGSNTR KKMQHNVL	[B565:588 B715:722]
BK444-BK673	50-60	C-intra	VKIQTVAAKQGESDPER LLTNKSVSDDSEK	[B672:688 B440:452]
BK72-BK638		C-intra	ALQSLACGKPTQR TMVLHKHGEKL	[B630:642 B63:73]
BK12-BK414		C-intra	GLTEQEVETILDKAMVL SKGTGSRKDTKM	[B402:418 B5:16]
BK326-BK336	40-50	C-intra	VSEEGEGKNPVDYIQGLL EQGKAL	[B329:346 B323:328]
BK326-BK452		C-intra	TNKSVSDDSEKNMISK LREQGKAL	[B442:457 B321:328]

BK349-BK689	C-intra	QGESDPERKETR IQGLLDLKSR	[B681:692 B342:351]
BK15-BK610	C-intra	NNREKYTFEEIQQETDIPER KDTKMR	[B606:625 B12:17]
BK289-BK638	C-intra	VHMLKNGKTEDL QSLACGKPTQR	[B285:296 B632:642]
BK395-BK743	C-intra	FLPSPVVIKKR SLFIDDKLK	[B734:744 B389:397]
BK521-BK712	C-intra	WPTQSATPKCNIPPAPR IMKSR	[B513:529 B710:714]
AK84-BK326	KC-inter	CDVTLQVKYQDAPAAQF EQGKAL	[A77:93 B323:328]
AK323-BK12	KC-inter	HKPTQVMPCRAPKVGR KDTK	[A311:326 B12:15]
BK223-BK638	C-intra	VRALQSLACGKPTQR QMESQKF	[B628:642 B218:224]
BK349-BK743	C-intra	FLPSPVVIKKRIEGL IQGLLDLKSR	[B734:748 B342:351]
BK689-BK742	C-intra	IQTVAAKQGESDPERKETRQK FLPSPVVIKKRIEGL	[B674:694 B734:748]

TABLE X

IDENTIFIED DEAD-ENDS IN THE KEAP1-CUL3 COMPLEX USING BS^3 CROSS-LINKING REAGENT FOLLOWED BY LTQ-ORBITRAP VELOS ANALYSIS

Lysine	Type	Lysine	Type
Keap1:		Cul3:	
K61	H_2O[a]	K398	H_2O/ Tris-HCl
K108	H_2O	K401	H_2O
K216	H_2O	K444	H_2O
K303	H_2O/ Tris-HCl	K457	Tris-HCl
K312	H_2O	K459	H_2O
K323	H_2O	K568	H_2O/ Tris-HCl
Cul3:		K569	H_2O/ Tris-HCl
K12	H_2O/ Tris-HCl	K610	H_2O
K15	H_2O/ Tris-HCl	K668	H_2O
K38	H_2O	K673	H_2O/ Tris-HCl
K88	H_2O	K680	H_2O
K236	Tris-HCl	K700	H_2O
K262	H_2O/ Tris-HCl	K715	H_2O
K326	H_2O	K731	H_2O
K336	H_2O	K742	H_2O
K367	H_2O	K743	H_2O/ Tris-HCl
K397	H_2O		

[a.] H_2O, Tris-HCl or H_2O/Tris-HCl indicates the dead-end introduced by quenching reagent H_2O, Tris-HCl or both, respectively.

5.3.3 Comparison of LTQ-FT ICR and LTQ-Orbitrap Velos mass spectrometer in cross-linking studies

Cross-linking coupled to mass spectrometry studies have been based on comparing the mass spectra of cross-linked samples with all the possible cross-linked peptide masses that the searching program computes and lists. Considering that a combination of two theoretical peptides leads to an exponential number of possible cross-linked peptides, identification of cross-linked peptides relies predominantly on the accuracy of mass spectra [144]. Thus, exact mass measurement using high-resolution FTICR or Orbitrap mass spectrometry offers distinct advantages for cross-linking analysis. With the help of the state-of-the-art mass spectrometric instrumentation, the sensitivity, throughput and false positive rate have dramatically improved [132, 140, 145]. However, our results showed that much more cross-links were identified with a significantly higher score by using LTQ-Orbitrap Velos. Three features of LTQ-Orbitrap Velos offer marked advantages over LTQ-FT ICR mass spectrometer in cross-linking studies.

First of all, for LTQ-FT ICR, isolation and dissociation of precursor ions in the 2-D linear trap and the exact mass measurement of precursor ions in ICR cell are achieved at the expense of loss of some ions and scan speed during the transmission. However, with a dual-pressure ion trap, the isolation and scanning rate are drastically accelerated in LTQ-Orbitrap Velos. It routinely enables acquisition of up to ten most intense peptide ions instead of five on LTQ-FT ICR mass spectrometer [79]. Therefore, better sequence coverage as well as more cross-linked peptides and dead-ends were observed from the LTQ-Orbitrap Velos run compared with the LTQ-FT ICR mass spectrometer run.

Secondly, HCD in the C-trap of LTQ-Orbitrap Velos offers better fragmentation efficiency than CID in the 2-D linear trap of LTQ-FT ICR mass spectrometer. Since the length of cross-linked peptides is usually longer than non-modified peptides and blind spots are generated by cross-linking, poor fragmentation patterns are always obtained due to insufficient fragmentation in CID and the low mass cut-off limit of ion trap (Figure 33A). In contrast, HCD has "triple quadrupole-like" behavior [79]. The dissociation occurs at a higher energy, so that more fragments are generated, which covered the preponderance of y-ions and the absence of a low mass cut-off for fragments (Figure 33B). Figure 33 showed the MS/MS spectra of a cross-linked peptide detected by both instruments. The fragment ions detected by LTQ-FT ICR mass spectrometer accumulate in the mass range of 400-1200 *m/z* due to the "1/3" limitation of ion trap. Whereas, more fragment ions were detected by LTQ-Orbitrap Velos and they were evenly spread in the mass range of 100-1400 *m/z*. Thus, the more efficient HCD fragmentation spectra resulted in a better sequence coverage and got a four times higher score than the one detected by LTQ-FT ICR mass spectrometer.

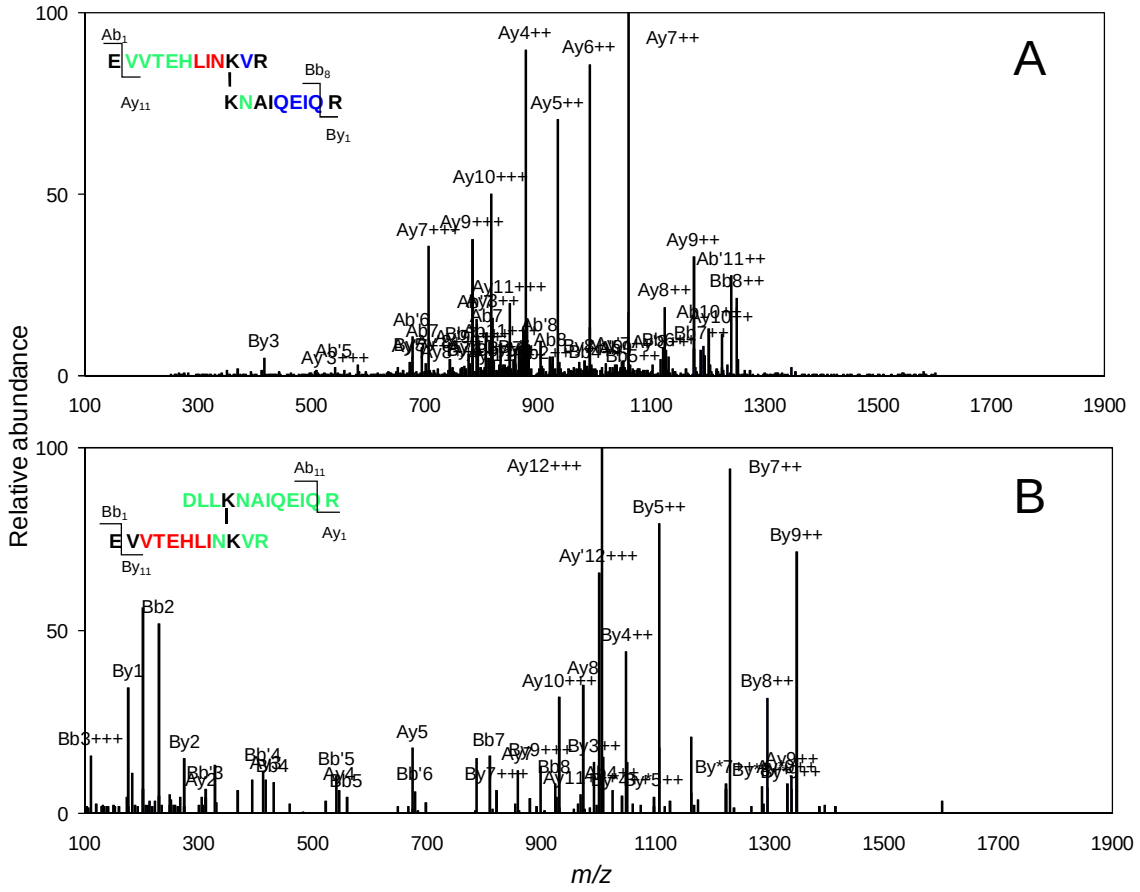

Figure 33. MS/MS spectra of intramolecular cross-linked peptides DLLK$_{38}^{\neq}$NAIQEIQR and EVVTEHLINK$_{88}^{\neq}$VR by BS^3 within Cul3. The peptide was detected by A) LTQ-FT ICR mass spectrometer with an XMapper score of 40.22, and B) LTQ-Orbitrap Velos with an XMapper score of 176.1. K$_{38}^{\neq}$ and K$_{88}^{\neq}$ represent the two lysine residues cross-linked by BS^3. The amino acid residues tagged in green, blue and red represent a pair of consecutive y ions, a pair of consecutive b ions and both pairs of consecutive y and b ions were detected, respectively. Product ions from neutral loss are labeled by * (loss of ammonia) and ′ (loss of water).

Furthermore, high resolution and high mass accuracy MS/MS was acquired in the Orbitrap as sensitive as relatively low mass accuracy MS/MS in the ion trap of LTQ-FT ICR mass spectrometer. The statistical significance of the improvement of the fragment mass accuracy is extremely crucial. Because the score is the negative logarithm of the probability that a match is random, raising mass accuracy has an immediate positive effect on the overall statistical confidence in peptide assignment by reducing false

positives and substantially improving peptide scores for true positives [85]. Owing to the intrinsic complex nature of the cross-linked peptides, they are more prone to false positives and harder to be identified compared to the non-modified peptides. Except type one cross-linked peptides illustrated in Figure 31 that allow good fragmentation sequence coverage, other peptide types can suffer from lower sequence coverage due to blind spots in the product ion series [87]. Therefore, improving the mass accuracy of fragment ions can dramatically reduce the false positives and increases the sensitivity of identification of true positive cross-linked peptides. Figure 34 showed a cross-linked peptide detected by both instruments with a blind spot KIQTVAAK introduced by the intrachain cross-link. With the limited residues can be sequenced in the peptide, mass accuracy is especially critical to peptide identification. LTQ-FT ICR mass spectrometer detected five pairs of consecutive y and b ions; whereas, LTQ-Orbitrap Velos detected seven pairs of consecutive y ions. Due to the high mass accuracy provided by the Orbitrap, the identified cross-linked peptide got a 2.5-fold higher score than using ion trap in LTQ-FT ICR mass spectrometer.

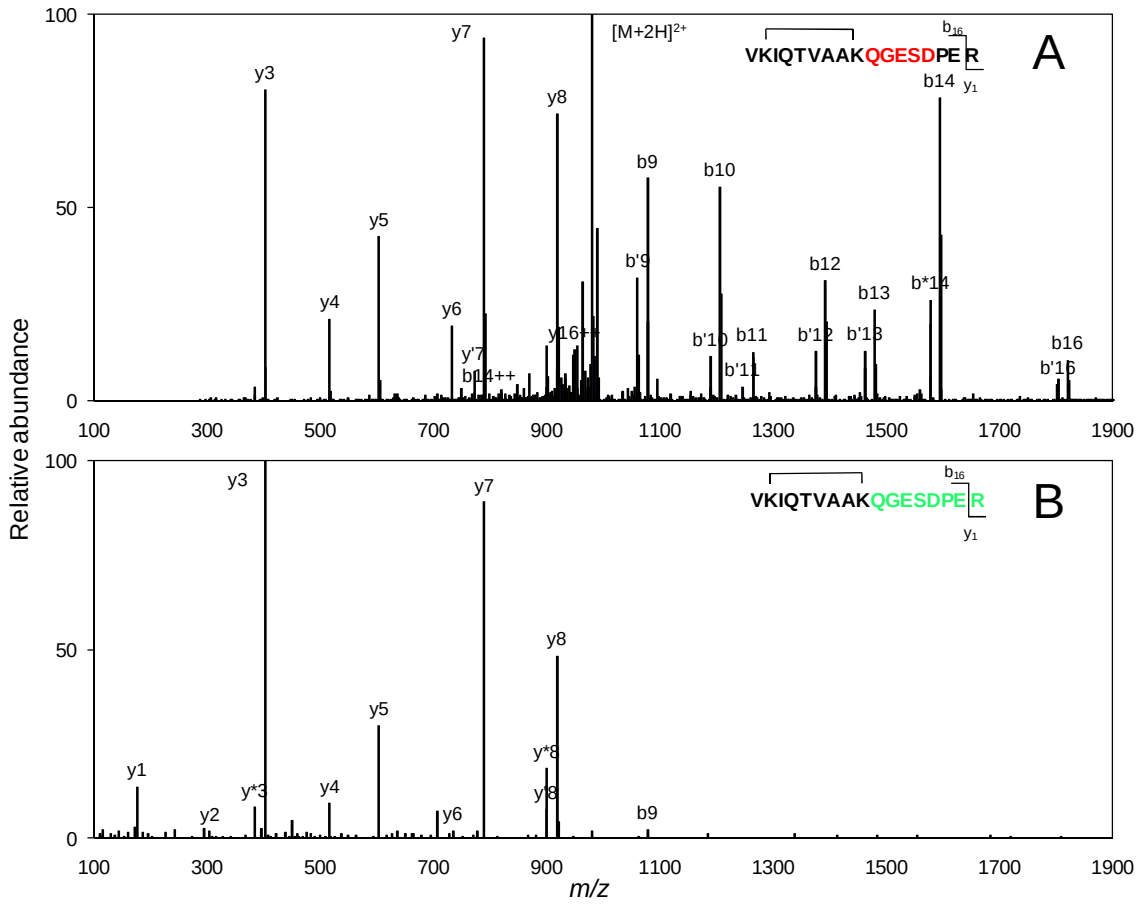

Figure 34. MS/MS spectra of intramolecular cross-linked peptide (intrachain) $VK_{673}^{\neq}IQTVAAK_{680}^{\neq}QGESDPER$ by BS^3 within Cul3. The peptide was detected by A) LTQ-FT ICR mass spectrometer with an XMapper score of 61.76, and B) LTQ-Orbitrap Velos with an XMapper score of 155.28. $K_{673}^{\neq}$ and $K_{680}^{\neq}$ represent the two lysine residues cross-linked by BS^3. The amino acid residues tagged in green, blue and red represent a pair of consecutive y ions, a pair of consecutive b ions and both pairs of consecutive y and b ions were detected, respectively. Product ions from neutral loss are labeled by * (loss of ammonia) and ′ (loss of water).

5.4 Summary

Interaction between Keap1 and Cul3 proteins has drawn attention due to its promising role in the mechanism of disturbing Nrf2 ubiquitination and ARE activation. Independent groups have shown evidence that the Keap1-Cul3 interaction was altered when the critical cysteine(s) on the Keap1 was modified by various techniques, such as immunoprecipitation, homology models, etc. [47-49, 59, 65]. However, no direct

evidence has been reported in terms of the location of the interface due to the unavailability of three-dimensional structure of either protein.

In this investigation, we used chemical cross-linking coupled with mass spectrometry to directly probe the protein structures and the interface. The information we got here is limited and in low resolution, but it is useful to facilitate the future protein structure modeling and mutation work. In the meantime, the cross-link data we obtained here for Keap1-Cul3 complex is the largest collection to date. It provides a valuable resource to understand method and instrument specific aspects on cross-linking studies.

Two cross-linkers glutaraldehyde and BS^3 were used to crosslink Keap1-Cul3 complex. In order to minimize the background cross-linking and protein aggregation, both protein complex and cross-linker should be kept at low concentration. In addition, gel filtration was used before and after cross-linking reaction to separate the cross-linked complex specifically. Considering the larger size of cross-linked peptides as well as the up to 2 cross-links searching limit, trypsin followed by chymotrypsin digestion were used to modulate the proper size of cross-linked peptides and it showed better efficiency and sequence coverage compared to using trypsin alone.

BS^3 showed much better cross-linking efficiency than glutaraldehyde. From a structural point of view, BS^3 has a longer spacer, which is more suitable to form intermolecular cross-links. Considering the chemical properties, glutaraldehyde is reactive to several amino acid residues besides lysine. Moreover, several forms of glutaraldehyde co-exist in solution that can form different cross-links. Thus, high background cross-links were found in the glutaraldehyde cross-linking experiments and it

is hard to distinguish the correct hit from the false positives. Whereas, with single target at lysine residue, BS^3 cross-linking experiments showed quite low background cross-links and some potential cross-linked hits had significantly high scores.

By comparing the results and the features of the two state-of-art instruments, we found that LTQ Orbitrap Velos is more suitable for cross-linking analysis in three aspects than LTQ-FT ICR mass spectrometer does. Faster scan speed allowed more low abundant cross-linked peptides to be identified; HCD generated better fragmentation patterns for assignment and high mass accuracy measurement of MS/MS in the Orbitrap improved the sensitivity and specificity of the database search identification. These features of LTQ-Orbitrap Velos dramatically increase the efficiency and confidence of cross-linked peptides identification, especially for a large protein complex.

6 MAIN CONCLUSIONS

Natural products play a promising role in cancer chemoprevention. In order for natural product-based drug discovery to continue to be successful, new and innovative approaches are required. As a reliable modern technique, mass spectrometry has emerged as a powerful tool to provide a mature platform for high throughput screening and in-depth protein characterization for molecular mechanism studies. The objective of this dissertation has been to develop and improve analytical methods for the Nrf2-Keap1 chemoprevention pathway study.

Human Keap1 and Nrf2 are important chemoprevention targets because of their role in regulating the ARE in response to oxidative stress and exposure to xenobiotics. First, a LC-MS based screening method was developed to improve our existing MALDI-TOF based screening method to discover natural products that modify Keap1. This new assay is based on the detection of adducts of BME with electrophiles that were reversibly bound to Keap1 using high resolution LC-MS with automated peak detection software. It can identify some potential chemopreventive agents with poor ionization in MALDI source such as sulforaphane, and permits approximately 20-fold more sensitive detection than MALDI-TOF MS-based assay with low false positive identification. Therefore, it can be a supplemental screening method to our existing assay. Together with these two assays, we can identify more low abundant chemopreventive agents from natural product extracts and accelerate structure elucidation of the lead compounds.

Modification of specific cysteine residues by chemopreventive agents has been demonstrated to be a critical step in up-regulation of ARE activation. Significant effort has been undertaken to identify the Keap1 modification pattern both in vitro and in vivo.

However, there are conflicting in vitro and in vivo data regarding which Keap1 cysteine residues become modified towards sulforaphane, a potent natural ARE activator. Here, we have reconciled these conflicting data using mass spectrometry with a revised sample preparation protocol and confirmed that C151 is indeed among the reactive sites of Keap1 towards sulforaphane. Previous mass spectrometry-based studies had used iodoacetamide during sample preparation to derivatize free cysteine sulfhydryl groups causing loss of sulforaphane from highly reactive and reversible cysteine residues on Keap1 including C151. By omitting iodoacetamide from the protocol and reducing sample preparation time, mass spectrometry-based studies now confirm previous cell studies indicating that sulforaphane modifies four highly reactive cysteine residues of Keap1 including C151. Considering the reversible feature of Michael addition acceptor, one of the common classes of ARE activators, the reversibility of five potential chemopreventive agents were investigated. The order of dissociation from Keap1 of the six activators including sulforaphane was CDDO-Im > sulforaphane > PGA_2 > isoliquiritigenin > xanthohumol = 15d-PGJ_2. The streamlined procedure was found also beneficial to compounds that form slightly less reversible adducts with Keap1 such as PGA_2 and isoliquiritigenin. However, Michael addition acceptors such as CDDO-Im that form much less stable adducts with Keap1 than does sulforaphane dissociated too quickly for any sites of Keap1 modification to be detected using even the modified sample processing procedure. In addition, the human Keap1 modification patterns by PGA_2 and 15d-PGJ_2 were also studied. We found that the five most readily modified cysteines towards PGA_2 are C226, C319, C273, C368 and C434; and the five most readily modified cysteines towards 15d-PGJ_2 are C241, C249, C273, C513 and C518. Our in

vitro “cysteine code” agreed well with other in vivo observations using mouse Keap1, which indicated that PGA_2 and 15d-PGJ_2 activators are C151 independent.

To support the molecular mechanistic study of how Keap1 modification at C151 alters Keap1-Cul3 interaction, mass spectrometry was applied to probe for protein conformational changes that altered cysteine modification on Keap1 and Cul3 by isoliquiritigenin before and after binding. By mutating Keap1 C151 to tryptophan to simulate the modification at this site, we found that it does not induce a significant change in Keap1 modification pattern by isoliquiritigenin. However, in the presence of Cul3, C636 in Cul3 was differentially modified by isoliquiritigenin when binding to human wt Keap1 or Keap1 C151W. By reversing the binding order of isoliquiritigenin and Cul3 to Keap1, we demonstrated that isoliquiritigenin is sufficient to alter the Keap1-Cul3 interaction at molar ratio of 1:2 (Keap1/isoliquiritigenin). In addition, Cul3 C636 is first reported as a reactive cysteine residue on Cul3. It is plausible to predict that C636 should be an important cysteine residue in Cul3 involved in the Nrf2-Keap1 signaling pathway. Further detailed investigation is needed to elucidate the role of Cul3 C636.

Next, a mass spectrometry-based cross-linking method was developed to study the Keap1 and Cul3 as well as their interface directly. With ultra-high resolution and mass accuracy, both LTQ-FT ICR and LTQ-Orbitrap Velos mass spectrometer facilitate detection of BS^3 cross-linked intra- and intermolecular peptides unambiguously based on exact mass measurements. These results are useful to support the future protein-docking model and mutation work. Meanwhile, by comparing the quantity and quality of the cross-linked peptides we detected, LTQ-Orbitrap Velos turns out to be more suitable than LTQ FT-ICR for cross-linking study, especially for the large complex. Since the data we

obtained for Keap1-Cul3 complex here is the largest collection to date, the method optimization, database searching, as well as instrument comparison are useful for further protein(s) structure analysis and elucidation.

CITED LITERATURE

1. Jemal, A., Siegel, R., Xu, J., and Ward, E.: Cancer Statistics, 2010. *CA Cancer J Clin*, 2010.

2. Austoker, J.: Cancer prevention in primary care. Current trends and some prospects for the future--II. *BMJ*, **309**: *517-520*, 1994.

3. Hajjar, R. R.: Cancer in the elderly: is it preventable? *Clin. Geriatr. Med.*, **20**: *293-316*, 2004.

4. Mackey, S.: Promoting lifestyle modification for cancer prevention. *J Am Diet Assoc*, **104**: *1568-1569*, 2004.

5. Sporn, M. B., Dunlop, N. M., Newton, D. L., and Smith, J. M.: Prevention of chemical carcinogenesis by vitamin A and its synthetic analogs (retinoids). *Fed. Proc.*, **35**: *1332-1338*, 1976.

6. Wattenberg, L. W.: Inhibition of carcinogenesis by minor anutrient constituents of the diet. *Proc Nutr Soc*, **49**: *173-183*, 1990.

7. Mehta, R. G., Murillo, G., Naithani, R., and Peng, X.: Cancer chemoprevention by natural products: how far have we come? *Pharm. Res.*, **27**: *950-961*, 2010.

8. Surh, Y. J.: Cancer chemoprevention with dietary phytochemicals. *Nat. Rev. Cancer*, **3**: *768-780*, 2003.

9. Kwon, K. H., Barve, A., Yu, S., Huang, M. T., and Kong, A. N.: Cancer chemoprevention by phytochemicals: potential molecular targets, biomarkers and animal models. *Acta Pharmacol. Sin.*, **28**: *1409-1421*, 2007.

10. Colic, M., and Pavelic, K.: Molecular, cellular and medical aspects of the action of nutraceuticals and small molecules therapeutics: from chemoprevention to new drug development. *Drugs Exp Clin Res*, **28**: *169-175*, 2002.

11. Ambrosone, C. B., and Tang, L.: Cruciferous vegetable intake and cancer prevention: role of nutrigenetics. *Cancer Prev Res (Phila Pa)*, **2**: *298-300*, 2009.

12. Reuter, S., Eifes, S., Dicato, M., Aggarwal, B. B., and Diederich, M.: Modulation of anti-apoptotic and survival pathways by curcumin as a strategy to induce apoptosis in cancer cells. *Biochem. Pharmacol.*, **76**: *1340-1351*, 2008.

13. Stewart, J. R., Artime, M. C., and O'Brian, C. A.: Resveratrol: a candidate nutritional substance for prostate cancer prevention. *J. Nutr.*, **133**: *2440S-2443S*, 2003.

14. Yang, C. S., Wang, X., Lu, G., and Picinich, S. C.: Cancer prevention by tea: animal studies, molecular mechanisms and human relevance. *Nat. Rev. Cancer,* **9**: *429-439*, 2009.

15. Dennis, T., Fanous, M., and Mousa, S.: Natural products for chemopreventive and adjunctive therapy in oncologic disease. *Nutr Cancer,* **61**: *587-597*, 2009.

16. Talalay, P., Fahey, J. W., Holtzclaw, W. D., Prestera, T., and Zhang, Y.: Chemoprotection against cancer by phase 2 enzyme induction. *Toxicol. Lett.,* **82-83**: *173-179*, 1995.

17. Rushmore, T. H., and Pickett, C. B.: Transcriptional regulation of the rat glutathione S-transferase Ya subunit gene. Characterization of a xenobiotic-responsive element controlling inducible expression by phenolic antioxidants. *J. Biol. Chem.,* **265**: *14648-14653*, 1990.

18. Rushmore, T. H., Morton, M. R., and Pickett, C. B.: The antioxidant responsive element. Activation by oxidative stress and identification of the DNA consensus sequence required for functional activity. *J. Biol. Chem.,* **266**: *11632-11639*, 1991.

19. Prestera, T., Talalay, P., Alam, J., Ahn, Y. I., Lee, P. J., and Choi, A. M.: Parallel induction of heme oxygenase-1 and chemoprotective phase 2 enzymes by electrophiles and antioxidants: regulation by upstream antioxidant-responsive elements (ARE). *Mol. Med.,* **1**: *827-837*, 1995.

20. Primiano, T., Sutter, T. R., and Kensler, T. W.: Antioxidant-inducible genes. *Adv. Pharmacol.,* **38**: *293-328*, 1997.

21. Nioi, P., McMahon, M., Itoh, K., Yamamoto, M., and Hayes, J. D.: Identification of a novel Nrf2-regulated antioxidant response element (ARE) in the mouse NAD(P)H:quinone oxidoreductase 1 gene: reassessment of the ARE consensus sequence. *Biochem. J.,* **374**: *337-348*, 2003.

22. Pi, J., Qu, W., Reece, J. M., Kumagai, Y., and Waalkes, M. P.: Transcription factor Nrf2 activation by inorganic arsenic in cultured keratinocytes: involvement of hydrogen peroxide. *Exp. Cell Res.,* **290**: *234-245*, 2003.

23. Jaiswal, A. K.: Regulation of antioxidant response element-dependent induction of detoxifying enzyme synthesis. *Methods Enzymol.,* **378**: *221-238*, 2004.

24. Jakel, R. J., Kern, J. T., Johnson, D. A., and Johnson, J. A.: Induction of the protective antioxidant response element pathway by 6-hydroxydopamine in vivo and in vitro. *Toxicol. Sci.,* **87**: *176-186*, 2005.

25. Ben-Dor, A., Steiner, M., Gheber, L., Danilenko, M., Dubi, N., Linnewiel, K., Zick, A., Sharoni, Y., and Levy, J.: Carotenoids activate the antioxidant response element transcription system. *Mol. Cancer Ther.,* **4**: *177-186*, 2005.

26. Eggler, A. L., Gay, K. A., and Mesecar, A. D.: Molecular mechanisms of natural products in chemoprevention: induction of cytoprotective enzymes by Nrf2. *Mol. Nutr. Food Res.*, **52 Suppl 1**: *S84-94*, 2008.

27. Zhang, D. D.: The Nrf2-Keap1-ARE signaling pathway: The regulation and dual function of Nrf2 in cancer. *Antioxid. Redox Signal.*, **13**: *1623-1626*, 2010.

28. Moi, P., Chan, K., Asunis, I., Cao, A., and Kan, Y. W.: Isolation of NF-E2-related factor 2 (Nrf2), a NF-E2-like basic leucine zipper transcriptional activator that binds to the tandem NF-E2/AP1 repeat of the beta-globin locus control region. *Proc. Natl. Acad. Sci. U. S. A.*, **91**: *9926-9930*, 1994.

29. Itoh, K., Igarashi, K., Hayashi, N., Nishizawa, M., and Yamamoto, M.: Cloning and characterization of a novel erythroid cell-derived CNC family transcription factor heterodimerizing with the small Maf family proteins. *Mol. Cell Biol.*, **15**: *4184-4193*, 1995.

30. Ramos-Gomez, M., Kwak, M. K., Dolan, P. M., Itoh, K., Yamamoto, M., Talalay, P., and Kensler, T. W.: Sensitivity to carcinogenesis is increased and chemoprotective efficacy of enzyme inducers is lost in nrf2 transcription factor-deficient mice. *Proc. Natl. Acad. Sci. U. S. A.*, **98**: *3410-3415*, 2001.

31. Moinova, H. R., and Mulcahy, R. T.: Up-regulation of the human gamma-glutamylcysteine synthetase regulatory subunit gene involves binding of Nrf-2 to an electrophile responsive element. *Biochem. Biophys. Res. Commun.*, **261**: *661-668*, 1999.

32. Alam, J., Stewart, D., Touchard, C., Boinapally, S., Choi, A. M., and Cook, J. L.: Nrf2, a Cap'n'Collar transcription factor, regulates induction of the heme oxygenase-1 gene. *J. Biol. Chem.*, **274**: *26071-26078*, 1999.

33. Wild, A. C., Moinova, H. R., and Mulcahy, R. T.: Regulation of gamma-glutamylcysteine synthetase subunit gene expression by the transcription factor Nrf2. *J. Biol. Chem.*, **274**: *33627-33636*, 1999.

34. Itoh, K., Chiba, T., Takahashi, S., Ishii, T., Igarashi, K., Katoh, Y., Oyake, T., Hayashi, N., Satoh, K., Hatayama, I., Yamamoto, M., and Nabeshima, Y.: An Nrf2/small Maf heterodimer mediates the induction of phase II detoxifying enzyme genes through antioxidant response elements. *Biochem. Biophys. Res. Commun.*, **236**: *313-322*, 1997.

35. Wakabayashi, N., Dinkova-Kostova, A. T., Holtzclaw, W. D., Kang, M. I., Kobayashi, A., Yamamoto, M., Kensler, T. W., and Talalay, P.: Protection against electrophile and oxidant stress by induction of the phase 2 response: fate of cysteines of the Keap1 sensor modified by inducers. *Proc. Natl. Acad. Sci. U. S. A.*, **101**: *2040-2045*, 2004.

36. Wakabayashi, N., Itoh, K., Wakabayashi, J., Motohashi, H., Noda, S., Takahashi, S., Imakado, S., Kotsuji, T., Otsuka, F., Roop, D. R., Harada, T., Engel, J. D., and Yamamoto, M.: Keap1-null mutation leads to postnatal lethality due to constitutive Nrf2 activation. *Nat. Genet.*, **35**: *238-245*, 2003.

37. Itoh, K., Wakabayashi, N., Katoh, Y., Ishii, T., Igarashi, K., Engel, J. D., and Yamamoto, M.: Keap1 represses nuclear activation of antioxidant responsive elements by Nrf2 through binding to the amino-terminal Neh2 domain. *Genes Dev.*, **13**: *76-86*, 1999.

38. Okawa, H., Motohashi, H., Kobayashi, A., Aburatani, H., Kensler, T. W., and Yamamoto, M.: Hepatocyte-specific deletion of the keap1 gene activates Nrf2 and confers potent resistance against acute drug toxicity. *Biochem. Biophys. Res. Commun.*, **339**: *79-88*, 2006.

39. Kang, K. W., Lee, S. J., Park, J. W., and Kim, S. G.: Phosphatidylinositol 3-kinase regulates nuclear translocation of NF-E2-related factor 2 through actin rearrangement in response to oxidative stress. *Mol. Pharmacol.*, **62**: *1001-1010*, 2002.

40. Kang, M. I., Kobayashi, A., Wakabayashi, N., Kim, S. G., and Yamamoto, M.: Scaffolding of Keap1 to the actin cytoskeleton controls the function of Nrf2 as key regulator of cytoprotective phase 2 genes. *Proc. Natl. Acad. Sci. U. S. A.*, **101**: *2046-2051*, 2004.

41. Velichkova, M., Guttman, J., Warren, C., Eng, L., Kline, K., Vogl, A. W., and Hasson, T.: A human homologue of Drosophila kelch associates with myosin-VIIa in specialized adhesion junctions. *Cell Motil. Cytoskeleton*, **51**: *147-164*, 2002.

42. Zipper, L. M., and Mulcahy, R. T.: The Keap1 BTB/POZ dimerization function is required to sequester Nrf2 in cytoplasm. *J. Biol. Chem.*, **277**: *36544-36552*, 2002.

43. Kobayashi, M., Itoh, K., Suzuki, T., Osanai, H., Nishikawa, K., Katoh, Y., Takagi, Y., and Yamamoto, M.: Identification of the interactive interface and phylogenic conservation of the Nrf2-Keap1 system. *Genes Cells*, **7**: *807-820*, 2002.

44. Tong, K. I., Kobayashi, A., Katsuoka, F., and Yamamoto, M.: Two-site substrate recognition model for the Keap1-Nrf2 system: a hinge and latch mechanism. *Biological chemistry*, **387**: *1311-1320*, 2006.

45. Zhang, D. D., and Hannink, M.: Distinct cysteine residues in Keap1 are required for Keap1-dependent ubiquitination of Nrf2 and for stabilization of Nrf2 by chemopreventive agents and oxidative stress. *Mol. Cell. Biol.*, **23**: *8137-8151*, 2003.

46. Cullinan, S. B., Gordan, J. D., Jin, J., Harper, J. W., and Diehl, J. A.: The Keap1-BTB protein is an adaptor that bridges Nrf2 to a Cul3-based E3 ligase: oxidative stress sensing by a Cul3-Keap1 ligase. *Mol. Cell Biol.,* **24**: *8477-8486*, 2004.

47. Zhang, D. D., Lo, S. C., Cross, J. V., Templeton, D. J., and Hannink, M.: Keap1 is a redox-regulated substrate adaptor protein for a Cul3-dependent ubiquitin ligase complex. *Mol. Cell Biol.,* **24**: *10941-10953*, 2004.

48. Kobayashi, A., Kang, M. I., Okawa, H., Ohtsuji, M., Zenke, Y., Chiba, T., Igarashi, K., and Yamamoto, M.: Oxidative stress sensor Keap1 functions as an adaptor for Cul3-based E3 ligase to regulate proteasomal degradation of Nrf2. *Mol. Cell. Biol.,* **24**: *7130-7139*, 2004.

49. Furukawa, M., and Xiong, Y.: BTB protein Keap1 targets antioxidant transcription factor Nrf2 for ubiquitination by the Cullin 3-Roc1 ligase. *Mol. Cell. Biol.,* **25**: *162-171*, 2005.

50. Kobayashi, M., and Yamamoto, M.: Molecular mechanisms activating the Nrf2-Keap1 pathway of antioxidant gene regulation. *Antioxid. Redox Signal.,* **7**: *385-394*, 2005.

51. Talalay, P., De Long, M. J., and Prochaska, H. J.: Identification of a common chemical signal regulating the induction of enzymes that protect against chemical carcinogenesis. *Proc. Natl. Acad Sci. U. S. A.,* **85**: *8261-8265*, 1988.

52. Dinkova-Kostova, A. T., Holtzclaw, W. D., Cole, R. N., Itoh, K., Wakabayashi, N., Katoh, Y., Yamamoto, M., and Talalay, P.: Direct evidence that sulfhydryl groups of Keap1 are the sensors regulating induction of phase 2 enzymes that protect against carcinogens and oxidants. *Proc. Natl. Acad. Sci. U. S. A.,* **99**: *11908-11913*, 2002.

53. Itoh, K., Ishii, T., Wakabayashi, N., and Yamamoto, M.: Regulatory mechanisms of cellular response to oxidative stress. *Free Radic. Res.,* **31**: *319-324*, 1999.

54. Levonen, A. L., Landar, A., Ramachandran, A., Ceaser, E. K., Dickinson, D. A., Zanoni, G., Morrow, J. D., and Darley-Usmar, V. M.: Cellular mechanisms of redox cell signalling: role of cysteine modification in controlling antioxidant defences in response to electrophilic lipid oxidation products. *Biochem. J.,* **378**: *373-382*, 2004.

55. Yamamoto, T., Suzuki, T., Kobayashi, A., Wakabayashi, J., Maher, J., Motohashi, H., and Yamamoto, M.: Physiological significance of reactive cysteine residues of Keap1 in determining Nrf2 activity. *Mol. Cell. Biol.,* **28**: *2758-2770*, 2008.

56. Eggler, A. L., Luo, Y., van Breemen, R. B., and Mesecar, A. D.: Identification of the highly reactive cysteine 151 in the chemopreventive agent-sensor Keap1 protein is method-dependent. *Chem. Res. Toxicol.,* **20**: *1878-1884*, 2007.

57. Luo, Y., Eggler, A. L., Liu, D., Liu, G., Mesecar, A. D., and van Breemen, R. B.: Sites of alkylation of human Keap1 by natural chemoprevention agents. *J. Am. Soc. Mass Spectrom.,* **18**: *2226-2232,* 2007.

58. Hong, F., Sekhar, K. R., Freeman, M. L., and Liebler, D. C.: Specific patterns of electrophile adduction trigger Keap1 ubiquitination and Nrf2 activation. *J. Biol. Chem.,* **280**: *31768-31775,* 2005.

59. Eggler, A. L., Small, E., Hannink, M., and Mesecar, A. D.: Cul3-mediated Nrf2 ubiquitination and antioxidant response element (ARE) activation are dependent on the partial molar volume at position 151 of Keap1. *Biochem. J.,* **422**: *171-180,* 2009.

60. Sakurai, T., Kanayama, M., Shibata, T., Itoh, K., Kobayashi, A., Yamamoto, M., and Uchida, K.: Ebselen, a seleno-organic antioxidant, as an electrophile. *Chem. Res. Toxicol.,* **19**: *1196-1204,* 2006.

61. Satoh, T., Okamoto, S. I., Cui, J., Watanabe, Y., Furuta, K., Suzuki, M., Tohyama, K., and Lipton, S. A.: Activation of the Keap1/Nrf2 pathway for neuroprotection by electrophilic [correction of electrophillic] phase II inducers. *Proc. Natl. Acad. Sci. U.S.A.,* **103**: *768-773,* 2006.

62. Kobayashi, M., Li, L., Iwamoto, N., Nakajima-Takagi, Y., Kaneko, H., Nakayama, Y., Eguchi, M., Wada, Y., Kumagai, Y., and Yamamoto, M.: The antioxidant defense system Keap1-Nrf2 comprises a multiple sensing mechanism for responding to a wide range of chemical compounds. *Mol. Cell. Biol.,* **29**: *493-502,* 2009.

63. Eggler, A. L., Liu, G., Pezzuto, J. M., van Breemen, R. B., and Mesecar, A. D.: Modifying specific cysteines of the electrophile-sensing human Keap1 protein is insufficient to disrupt binding to the Nrf2 domain Neh2. *Proc. Natl. Acad. Sci. U. S. A.,* **102**: *10070-10075,* 2005.

64. Gao, L., Wang, J., Sekhar, K. R., Yin, H., Yared, N. F., Schneider, S. N., Sasi, S., Dalton, T. P., Anderson, M. E., Chan, J. Y., Morrow, J. D., and Freeman, M. L.: Novel n-3 fatty acid oxidation products activate Nrf2 by destabilizing the association between Keap1 and Cullin3. *J. Biol. Chem.,* **282**: *2529-2537,* 2007.

65. Rachakonda, G., Xiong, Y., Sekhar, K. R., Stamer, S. L., Liebler, D. C., and Freeman, M. L.: Covalent modification at Cys151 dissociates the electrophile sensor Keap1 from the ubiquitin ligase CUL3. *Chem. Res. Toxicol.,* **21**: *705-710,* 2008.

66. Liu, G., Eggler, A. L., Dietz, B. M., Mesecar, A. D., Bolton, J. L., Pezzuto, J. M., and van Breemen, R. B.: Screening method for the discovery of potential cancer chemoprevention agents based on mass spectrometric detection of alkylated Keap1. *Anal. Chem.,* **77**: *6407-6414,* 2005.

67. Hong, F., Freeman, M. L., and Liebler, D. C.: Identification of sensor cysteines in human Keap1 modified by the cancer chemopreventive agent sulforaphane. *Chem. Res. Toxicol.,* **18**: *1917-1926*, 2005.

68. Aebersold, R., and Mann, M.: Mass spectrometry-based proteomics. *Nature,* **422**: *198-207,* 2003.

69. Fenn, J. B., Mann, M., Meng, C. K., Wong, S. F., and Whitehouse, C. M.: Electrospray ionization for mass spectrometry of large biomolecules. *Science,* **246**: *64-71*, 1989.

70. Karas, M., and Hillenkamp, F.: Laser desorption ionization of proteins with molecular masses exceeding 10,000 daltons. *Anal. Chem.,* **60**: *2299-2301*, 1988.

71. Karas, M., Gluckmann, M., and Schafer, J.: Ionization in matrix-assisted laser desorption/ionization: singly charged molecular ions are the lucky survivors. *J Mass Spectrom,* **35**: *1-12*, 2000.

72. Hillenkamp, F., Karas, M., Beavis, R. C., and Chait, B. T.: Matrix-assisted laser desorption/ionization mass spectrometry of biopolymers. *Anal. Chem.,* **63**: *1193A-1203A*, 1991.

73. Classon, R., Arakawa, K., Kobayashi, M., Hamada, N., Takatori, S., Kitagawa, M., and Fujito, Y.: Screening method for residual pesticides in processed foods by accurate mass measurement using LCMS-IT-TOF. *46th Annual Florida Pesticide Residue Workshop*, 24, 2009.

74. Comisarow, M. B., and Marshall, A. G.: Fourier transform ion cyclotron resonance spectroscopy. *Chem. Phys. Lett.,* **25**: *282-283,* 1974.

75. Sihlbom, C.: Mass spectrometry for comparative proteomics of degenerative and regenerative processes in the brain. 27, Doctoral thesis, Göteborg University, Sweden, 2006.

76. Peterman, S. M., and Mulholland, J. J.: A novel approach for identification and characterization of glycoproteins using a hybrid linear ion trap/FT-ICR mass spectrometer. *J. Am. Soc. Mass Spectrom.,* **17**: *168-179,* 2006.

77. Nielsen, P. A., Olsen, J. V., Podtelejnikov, A. V., Andersen, J. R., Mann, M., and Wisniewski, J. R.: Proteomic mapping of brain plasma membrane proteins. *Mol. Cell Proteomics,* **4**: *402-408*, 2005.

78. Scigelova, M., and Makarov, A.: Orbitrap mass analyzer--overview and applications in proteomics. *Proteomics,* **6 Suppl 2**: *16-21,* 2006.

79. Olsen, J. V., Schwartz, J. C., Griep-Raming, J., Nielsen, M. L., Damoc, E., Denisov, E., Lange, O., Remes, P., Taylor, D., Splendore, M., Wouters, E. R., Senko, M., Makarov, A., Mann, M., and Horning, S.: A dual pressure linear ion

trap Orbitrap instrument with very high sequencing speed. *Mol. Cell Proteomics*, **8**: *2759-2769*, 2009.

80. Sadygov, R. G., Cociorva, D., and Yates, J. R., 3rd: Large-scale database searching using tandem mass spectra: looking up the answer in the back of the book. *Nat. Methods*, **1**: *195-202*, 2004.

81. Qian, W. J., Liu, T., Monroe, M. E., Strittmatter, E. F., Jacobs, J. M., Kangas, L. J., Petritis, K., Camp, D. G., 2nd, and Smith, R. D.: Probability-based evaluation of peptide and protein identifications from tandem mass spectrometry and SEQUEST analysis: the human proteome. *J. Proteome Res.*, **4**: *53-62*, 2005.

82. Eng, J. K., McCormack, A. L., and Yates Iii, J. R.: An approach to correlate tandem mass spectral data of peptides with amino acid sequences in a protein database. *J. Am. Soc. Mass Spectrom.*, **5**: *976-989*, 1994.

83. MacCoss, M. J., Wu, C. C., and Yates, J. R.: Probability-based validation of protein identifications using a modified SEQUEST algorithm. *Anal. Chem.*, **74**: *5593-5599*, 2002.

84. Peng, J., Schwartz, D., Elias, J. E., Thoreen, C. C., Cheng, D., Marsischky, G., Roelofs, J., Finley, D., and Gygi, S. P.: A proteomics approach to understanding protein ubiquitination. *Nat. Biotechnol.*, **21**: *921-926*, 2003.

85. Xu, H., and Freitas, M. A.: MassMatrix: a database search program for rapid characterization of proteins and peptides from tandem mass spectrometry data. *Proteomics*, **9**: *1548-1555*, 2009.

86. Xu, H., and Freitas, M. A.: A mass accuracy sensitive probability based scoring algorithm for database searching of tandem mass spectrometry data. *BMC Bioinformatics*, **8**: *133*, 2007.

87. Xu, H., Zhang, L., and Freitas, M. A.: Identification and characterization of disulfide bonds in proteins and peptides from tandem MS data by use of the MassMatrix MS/MS search engine. *J. Proteome Res.*, **7**: *138-144*, 2008.

88. Elias, J. E., and Gygi, S. P.: Target-decoy search strategy for increased confidence in large-scale protein identifications by mass spectrometry. *Nat. Methods*, **4**: *207-214*, 2007.

89. Huttlin, E. L., Hegeman, A. D., Harms, A. C., and Sussman, M. R.: Prediction of error associated with false-positive rate determination for peptide identification in large-scale proteomics experiments using a combined reverse and forward peptide sequence database strategy. *J. Proteome Res.*, **6**: *392-398*, 2007.

90. Xu, H., Hsu, P. H., Zhang, L., Tsai, M. D., and Freitas, M. A.: Database search algorithm for identification of intact cross-links in proteins and peptides using tandem mass spectrometry. *J. Proteome Res.*, **9**: *3384-3393*, 2010.

91. Fahey, J. W., Zhang, Y., and Talalay, P.: Broccoli sprouts: an exceptionally rich source of inducers of enzymes that protect against chemical carcinogens. *Proc. Natl. Acad. Sci. U.S.A.,* **94**: *10367-10372,* 1997.

92. Stevens, J. F., and Page, J. E.: Xanthohumol and related prenylflavonoids from hops and beer: to your good health! *Phytochemistry,* **65**: *1317-1330,* 2004.

93. Kim, D. C., Choi, S. Y., Kim, S. H., Yun, B. S., Yoo, I. D., Reddy, N. R., Yoon, H. S., and Kim, K. T.: Isoliquiritigenin selectively inhibits H(2) histamine receptor signaling. *Mol. Pharmacol.,* **70**: *493-500,* 2006.

94. Tanigawa, S., Fujii, M., and Hou, D. X.: Action of Nrf2 and Keap1 in ARE-mediated NQO1 expression by quercetin. *Free Radic. Biol. Med.,* **42**: *1690-1703,* 2007.

95. Schopfer, F. J., Batthyany, C., Baker, P. R., Bonacci, G., Cole, M. P., Rudolph, V., Groeger, A. L., Rudolph, T. K., Nadtochiy, S., Brookes, P. S., and Freeman, B. A.: Detection and quantification of protein adduction by electrophilic fatty acids: mitochondrial generation of fatty acid nitroalkene derivatives. *Free Radic. Biol. Med.,* **46**: *1250-1259,* 2009.

96. Calderon, A. I., Wright, B. J., Hurst, W. J., and van Breemen, R. B.: Screening antioxidants using LC-MS: case study with cocoa. *Journal of agricultural and food chemistry,* **57**: *5693-5699,* 2009.

97. Cuendet, M., Oteham, C. P., Moon, R. C., and Pezzuto, J. M.: Quinone reductase induction as a biomarker for cancer chemoprevention. *J. Nat. Prod.,* **69**: *460-463,* 2006.

98. Rudolph, T. K., and Freeman, B. A.: Transduction of redox signaling by electrophile-protein reactions. *Sci Signal,* **2**: *re7,* 2009.

99. Zhang, Y., Kensler, T. W., Cho, C. G., Posner, G. H., and Talalay, P.: Anticarcinogenic activities of sulforaphane and structurally related synthetic norbornyl isothiocyanates. *Proc. Natl. Acad. Sci. U.S.A.,* **91**: *3147-3150,* 1994.

100. Dinkova-Kostova, A. T., Fahey, J. W., Wade, K. L., Jenkins, S. N., Shapiro, T. A., Fuchs, E. J., Kerns, M. L., and Talalay, P.: Induction of the phase 2 response in mouse and human skin by sulforaphane-containing broccoli sprout extracts. *Cancer Epidemiol. Biomarkers Prev.,* **16**: *847-851,* 2007.

101. Brooks, J. D., Paton, V. G., and Vidanes, G.: Potent induction of phase 2 enzymes in human prostate cells by sulforaphane. *Cancer Epidemiol. Biomarkers Prev.,* **10**: *949-954,* 2001.

102. Kensler, T. W., and Wakabayashi, N.: Nrf2: friend or foe for chemoprevention? *Carcinogenesis,* **31**: *90-99,* 2010.

103. Loub, W. D., Farnsworth, N. R., Soejarto, D. D., and Quinn, M. L.: NAPRALERT: computer handling of natural product research data. *J Chem Inf Comput Sci*, **25**: *99-103*, 1985.

104. Liu, H., Dinkova-Kostova, A. T., and Talalay, P.: Coordinate regulation of enzyme markers for inflammation and for protection against oxidants and electrophiles. *Proceedings of the National Academy of Sciences of the United States of America*, **105**: *15926-15931*, 2008.

105. Keum, Y. S., Khor, T. O., Lin, W., Shen, G., Kwon, K. H., Barve, A., Li, W., and Kong, A. N.: Pharmacokinetics and pharmacodynamics of broccoli sprouts on the suppression of prostate cancer in transgenic adenocarcinoma of mouse prostate (TRAMP) mice: implication of induction of Nrf2, HO-1 and apoptosis and the suppression of Akt-dependent kinase pathway. *Pharm. Res.*, **26**: *2324-2331*, 2009.

106. Yoon, H. Y., Kang, N. I., Lee, H. K., Jang, K. Y., Park, J. W., and Park, B. H.: Sulforaphane protects kidneys against ischemia-reperfusion injury through induction of the Nrf2-dependent phase 2 enzyme. *Biochem. Pharmacol.*, **75**: *2214-2223*, 2008.

107. Jeong, W. S., Keum, Y. S., Chen, C., Jain, M. R., Shen, G., Kim, J. H., Li, W., and Kong, A. N.: Differential expression and stability of endogenous nuclear factor E2-related factor 2 (Nrf2) by natural chemopreventive compounds in HepG2 human hepatoma cells. *J. Biochem. Mol. Biol.*, **38**: *167-176*, 2005.

108. Gao, X., and Talalay, P.: Induction of phase 2 genes by sulforaphane protects retinal pigment epithelial cells against photooxidative damage. *Proc. Natl. Acad. Sci. U. S. A.*, **101**: *10446-10451*, 2004.

109. Chung, F. L., Conaway, C. C., Rao, C. V., and Reddy, B. S.: Chemoprevention of colonic aberrant crypt foci in Fischer rats by sulforaphane and phenethyl isothiocyanate. *Carcinogenesis*, **21**: *2287-2291*, 2000.

110. Xu, C., Huang, M. T., Shen, G., Yuan, X., Lin, W., Khor, T. O., Conney, A. H., and Kong, A. N.: Inhibition of 7,12-dimethylbenz(a)anthracene-induced skin tumorigenesis in C57BL/6 mice by sulforaphane is mediated by nuclear factor E2-related factor 2. *Cancer Res.*, **66**: *8293-8296*, 2006.

111. Ahn, Y. H., Hwang, Y., Liu, H., Wang, X. J., Zhang, Y., Stephenson, K. K., Boronina, T. N., Cole, R. N., Dinkova-Kostova, A. T., Talalay, P., and Cole, P. A.: Electrophilic tuning of the chemoprotective natural product sulforaphane. *Proc. Natl. Acad. Sci. U. S. A.*, 2010.

112. Itoh, K., Mochizuki, M., Ishii, Y., Ishii, T., Shibata, T., Kawamoto, Y., Kelly, V., Sekizawa, K., Uchida, K., and Yamamoto, M.: Transcription factor Nrf2 regulates inflammation by mediating the effect of 15-deoxy-Delta(12,14)-prostaglandin j(2). *Mol. Cell. Biol.*, **24**: *36-45*, 2004.

113. Mochizuki, M., Ishii, Y., Itoh, K., Iizuka, T., Morishima, Y., Kimura, T., Kiwamoto, T., Matsuno, Y., Hegab, A. E., Nomura, A., Sakamoto, T., Uchida, K., Yamamoto, M., and Sekizawa, K.: Role of 15-deoxy delta(12,14) prostaglandin J2 and Nrf2 pathways in protection against acute lung injury. *Am. J. Respir. Crit. Care Med.*, **171**: *1260-1266*, 2005.

114. Xu, H., and Freitas, M. A.: Monte carlo simulation-based algorithms for analysis of shotgun proteomic data. *J. Proteome Res.*, **7**: *2605-2615*, 2008.

115. Xu, H., Yang, L., and Freitas, M. A.: A robust linear regression based algorithm for automated evaluation of peptide identifications from shotgun proteomics by use of reversed-phase liquid chromatography retention time. *BMC Bioinformatics*, **9**: *347*, 2008.

116. Small, E., Eggler, A., and Mesecar, A. D.: Development of an efficient E. coli expression and purification system for a catalytically active, human Cullin3-RINGBox1 protein complex and elucidation of its quaternary structure with Keap1. *Biochem. Biophys. Res. Commun.*, **400**: *471-475*, 2010.

117. Holland, R., Hawkins, A. E., Eggler, A. L., Mesecar, A. D., Fabris, D., and Fishbein, J. C.: Prospective type 1 and type 2 disulfides of Keap1 protein. *Chem. Res. Toxicol.*, **21**: *2051-2060*, 2008.

118. Nioi, P., and Nguyen, T.: A mutation of Keap1 found in breast cancer impairs its ability to repress Nrf2 activity. *Biochem. Biophys. Res. Commun.*, **362**: *816-821*, 2007.

119. Cao, Y., Wang, Y., Ji, C., and Ye, J.: Determination of liquiritigenin and isoliquiritigenin in Glycyrrhiza uralensis and its medicinal preparations by capillary electrophoresis with electrochemical detection. *J Chromatogr A*, **1042**: *203-209*, 2004.

120. Gerhauser, C.: Beer constituents as potential cancer chemopreventive agents. *Eur J Cancer*, **41**: *1941-1954*, 2005.

121. Gutierrez, L. L., Maslinkiewicz, A., Curi, R., and de Bittencourt, P. I., Jr.: Atherosclerosis: a redox-sensitive lipid imbalance suppressible by cyclopentenone prostaglandins. *Biochem. Pharmacol.*, **75**: *2245-2262*, 2008.

122. Hosoya, T., Maruyama, A., Kang, M. I., Kawatani, Y., Shibata, T., Uchida, K., Warabi, E., Noguchi, N., Itoh, K., and Yamamoto, M.: Differential responses of the Nrf2-Keap1 system to laminar and oscillatory shear stresses in endothelial cells. *J. Biol. Chem.*, **280**: *27244-27250*, 2005.

123. Gong, P., Stewart, D., Hu, B., Li, N., Cook, J., Nel, A., and Alam, J.: Activation of the mouse heme oxygenase-1 gene by 15-deoxy-Delta(12,14)-prostaglandin J(2) is mediated by the stress response elements and transcription factor Nrf2. *Antioxid. Redox Signal.*, **4**: *249-257*, 2002.

124. Copple, I. M., Goldring, C. E., Jenkins, R. E., Chia, A. J., Randle, L. E., Hayes, J. D., Kitteringham, N. R., and Park, B. K.: The hepatotoxic metabolite of acetaminophen directly activates the Keap1-Nrf2 cell defense system. *Hepatology (Baltimore, Md,* **48**: *1292-1301,* 2008.

125. Sekhar, K. R., Rachakonda, G., and Freeman, M. L.: Cysteine-based regulation of the CUL3 adaptor protein Keap1. *Toxicol. Appl. Pharmacol.,* **244**: *21-26,* 2009.

126. Kobayashi, A., Kang, M. I., Watai, Y., Tong, K. I., Shibata, T., Uchida, K., and Yamamoto, M.: Oxidative and electrophilic stresses activate Nrf2 through inhibition of ubiquitination activity of Keap1. *Mol. Cell. Biol.,* **26**: *221-229,* 2006.

127. Helten, A., and Koch, K. W.: Calcium-dependent conformational changes in guanylate cyclase-activating protein 2 monitored by cysteine accessibility. *Biochem. Biophys. Res. Commun.,* **356**: *687-692,* 2007.

128. Goldberg, N. R., Beuming, T., Soyer, O. S., Goldstein, R. A., Weinstein, H., and Javitch, J. A.: Probing conformational changes in neurotransmitter transporters: a structural context. *Eur. J. Pharmacol.,* **479**: *3-12,* 2003.

129. Sinz, A.: Chemical cross-linking and mass spectrometry to map three-dimensional protein structures and protein-protein interactions. *Mass Spectrom Rev,* **25**: *663-682,* 2006.

130. Rinner, O., Seebacher, J., Walzthoeni, T., Mueller, L. N., Beck, M., Schmidt, A., Mueller, M., and Aebersold, R.: Identification of cross-linked peptides from large sequence databases. *Nat. Methods,* **5**: *315-318,* 2008.

131. Zelter, A., Hoopmann, M. R., Vernon, R., Baker, D., Maccoss, M. J., and Davis, T. N.: Isotope Signatures Allow Identification of Chemically Cross-Linked Peptides by Mass Spectrometry: A Novel Method to Determine Interresidue Distances in Protein Structures through Cross-Linking. *J. Proteome Res.,* **9**: *3583-3589,* 2010.

132. Schulz, D. M., Ihling, C., Clore, G. M., and Sinz, A.: Mapping the topology and determination of a low-resolution three-dimensional structure of the calmodulin-melittin complex by chemical cross-linking and high-resolution FTICRMS: direct demonstration of multiple binding modes. *Biochemistry,* **43**: *4703-4715,* 2004.

133. Lee, Y. J., Lackner, L. L., Nunnari, J. M., and Phinney, B. S.: Shotgun cross-linking analysis for studying quaternary and tertiary protein structures. *J. Proteome Res.,* **6**: *3908-3917,* 2007.

134. Ogura, T., Tong, K. I., Mio, K., Maruyama, Y., Kurokawa, H., Sato, C., and Yamamoto, M.: Keap1 is a forked-stem dimer structure with two large spheres enclosing the intervening, double glycine repeat, and C-terminal domains. *Proc. Natl. Acad. Sci. U.S.A.,* **107**: *2842-2847,* 2010.

135. Quiocho, F. A., and Richards, F. M.: Intermolecular cross linking of a protein in the crystalline state: carboxypeptidase-A. *Proc. Natl. Acad. Sci. U.S.A.,* **52**: *833-839,* 1964.

136. Korn, A. H., Feairheller, S. H., and Filachione, E. M.: Glutaraldehyde: nature of the reagent. *J. Mol. Biol.,* **65**: *525-529,* 1972.

137. Okuda, K., Urabe, I., Yamada, Y., and Okada, H.: Reaction of glutaraldehyde with amino and thiol compounds. *J. Ferment. Bioeng.,* **71**: *100-105,* 1991.

138. Migneault, I., Dartiguenave, C., Bertrand, M. J., and Waldron, K. C.: Glutaraldehyde: behavior in aqueous solution, reaction with proteins, and application to enzyme crosslinking. *Biotechniques,* **37**: *790-796, 798-802,* 2004.

139. Kawahara, J., Ohmori, T., Ohkubo, T., Hattori, S., and Kawamura, M.: The structure of glutaraldehyde in aqueous solution determined by ultraviolet absorption and light scattering. *Anal. Biochem.,* **201**: *94-98,* 1992.

140. Chen, Z. A., Jawhari, A., Fischer, L., Buchen, C., Tahir, S., Kamenski, T., Rasmussen, M., Lariviere, L., Bukowski-Wills, J. C., Nilges, M., Cramer, P., and Rappsilber, J.: Architecture of the RNA polymerase II-TFIIF complex revealed by cross-linking and mass spectrometry. *EMBO J.,* **29**: *717-726,* 2010.

141. Li, X., Zhang, D., Hannink, M., and Beamer, L. J.: Crystal structure of the Kelch domain of human Keap1. *J. Biol. Chem.,* **279**: *54750-54758,* 2004.

142. Zhang, D. D., Lo, S. C., Sun, Z., Habib, G. M., Lieberman, M. W., and Hannink, M.: Ubiquitination of Keap1, a BTB-Kelch substrate adaptor protein for Cul3, targets Keap1 for degradation by a proteasome-independent pathway. *J. Biol. Chem.,* **280**: *30091-30099,* 2005.

143. Ohnuma, T., Nakayama, S., Anan, E., Nishiyama, T., Ogura, K., and Hiratsuka, A.: Activation of the Nrf2/ARE pathway via S-alkylation of cysteine 151 in the chemopreventive agent-sensor Keap1 protein by falcarindiol, a conjugated diacetylene compound. *Toxicol. Appl. Pharmacol.,* **244**: *27-36,* 2010.

144. Ihling, C., Schmidt, A., Kalkhof, S., Schulz, D. M., Stingl, C., Mechtler, K., Haack, M., Beck-Sickinger, A. G., Cooper, D. M., and Sinz, A.: Isotope-labeled cross-linkers and Fourier transform ion cyclotron resonance mass spectrometry for structural analysis of a protein/peptide complex. *J. Am. Soc. Mass Spectrom.,* **17**: *1100-1113,* 2006.

145. Heeren, R. M., Kleinnijenhuis, A. J., McDonnell, L. A., and Mize, T. H.: A mini-review of mass spectrometry using high-performance FTICR-MS methods. *Anal Bioanal Chem,* **378**: *1048-1058,* 2004.

VITA

NAME	Chenqi Hu
EDUCATION	B.E., Environmental Engineering, Shanghai Jiao Tong University, China, 2003 B.S., International Economics and Trade, Shanghai Jiao Tong University, China, 2003 M.S., Environmental Science and Engineering, Nanyang Technological University, Singapore and Stanford University, Palo Alto, CA, 2004 Ph.D., Medicinal Chemistry, University of Illinois at Chicago, Chicago, Illinois, 2011
TEACHING EXPERIENCE	Division of Environmental and Water Resources Engineering, Nanyang Technological University, Singapore. Aquatic Chemistry Laboratory, 2005 College of Pharmacy, University of Illinois at Chicago, Chicago, Illinois. Experiential III, 2007. College of Pharmacy, University of Illinois at Chicago, Chicago, Illinois. Principles of drug action & therapeutics III, 2007-2008.
HONORS	Joseph Frank Celer Scholarship, University of Illinois at Chicago, College of Pharmacy, Chicago, Illinois, 2009 Singapore Stanford Partnership Fellowship, Nanyang Technological University, Singapore, 2003-2004 Shanghai Jiao Tong University Excellent Academic Scholarship, Shanghai Jiao Tong University, China, 1999-2003
PROFESSIONAL MEMBERSHIP	The American Society of Mass Spectrometry
PUBLICATIONS	**Hu, C.**, Eggler, A.L., Mesecar, A.D., and van Breemen, R.B.: Modification of Keap1 cysteine residues by sulforaphane. *Chem. Res. Toxicol.*, **24**: *515-521*, 2011. **Hu, C.**, Nikolic, D., Eggler, A.L., Mesecar, A.D., and van Breemen, R.B.: Screening for natural chemoprevention agents that modify human Keap1. Anal. Biochem. 2011 (Epub)

SELECTED PRESENTATIONS

Hu, C., Nikolic, D., Eggler, A.L., Mesecar, A.D., and van Breemen, R.B.: Screening for natural chemoprevention agents that reversibly modify human Keap1. Proceedings of the 58th ASMS Conference on Mass Spectrometry and Allied Topics, Salt Lake City, Utah, May 23-27, 2010.

Qiu, X., Yuan, Y., **Hu, C.**, Vaishnav, A., Nonn, L., and van Breemen, R.B.: Quantitative proteomics of lycopene effects on prostate primary epithelial cells by LC-MS/MS. Proceedings of the 58th ASMS Conference on Mass Spectrometry and Allied Topics, Salt Lake City, Utah, May 23-27, 2010.

Pituch, K., Lopez-Rosas, A., **Hu, C.**, and Givogri, M.I.: Analysis of sulfatides in neural stem cells. Proceedings of the 41st Annual American Society for Neurochemistry (ASN) Meeting, Santa Fe, New Mexico, March 06-10, 2010.

Hu, C., Small, E., Eggler, A.L., Mesecar, A.D., and van Breemen, R.B.: Sites of alkylation by botanical chemoprevention agents of human Keap1 bound to Cul3. Proceedings of the 57th ASMS Conference on Mass Spectrometry and Allied Topics, Philadelphia, PA, May 31-June 4, 2009.